A-91

NATIONAL ADVISORY COMMITTEE FOR AERONAUTICS

WARTIME REPORT

ORIGINALLY ISSUED

December 1942 as
Memorandum Report

HIGH-SPEED WIND-TUNNEL TESTS OF A 1/6-SCALE MODEL OF A TWIN-ENGINE PURSUIT AIRPLANE

By Victor M. Ganzer

Ames Aeronautical Laboratory
Moffett Field, California

JPL LIBRARY
CALIFORNIA INSTITUTE OF TECHNOLOGY

NACA

WASHINGTON

MAR 23 1948

NACA WARTIME REPORTS are reprints of papers originally issued to provide rapid distribution of advance research results to an authorized group requiring them for the war effort. They were previously held under a security status but are now unclassified. Some of these reports were not technically edited. All have been reproduced without change in order to expedite general distribution.

NATIONAL ADVISORY COMMITTEE FOR AERONAUTICS

MEMORANDUM REPORT

for the

Air Materiel Command, U.S. Army Air Forces

HIGH-SPEED WIND-TUNNEL TESTS OF A 1/6-SCALE MODEL OF A TWIN-ENGINE PURSUIT AIRPLANE

By Victor M. Ganzer

SUMMARY

At the request of the Air Materiel Command, U.S. Army Air Forces, a 1/6-scale model of a twin-engine pursuit airplane was tested in the Ames 16-foot high-speed wind tunnel. The main purpose of the tests was to investigate the possibility of high-speed diving difficulties with this airplane and to find remedies for them.

Most of the data were obtained in force tests, although some pressure-distribution measurements, elevator hinge moments, and wake surveys were also made.

The tests showed that the airplane with the original 230-series wing will experience serious diving moments above lift coefficients of 0.5 at a Mach number of 0.65, and 0.1 at a Mach number of 0.725.

Modifications to the fuselage, booms, and the profile of the wing center-section proved ineffective in alleviating the diving tendency, but the substitution of a 66-series wing for the original 230-series wing increased the speed to which the airplane could go before encountering serious diving moments by a Mach number of 0.07 (50 mph at 20,000 feet).

INTRODUCTION

The model was furnished by the manufacturer. The airplane is a twin-engine, twin-boom, two-place pursuit similar in configuration to the airplane in reference 2. Two wings were

provided: an NACA 230-series wing and an NACA 66-series wing.

The purposes of the test were:

1. To investigate the model for high-speed diving tendencies and to investigate possible solutions to any difficulties that might appear

2. To investigate the airplane model for maneuvering and pull-out lifts

3. To investigate elevator hinge moments and elevator effectiveness, particularly at high speeds

4. To compare airplane model characteristics with the 230-series and the 66-series wings

5. To investigate the relative positions of wing wake and tail because of their bearing on tail buffeting

A-91

APPARATUS

Model

A three-view drawing of the model is shown in figure 1. Figure 2 shows the model mounted in the wind tunnel.

The 230-series wing consisted of a plywood skin fastened to a built-up steel spar. Designating the spanwise location of wing sections by the station as measured in inches on the model from the model center line, the wing from wing station 0 to station 36.67 had a constant-chord NACA 23016 profile set at an angle of incidence of +2° to the fuselage reference line. The tip section (wing station 67.83) was an NACA 4412 section set at 0° to the fuselage reference line, giving a geometrical washout of 2°. Straight-line elements joined the two sections.

The 66-series wing was similar in construction to the 230-series wing except that solid mahogany was used in place of the plywood. An NACA 66, 2-116 section set at an angle of incidence of +1-1/2° was used from wing station 0 to station 36.67, and an NACA 66, 2-216 section set at -1/2° to the fuselage reference line was used at station 67.83, also giving

a geometrical washout of 2°. Both wings had the same plan form and area.

Figure 3 shows the plan form and section of a third wing modification which was effected by means of a glove fastened to the original 230-series wing.

Two sets of booms were provided, designated in this report as the "large booms" and the "small booms." The outlines of the two sets of booms are shown in figure 4. The booms were constructed of mahogany bolted to steel backbones. The large booms were used in the standard configuration. The small booms were the same as the large booms from the Prestone radiators aft, but had a smaller cross section at the wing and had fillets between the wing and booms. The oil-cooler installation on the small booms was also different in that the frontal area of the booms was reduced and, on the model, there was no provision for air to pass through the oil coolers. Boom accessories consisted of Prestone radiators, oil coolers, and turbosuperchargers. There was airflow through the Prestone radiators.

The fuselage shown in figure 1 was used for all except one run when the modification shown in figure 5 was used. The fuselage was constructed of mahogany and was bolted through the wing. Fuselage accessories consisted of two turrets with guns. In this report, "fuselage" denotes the clean condition of the fuselage, without turrets.

The stabilizer and elevator were constructed of solid aluminum alloy with steel hinges and lead counterweights. A modified inverted 23010 section was used for the stabilizer. The elevator was hinged and was held in position by two steel arms extending forward from the elevator hinge line into the booms. Upon the upper and lower surfaces of each of these arms were mounted wire strain gages, which were calibrated by means of weights on a lever to read elevator hinge moment. Stabilizer angles were +2° for the tests with the 230-series wing and +2.25° for the tests with the 66-series wing. Fins and rudders were made of solid brass with no movable parts.

Pressure orifices were at wing station 9.6 (between the fuselage and booms), at wing station 28.85 (outboard of booms), and along the top of the fuselage where the sharp curvature occurred.

Wind Tunnel and Equipment

The tests were run in the 16-foot high-speed wind tunnel at Ames Aeronautical Laboratory. The tunnel has a circular test section, and has a single return. Pressure orifices were connected to mercury-in-glass manometers which were photographed. Wake surveys were made with a calibrated pitot-static pitch-yaw head mounted on a survey strut. Forces and moments were measured on automatic balancing and recording scales.

RESULTS

Reduction and Correction of Data

The following tunnel-wall corrections were applied to the test results (reference 1):

$$\Delta\alpha \text{ (deg)} = 0.629\ C_L$$

$$\Delta C_D = 0.01097\ C_L^2$$

$$\Delta C_M = 0.0155\ C_L$$

The results are expressed in the following forms:

C_L lift coefficient (L/qS)

C_D drag coefficient (D/qS)

C_M pitching-moment coefficient (M/qSc)

C_{H_e} elevator-hinge-moment coefficient (hinge moment/qS_ec_e)

S pressure coefficient $\left(\frac{\text{total pressure} - \text{local static pressure}}{q}\right)$

S_{cr} pressure coefficient at which the local velocity reaches the velocity of sound

q free-stream dynamic pressure $(\frac{1}{2}\rho V^2)$

q_w q in the wake of the wing or fuselage

A-91

α angle of attack corrected for tunnel-wall effects

M Mach number

R Reynolds number

The following dimensions were used in computing the coefficients:

S wing area, 16.67 square feet

c mean aerodynamic chord, 1.525 feet

S_e elevator area, 0.903 square feet

c_e elevator chord, 3.5 inches

Pitching moments are expressed about the 31.8-percent point on the mean aerodynamic chord as shown in figure 1.

Drag and pitching-moment tares were taken from the NACA test reported in reference 2. No buoyancy or upflow corrections have been made to the data. The drag data should therefore be used for comparison purposes only.

Presentation of Results

The test results are presented in the following groups:

(1) Build-up and modifications with the 230-series wing:

Figures 6 through 14 show the results of force and pressure measurements for the model with the 230 wing as various units were added and modifications made. With the fuselage off, the pressure at wing stations 9.6 and 28.85 were alike, hence pressure coefficients for only one station are shown.

(2) Build-up with the 66 series wing:

Plots similar to those described in (1) are included in figures 15 through 19 for the 66 wing.

(3) Elevator effectiveness with the 66-series wing:

Figure 20 shows the change in pitching-moment coefficient ΔC_M resulting from elevator deflections at various lift coefficients and Mach numbers for the 66 wing. With the 230-series wing on the model, elevator effectiveness at elevator angles to -4° agreed with that shown.

(4) Elevator hinge moments with the 230-series wing:

Figures 21 and 22 show the results of elevator hinge-moment tests with the 230-series wing on the model. With the 66-series wing on the model, elevator hinge moments at elevator angles of 0° and -3.5° agreed with those shown.

(5) Wake positions and flow angles at the tail:

Figures 23 through 26 show the relative positions of the tail and the wake, the size of the wake, the ratio of q in the wake to q outside the wake, and the flow angles at the tail for both the 230 and 66 wings.

DISCUSSION

Diving Characteristics of the Complete Airplane With the 230-Series Wing

The rapid decrease in the lift coefficient of a wing at constant angle of attack as the speed increases beyond the critical speed is attended by a reduction in the angle of downwash behind the wing. An example of this drop in lift coefficient can be seen in figure 10(c). This reduction in downwash angle causes an increase in the angle of attack of the horizontal tail, which produces a diving moment on the airplane. If a constant value of the lift coefficient were maintained, the angle of attack would have to be increased at speeds above the critical. As an example, from figure 10(b) at a Mach number of 0.675 the model attained a lift coefficient of 0.4 with an angle of attack of 1.1°, while at a Mach number of 0.75 an angle of attack of 4.3° was necessary - an increase of 3.2°. Since the average downwash angle is constant with constant lift coefficient, this increase in the angle of

attack of the model produces a corresponding increase in the angle of attack of the tail, which results in a diving moment. Whether at constant lift coefficient or constant angle of attack, a diving moment can be expected when the critical speed of the wing is exceeded. It is possible that the performance range of an airplane might not encompass this condition, but with the present trend toward more speed and higher wing loadings, it is to be expected that this dangerous diving condition could be present. It is possible that in flying an airplane with this characteristic, a pilot could get the airplane into a high-speed dive from which he could not recover. The principal object of these tests was to determine the characteristics of the airplane in this high-speed region and to attempt to correct any difficulties found.

Figure 10 shows the results of the test of the complete model with the 230-series wing. The curves showing the variation of pitching-moment coefficient with Mach number at constant values of the lift coefficient indicate the conditions for which diving tendencies were present at high speed. For instance, according to the pitching-moment curves in figure 10(c), at a lift coefficient of zero there was no large change in pitching-moment coefficient as Mach number increased, but at a lift coefficient of 0.1 a marked decrease in the pitching-moment coefficient occurred at Mach numbers above 0.725. Hence, it can be said that a "usable" lift coefficient of 0.1 was available at a Mach number of 0.725. Similarly, a usable lift coefficient of between 0.2 and 0.3 was available at a Mach number of 0.7. Since these lift coefficients permit only small accelerations, it is desirable to increase the usable lift coefficient at diving and maneuvering speeds.

Effect of Fuselage and Accessories

The portion of the wing between the booms undoubtedly has more effect on the horizontal tail, which is between the booms, than do the outer portions of the wing. The critical speed of any wing can be affected by bodies such as a fuselage and booms placed upon the wing due to the change in pressure distribution over the wing near the body. The model was tested without the fuselage and accessories and was then tested with these items in place in order to determine the effect on the speed and lift at which diving moments occurred. Figures 27 and 28 show the results for both wings. In each case, the fuselage alone had a

detrimental effect in that it caused the pitching-moment curves to break at about 0.025 lower Mach number for corresponding lift coefficients. The boom accessories, including Prestone radiators, oil coolers, and turbosuperchargers, had little effect but the turrets on the fuselage neutralized the adverse effects of the fuselage itself and caused the characteristics of the complete airplane to resemble those of the wing, booms, and tail.

The effect on the lift coefficient and the minimum drag coefficient of adding the fuselage is shown in figures 29 and 30. At speeds above the critical, a loss of lift is indicated because of the fuselage. The increment added to the minimum drag was practically constant up to a Mach number of 0.675, where the drag started to rise, but increased as the Mach number increased above the value.

The pressure plots in figure 8 indicate a high peak pressure on the top of the fuselage just forward of the wing leading edge. It was thought possible that this peak pressure could cause compressibility shock to occur on the upper surface of the wing at an excessively low speed which might have a detrimental effect on the lift and thus contribute to the diving moment. The canopy was revised, as shown in figure 5, to reduce this pressure peak. Figure 31 indicates that the revision had a detrimental effect on both the high-speed pitching moments and the high-speed drag. This effect could have resulted from moving the pressure peak, even though lower in magnitude, back to a point where it added to the wing pressures and caused compressibility effects to occur earlier.

Effect of Reducing the Cross Section of the Booms

The purpose of the small booms was to reduce the cross-sectional area along the wing intersection in an attempt to reduce the interference between the wing and booms and thus to preserve the lift and pitching-moment coefficients to a higher speed. Figure 32 shows that the reduction in boom size had no beneficial effect on pitching moments but reduced the minimum drag coefficient by 0.002 at a Mach number of 0.3 and by 0.003 at a Mach number of 0.6. Some of this drag change was probably due to the revision of the oil-cooler installation with the attendant reduction in frontal area and to the fact that on the model there was no air flow through the oil

coolers on the small booms.

Effect of the Glove on the Wing Center Section

Plots of the normal force coefficient C_N from the integration of the pressures separately on the lower and upper surfaces of the 230 and 66 wings showed that the downward normal force on the lower surface increased more rapidly with Mach number than did the upward force on the upper surface, thus giving a reduction in net lift even when the lift on the upper surface was still increasing (figs. 33 and 34). If it were possible to keep the downward force on the lower surface from increasing with Mach number, the lift could be maintained to a higher speed which would preserve the downwash angle and remove the cause for the diving moments to a higher speed. In an attempt to accomplish this improvement, a wing section was designed by the manufacturer to have positive pressures relative to the stream pressure over a greater part of the lower surface of the wing. The glove, as shown in figure 3, was installed using this section. The effect of the glove on lift coefficient and pitching-moment coefficient is shown in figure 35, and on normal-force coefficients in figure 36. Since there was only a slight increase in lift coefficient at speeds above the critical and since the pitching-moment curves broke at approximately the same Mach numbers as without the glove, the improvement due to the glove was not large enough to be of practical value.

Effect of Changing to the 66-Series Wing

Figure 37 shows a comparison of the results for the 230 and 66 wings with regard to lift and pitching moment. Figure 38 shows the lift coefficient available before the moment curves broke, the maximum lift coefficient, and the lift coefficient required for level flight at various altitudes. The break in the moment curves is considered the limiting condition on the lift coefficient available for flight and maneuvering, for even though more lift coefficients were available at higher angles of attack, the pilot might have difficulty producing the pitching moment necessary to attain these angles. This criterion will be less applicable as Mach number decreases because the moment differences will decrease directly in proportion to the decreased dynamic pressure. Figures 37 and 38 show the superiority of the

66 wing over the 230 wing. At Mach numbers greater than 0.55 an increase in the critical Mach number, as determined by moment-curve break, of about 0.07 (50 miles per hour at 20,000 feet) is available at lift coefficients of 0.3 and less.

The maximum lift coefficient with the 66-series wing was 0.33 lower than that with the 230-series wing at a Mach number of 0.2. Tests with and without the fuselage showed that, at this scale and speed, the interference effects on maximum lift coefficient due to the fuselage were negligible. Figure 39 shows the test Reynolds number variation with Mach number for the model. At a Mach number of 0.2 the Reynolds number was only 1,900,000. References 3 and 4 indicate that the maximum lift coefficients of 66-series airfoils are low at low Reynolds numbers, but that they compare favorably with maximum lift coefficients of conventional wings at higher Reynolds numbers. Tests at larger Reynolds numbers but at the same Mach numbers (corresponding to approach and landing speeds) are necessary to predict the maximum lift coefficient of the airplane in flight.

A comparison of the drag of the complete model with the different wings is shown in figure 40. At Mach numbers of 0.6 and greater, the 66 wing gave a lower drag at all lift coefficients while at lower speeds the 66 wing was superior at lift coefficients of 0.4 and less, with the drag curves crossing at that point. It is possible that the 66 wing would show to even greater advantage, especially at high lift coefficients, if the test Reynolds number were more nearly equivalent to flight Reynolds numbers.

Due to the high wing loading of this airplane (60.5 pounds per square foot), it is believed that further improvement could be realized if more camber were built into the 66-series wing. The wing tested was cambered for a lift coefficient of 0.1. Figure 38 shows that in any condition except a dive the airplane requires a higher lift coefficient than 0.1, and it would therefore be desirable to design the wing for a higher lift coefficient. This increase in camber should extend the usable lift-coefficient range of the airplane and should also show a beneficial result on maximum lift coefficient, allowing more lift for maneuvering at high speed, and improving the landing characteristics over the 66-series wing as tested. Figure 40 shows that the 66 wing was superior to the 230 wing with respect to subcritical drag coefficients at lift

coefficients of at least ±0.2 from the lift coefficient of 0.1 for which the 66 wing was cambered. Any increase in lift coefficient by means of added camber should raise the lift coefficient at which this drag saving is available to values more in keeping with the level-flight lift coefficients for this airplane.

The 66-series wing as tested on the model was aerodynamically smooth and the Reynolds number was low, which are ideal conditions for the maintenance of laminar flow. Since the actual airplane would have the turbulence due to the propellers and the increased Reynolds number, these ideal conditions would not exist and the transition point between laminar and turbulent flow might move forward. This forward movement would cause some change in the characteristics of the wing. In an attempt to determine the effect of moving the transition point forward, an extreme case was tested on the model. Transition was fixed with number 60 carborundum at the 10-percent-chord point. Figure 41 shows the results of this test. There was a detrimental effect on lift, particularly in the low lift range where this wing ordinarily had laminar-flow characteristics, and the pitching-moment curves broke more sharply but at the same Mach number as without transition. Since the device of arbitrarily fixing the transition with carborundum is not necessarily directly comparable with the normal transition on the full-scale airplane, these results may not accurately represent flight conditions.

Elevator Effectiveness

Figure 20 shows that for the range of lift coefficients covered in this test the elevator effectiveness was essentially constant with speed. However, the fact that the elevator remains effective does not indicate that the pilot could pull out of a high-speed dive without difficulty, as the airplane becomes extremely stable at high speed and an elevator deflection which would allow the pilot to pull out of a dive at speeds below the critical would have must less effect at speeds above the critical. An example of the increase in stability with speed is shown in figure 10(b).

Elevator Hinge Moments

Difficulty was experienced in the measurement of hinge moments with the electrical strain gages in that hysteresis was

indicated in the zero readings before and after a run. For this reason the absolute values of the hinge-moment coefficients cannot be relied upon, but any large variation of hinge-moment coefficient with Mach number could be detected. No such variation was found.

Wake Positions at the Tail

The wake surveys (figs. 23 through 26) show that the tail was in the wake of the fuselage at all conditions of the test. At attitudes and speeds corresponding to level flight the tail was not in the wake of the wing. However, at an angle of attack of 5.5° and a Mach number of 0.60 the wake of the 230 wing included the tail, and at the same angle at a Mach number of 0.65 the wake of the 66 wing also included the tail. These attitudes and speeds might be attained in accelerated flight. Wake measurements shown in reference 2 indicate that the wake would widen considerably if the speed were increased above a Mach number of 0.65. It is possible that the wake might widen to include the tail at attitudes corresponding to unaccelerated flight if the speed were increased above that investigated in these surveys. Since conditions are conducive to tail buffeting when the tail is in the wake of the wing and fuselage, it is concluded that under certain conditions it is possible that the airplane will experience buffeting.

CONCLUSIONS

1. At lift coefficients corresponding to level flight, the limiting speeds as determined by the development of unsatisfactory diving moments range from a Mach number of 0.65 (432 miles per hour at 40,000 feet altitude) to 0.73 (555 miles per hour at sea level).

2. Substitution of the 66-series wing for the original 230-series wing resulted in an increase in the allowable diving speed and the lift coefficient available for maneuvering at high speed.

3. Elevator effectiveness was essentially constant at all speeds, but the stability of the airplane increased rapidly at speeds above the critical.

4. Elevator hinge moments did not show any erratic characteristics at high speed.

5. At level-flight speeds and attitudes, the tail was above the wake of the wing, but was in the wake of the fuselage for all conditions of the test. Above the critical speed, the tail was in the wake in some accelerated flight conditions. At higher speeds than were included in the wake surveys, it is possible that the tail might be in the wake even in unaccelerated flight. Other experience indicates that tail buffeting is likely to be encountered when the tail is in the wake.

Ames Aeronautical Laboratory,
National Advisory Committee for Aeronautics,
Moffett Field, Calif.

REFERENCES

1. Silverstein, Abe, and White, James A.: Wind-Tunnel Interference with Particular Reference to Off-Center Positions of the Wing and to the Downwash at the Tail. NACA Rep. 547, 1935.

2. Erickson, Albert L.: Investigation of Diving Moments of a Pursuit Airplane in the Ames 16-Foot High-Speed Wind Tunnel. NACA CMR, Oct. 1942.

3. Muse, Thomas C., and Neely, Robert H.: Wind-Tunnel Investigation of an NACA Low-Drag Tapered Wing with Straight Trailing Edge and Simple Split Flaps. NACA ACR, Dec. 1941.

4. Jacobs, Eastman N., Abbott, Ira H., and Davidson, Milton: Preliminary Low-Drag-Airfoil and Flap Data from Tests at Large Reynolds Numbers and Low Turbulence. NACA ACR, Mar. 1942.

A-91

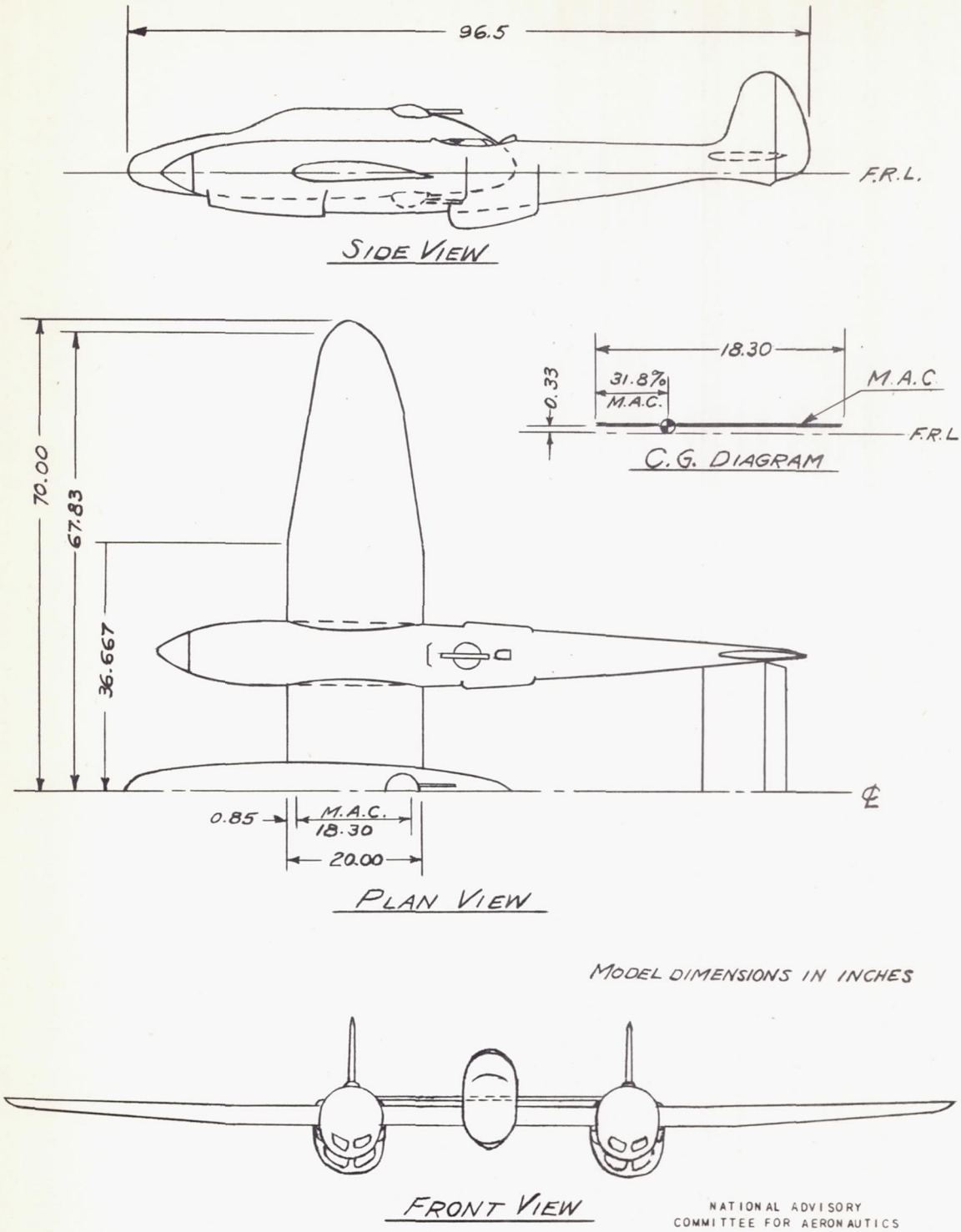

Figure 1.- General arrangement of the 1/6- scale model.

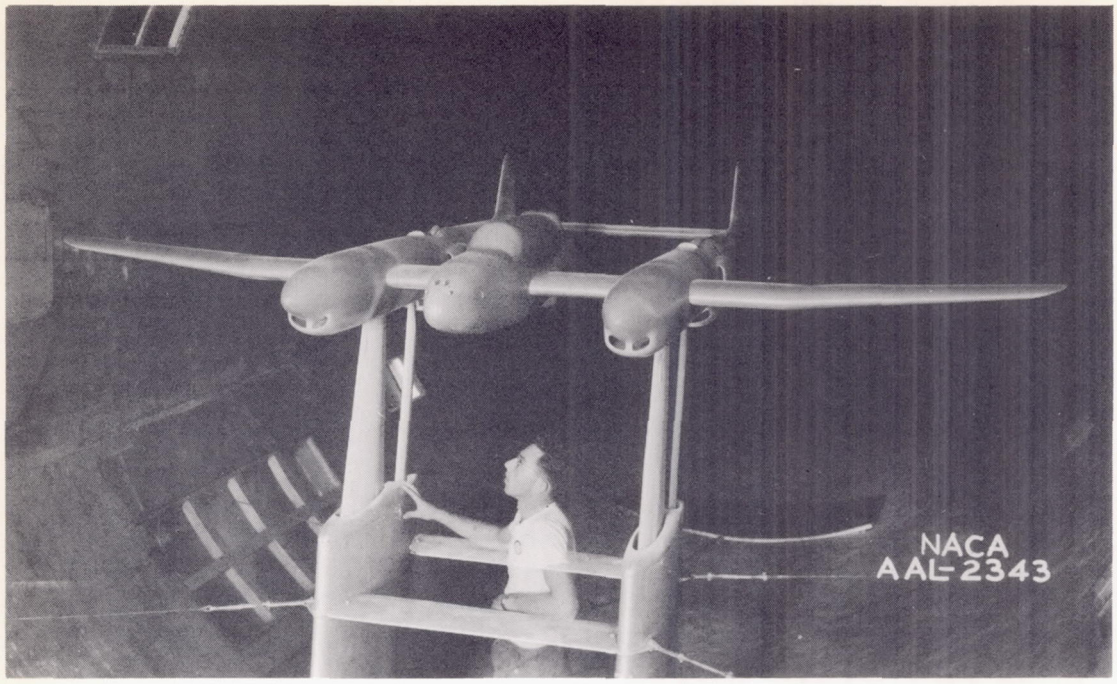

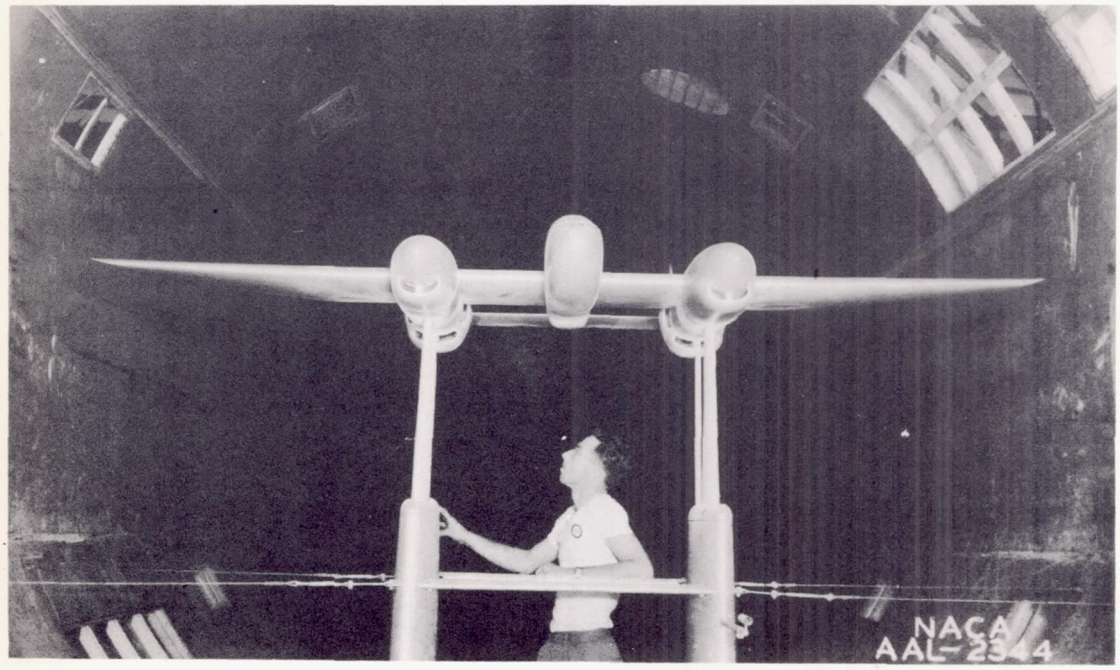

Figure 2.- The model mounted in the 16-foot wind tunnel.

A-91

MODIFIED SECTION

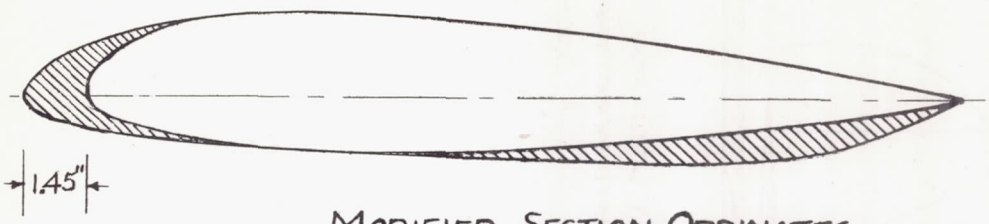

MODIFIED SECTION ORDINATES

STA. - IN.	UPPER ORDINATE-IN.	LOWER ORDINATE-IN.
0.0	0.0	0.0
0.5	0.66	0.53
1.0	0.94	0.67
2.0	1.35	0.86
3.0	1.62	1.00
4.0	1.80	1.08
6.0	1.93	1.23
8.0		1.33
10.0	SAME AS	1.43
12.0	23016	1.52
14.0	UPPER	1.55
16.0	SURFACE	1.48
18.0	ORDINATES	1.25
20.0		.67
21.45		0.0

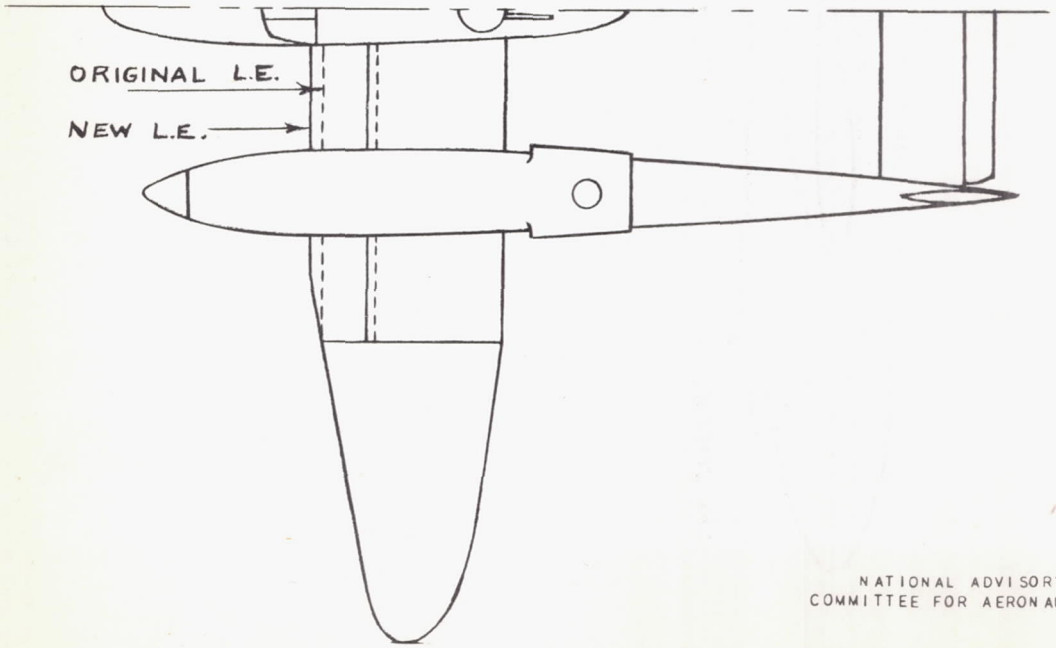

NATIONAL ADVISORY
COMMITTEE FOR AERONAUTICS

Figure 3.- Modification of the 23016 wing section.

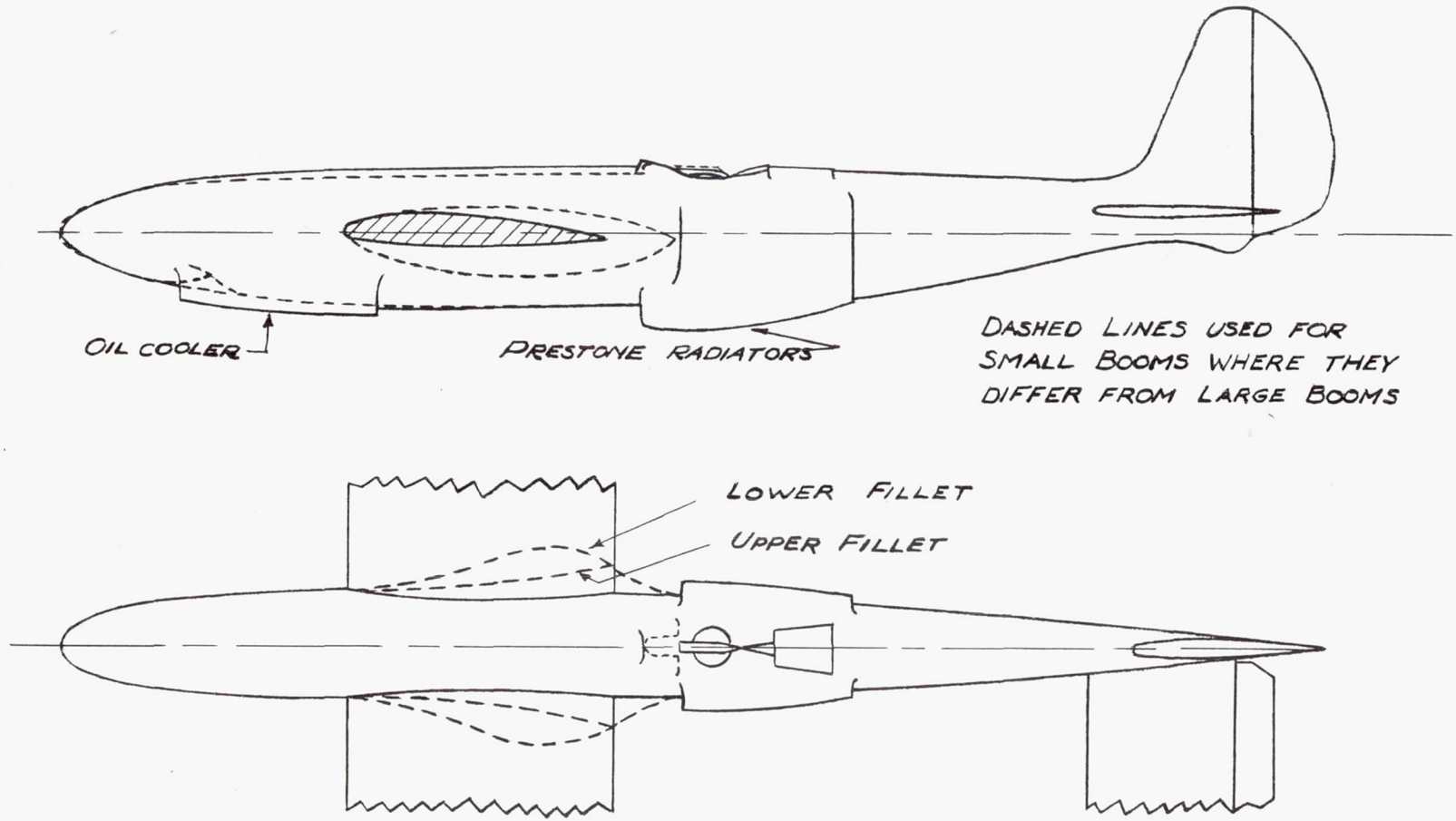

NATIONAL ADVISORY
COMMITTEE FOR AERONAUTICS

Figure 4.- Outlines of the large and small booms.

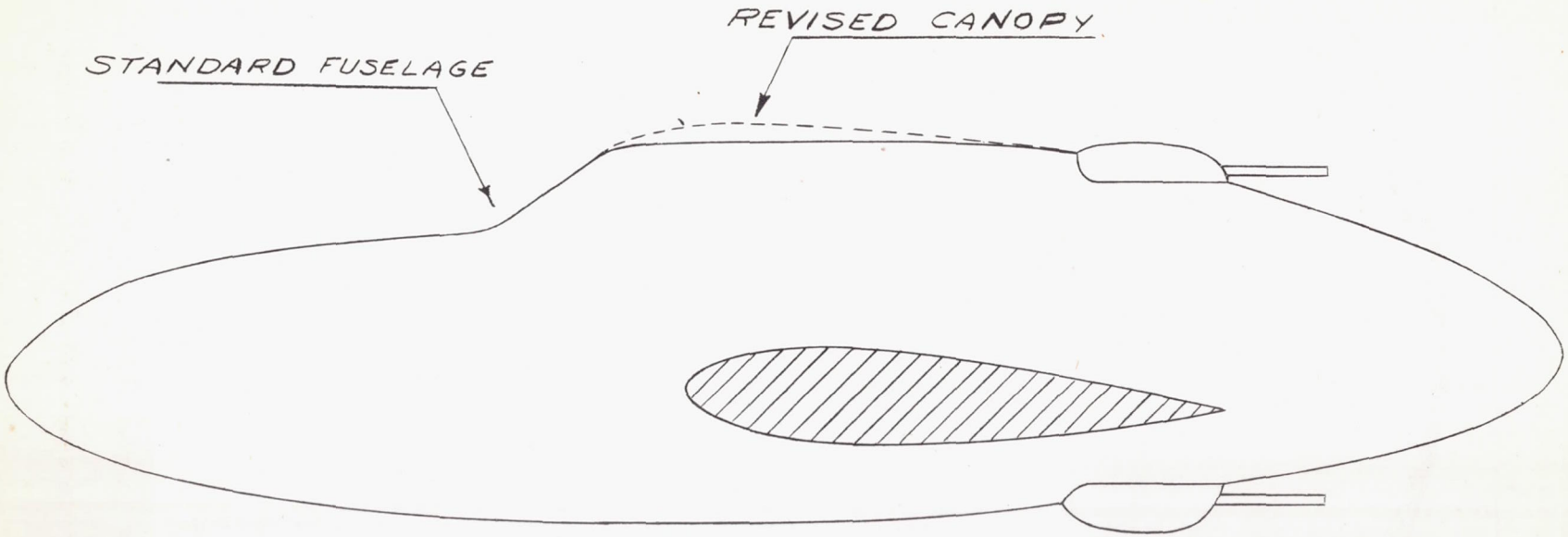

NATIONAL ADVISORY
COMMITTEE FOR AERONAUTICS

Figure 5.- Fuselage canopy revision.

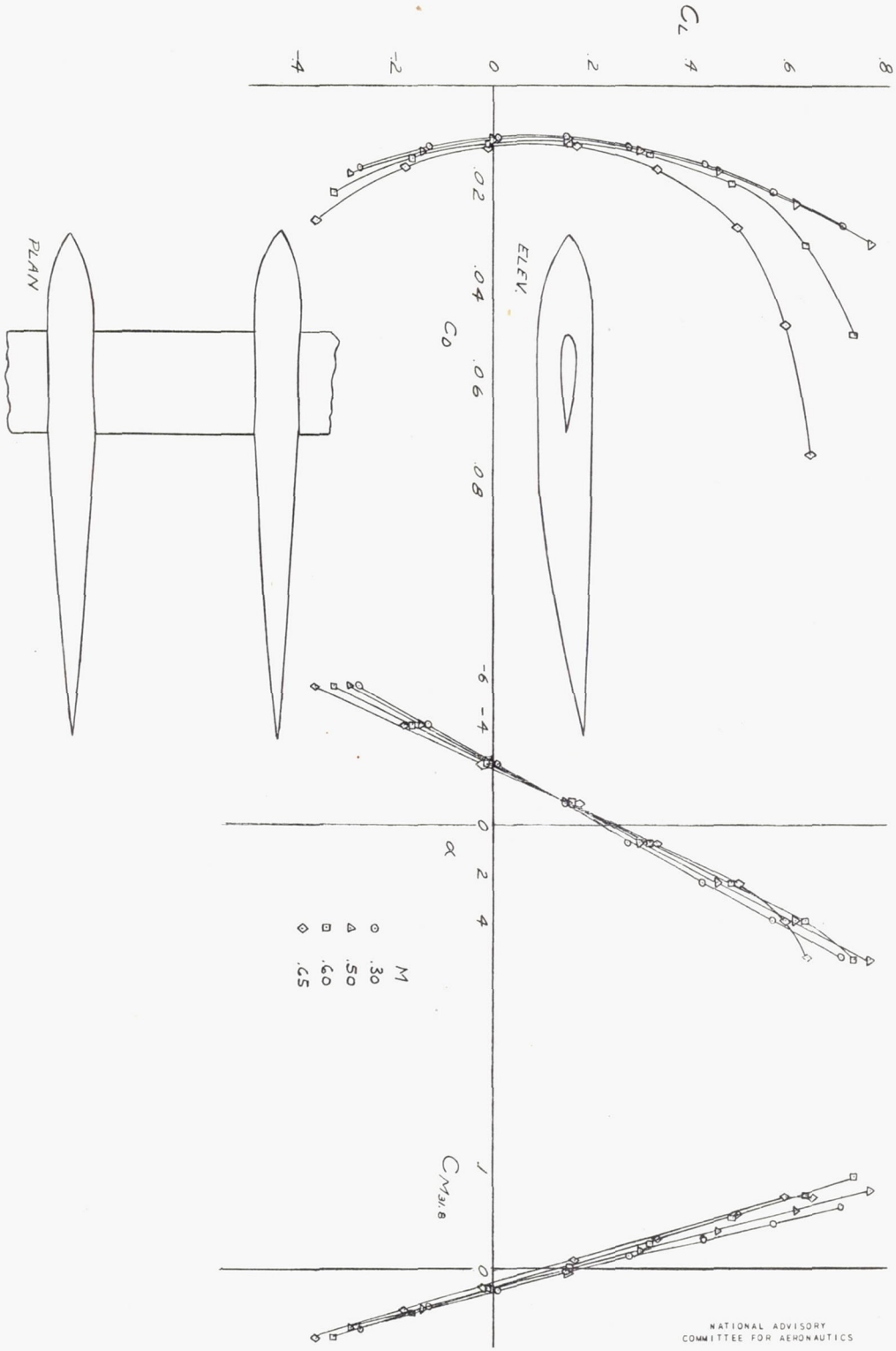

(a) Mach number 0.3 through 0.65.

Figure 6.- Characteristics with 230 wing, large booms.

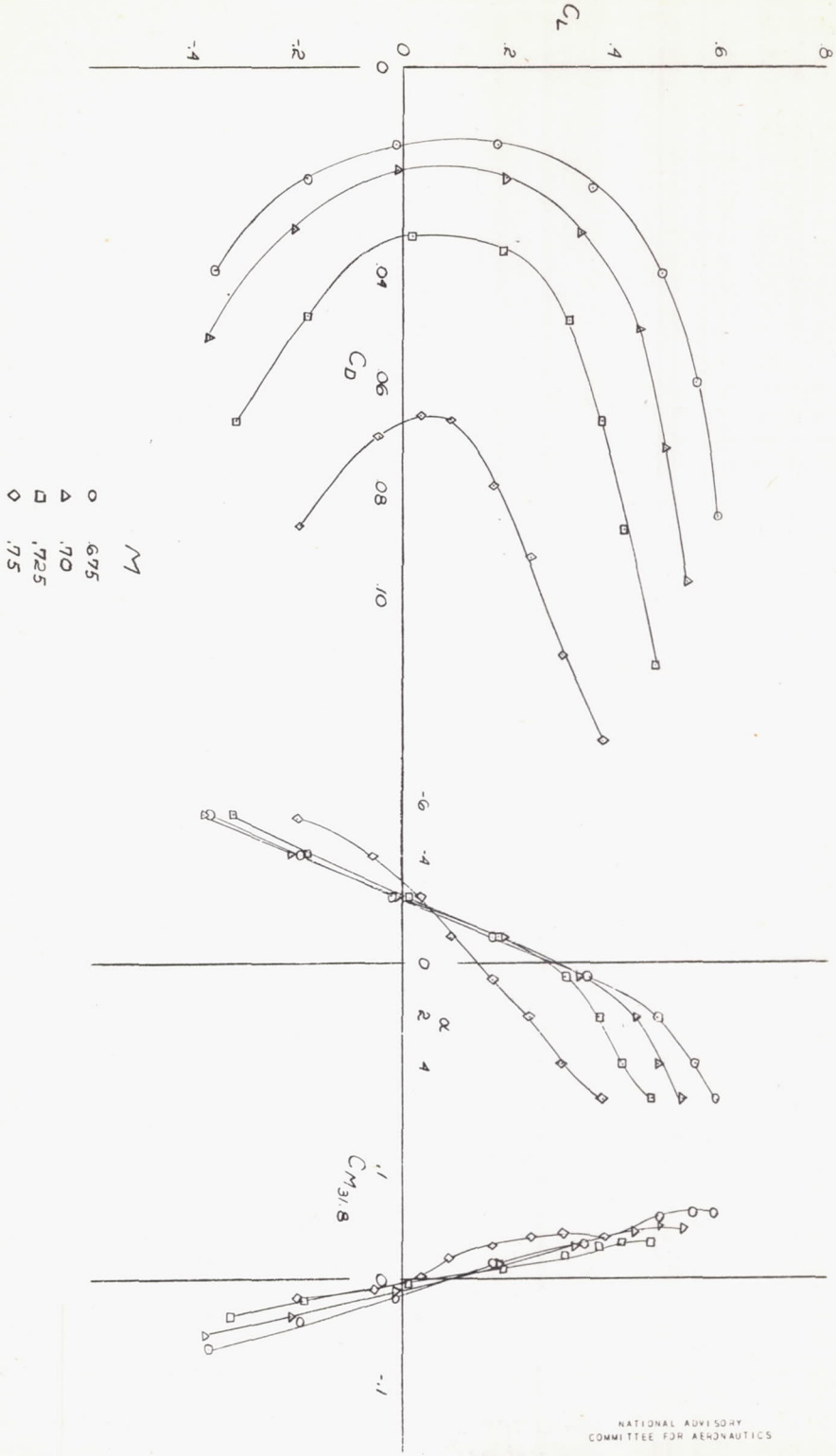

(b) Mach number, 0.675 through 0.75.

Figure 6. – Continued.

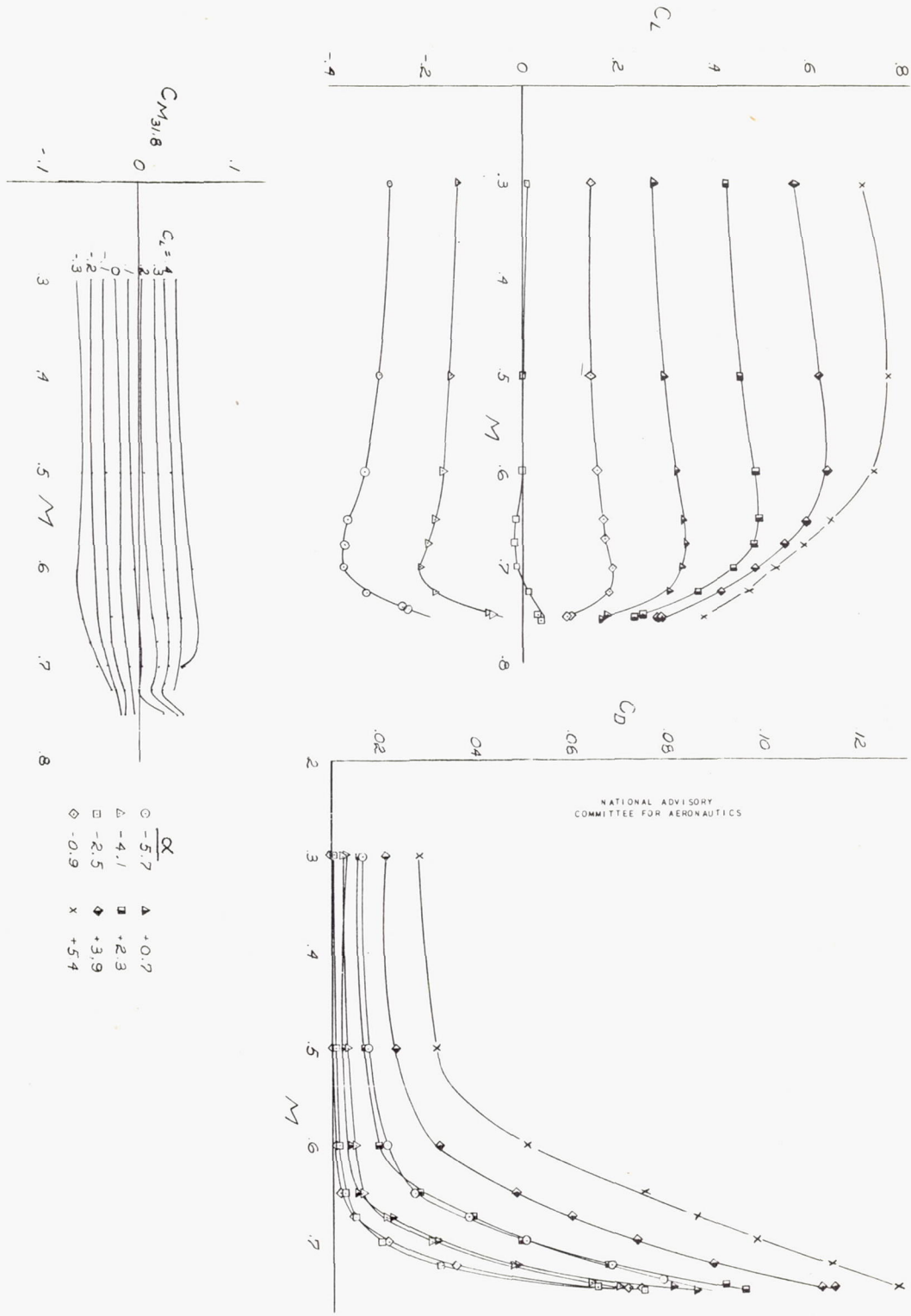

(c) Variation C_L, C_D, and C_M with Mach number.

Figure 6.– Continued.

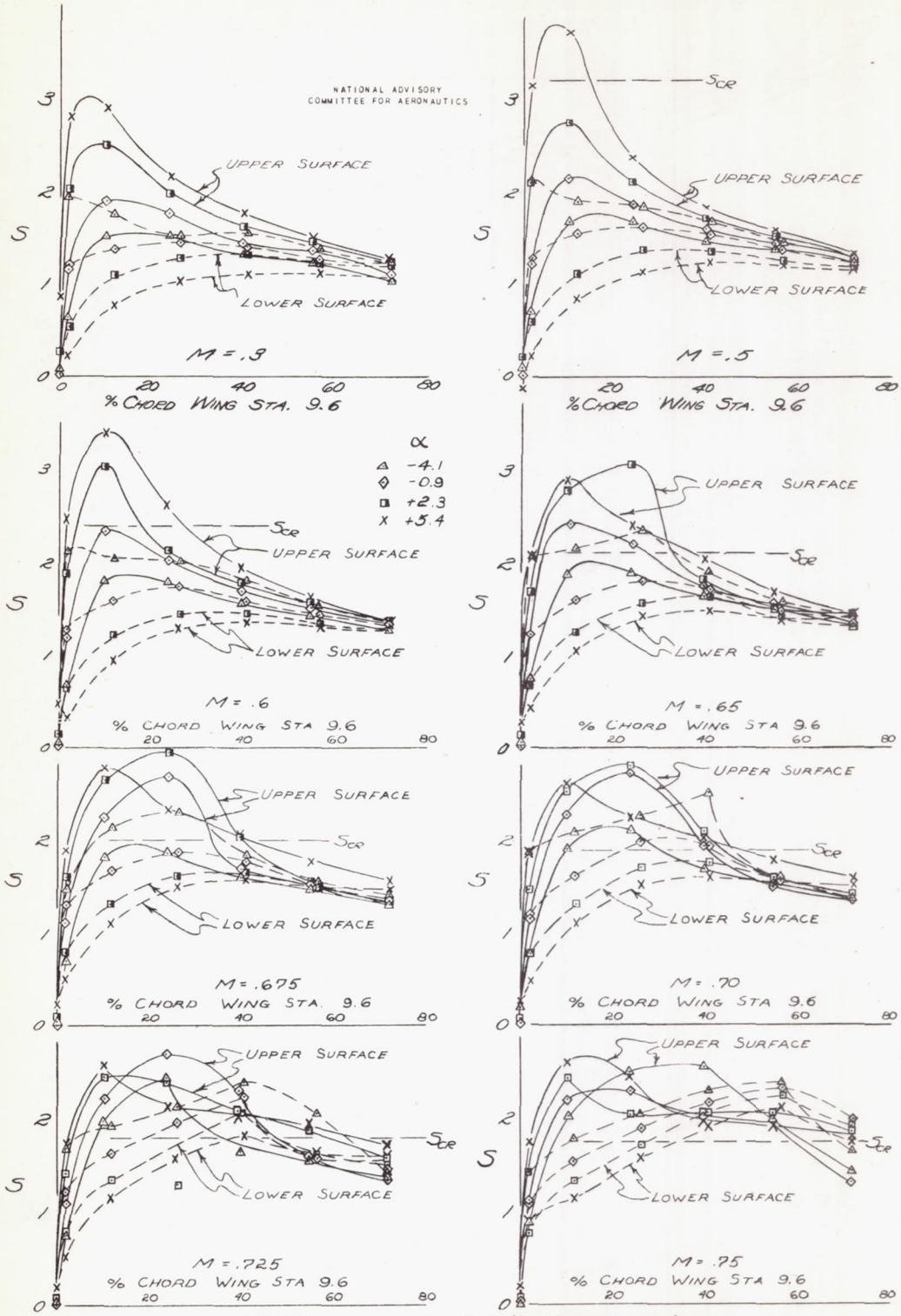

(d) Wing pressure distribution at various Mach numbers.

Figure 6. – Concluded.

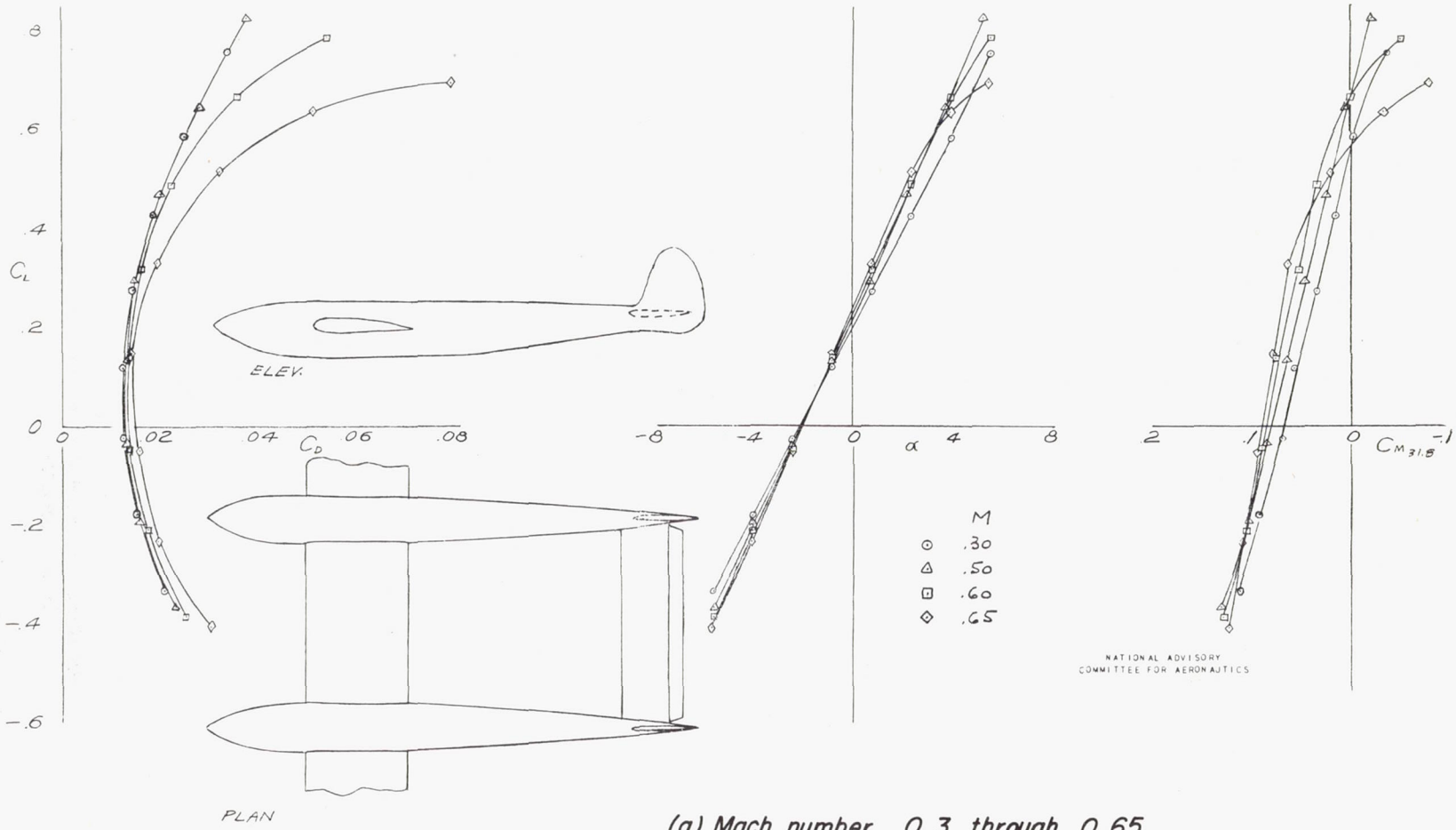

(a) Mach number, 0.3 through 0.65.

Figure 7.- Characteristics with 230 wing, large booms, tail.

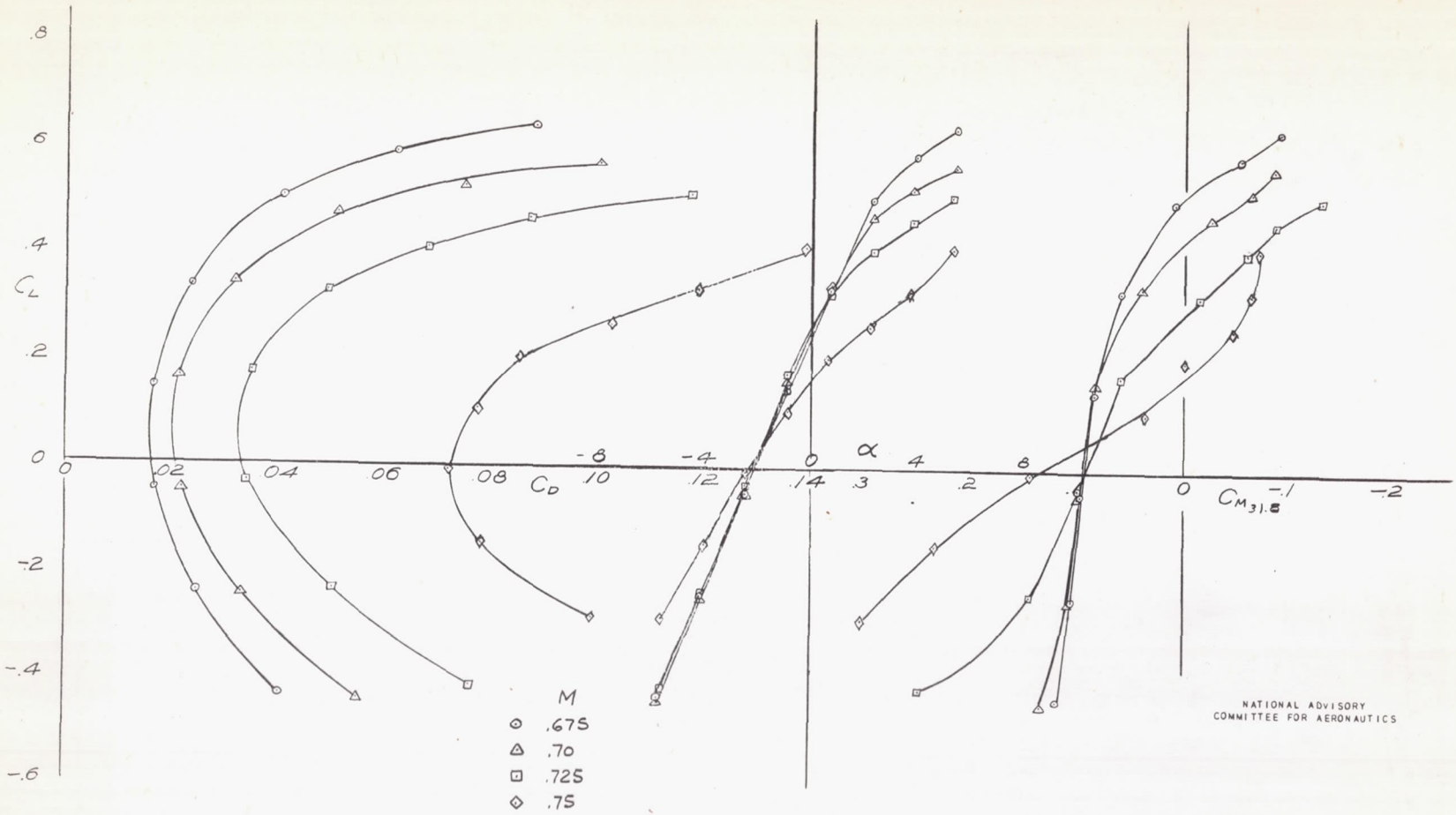

(b) Mach number, 0.675 through 0.75.

Figure 7.- Continued.

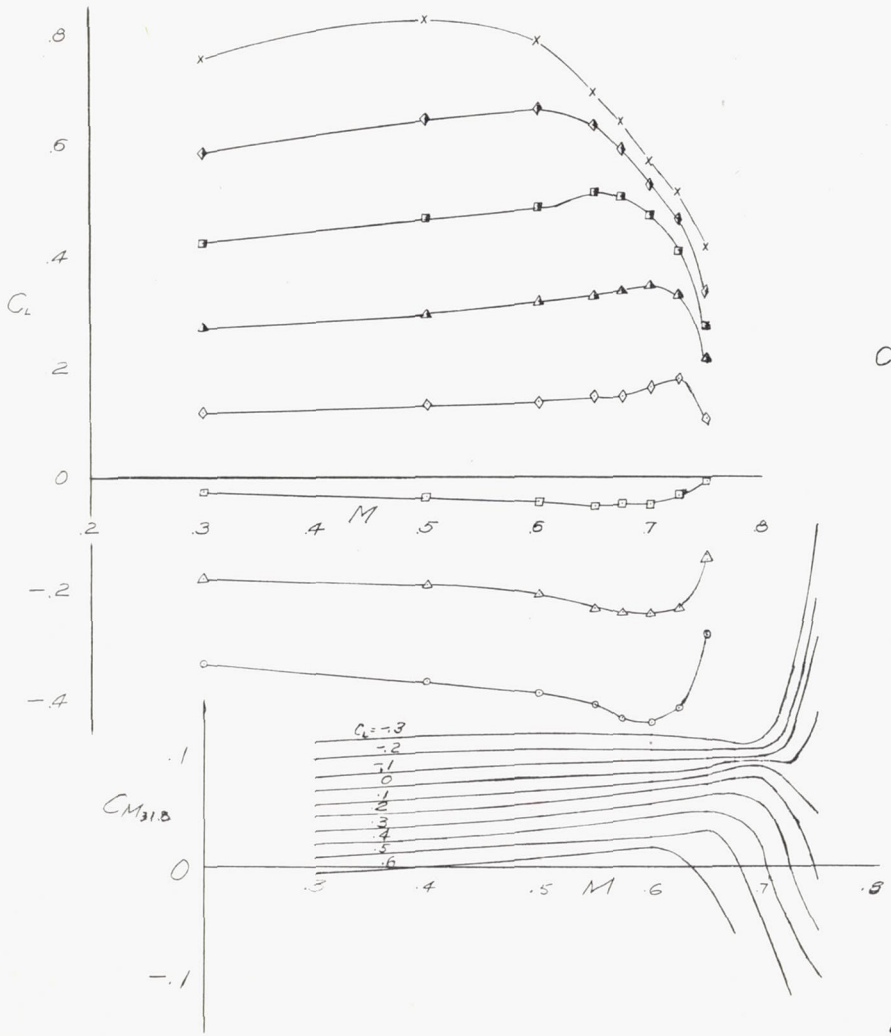

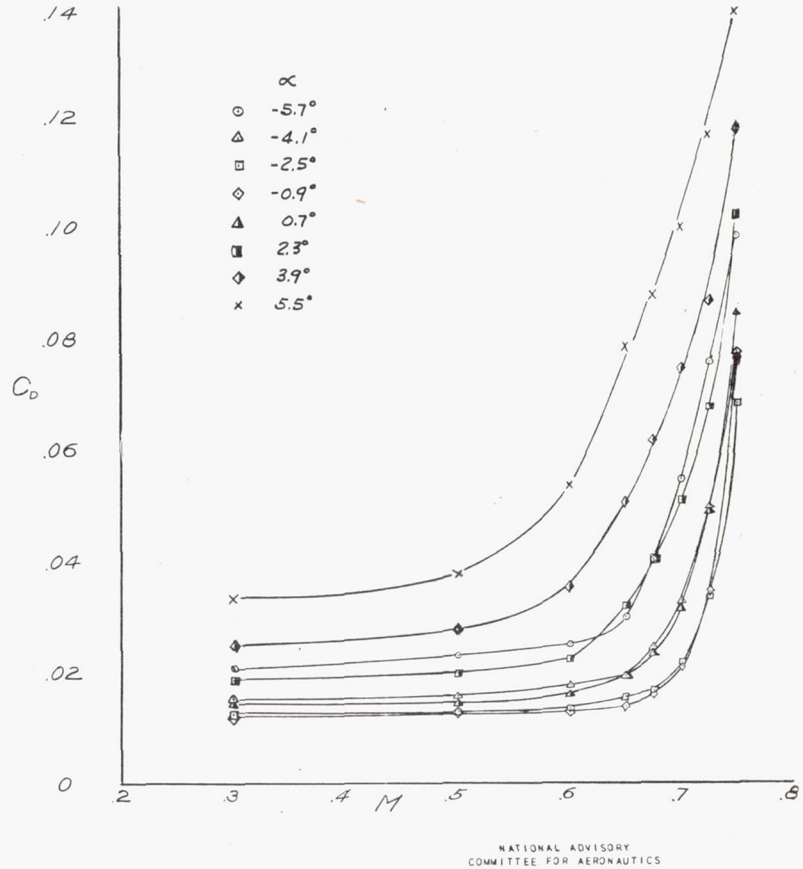

(c) Variation of C_L, C_D, and C_M with Mach number.

Figure 7.– Concluded.

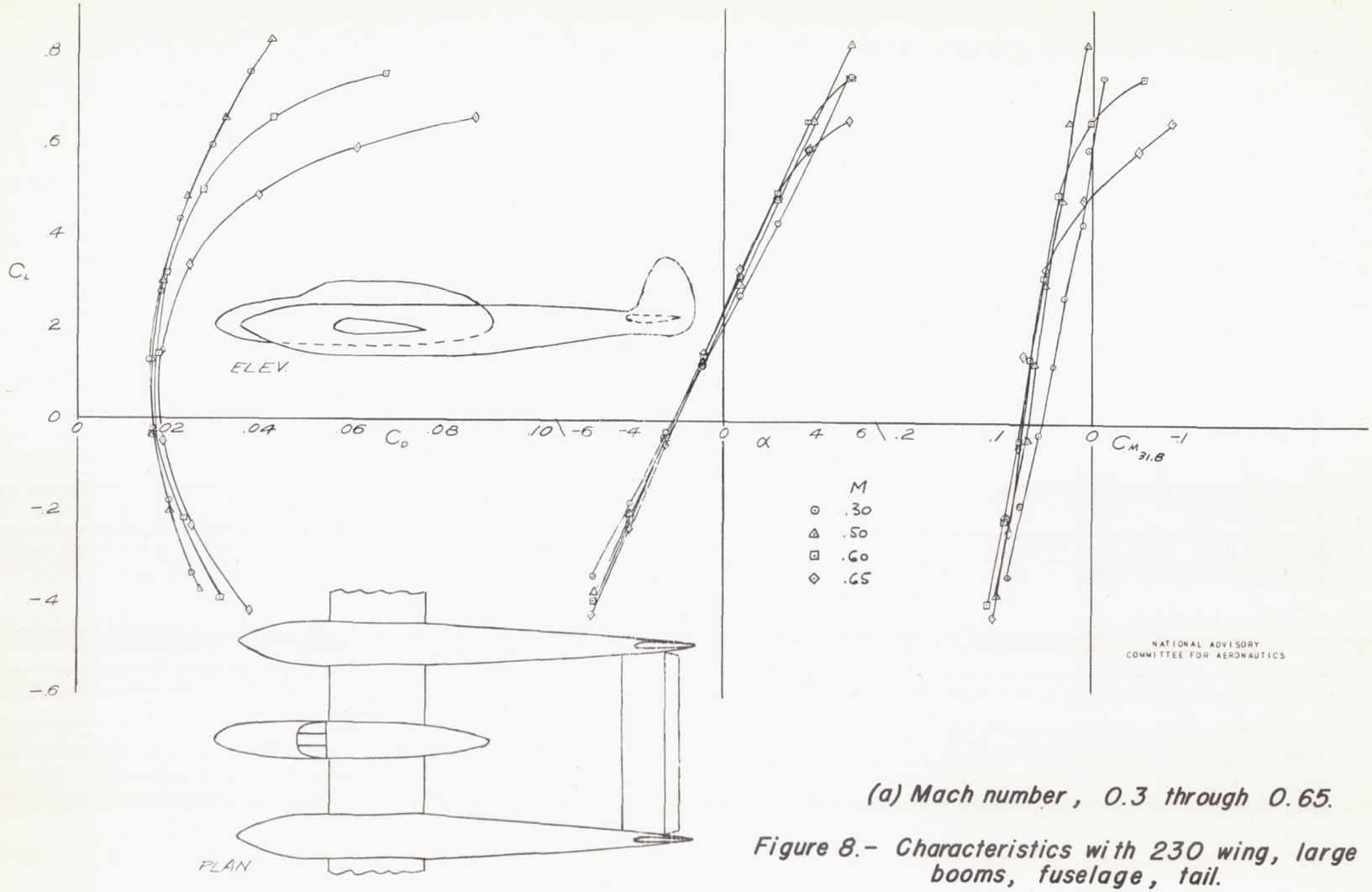

(a) Mach number, 0.3 through 0.65.

Figure 8.- Characteristics with 230 wing, large booms, fuselage, tail.

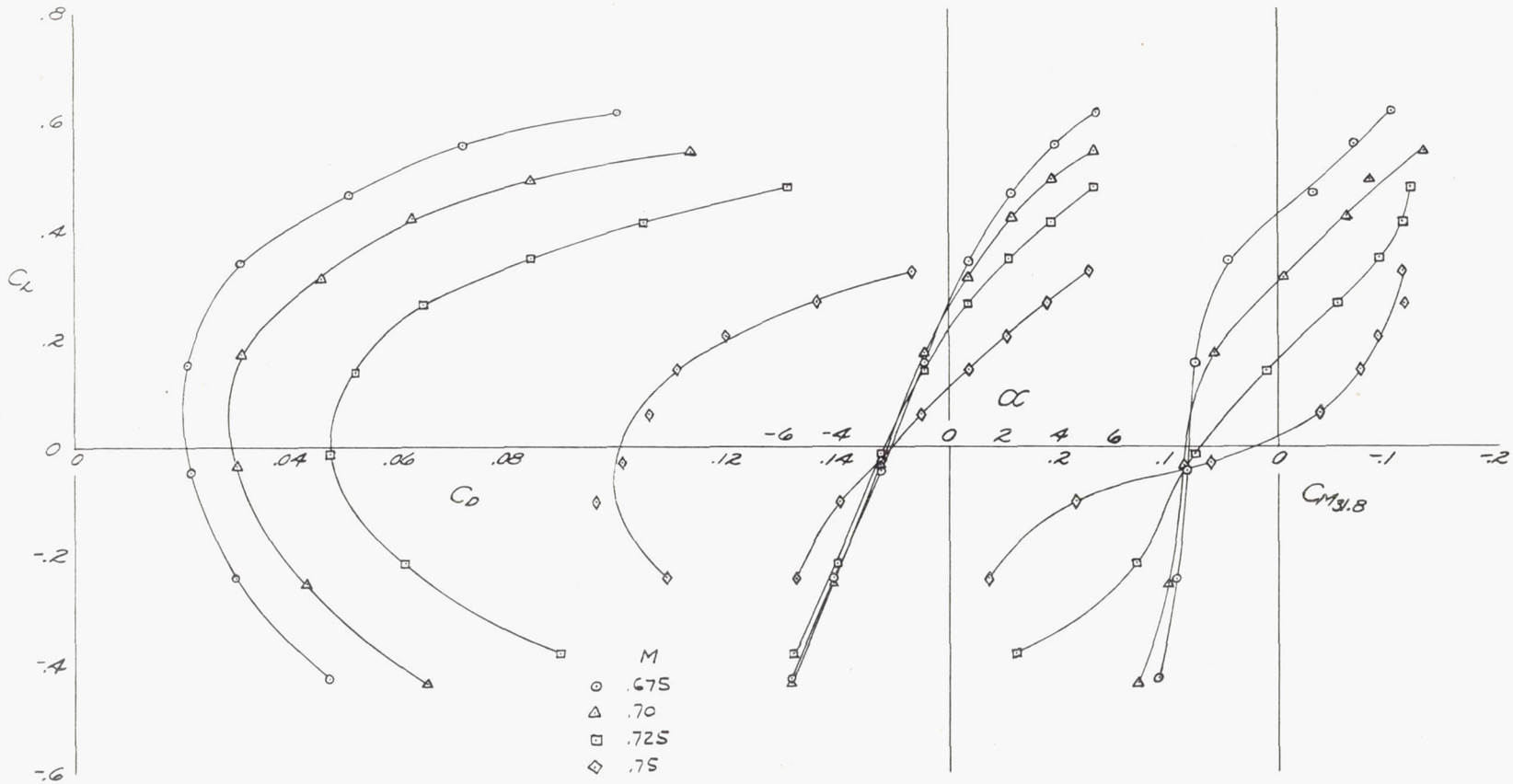

NATIONAL ADVISORY
COMMITTEE FOR AERONAUTICS

(b) Mach number, 0.675 through 0.75.

Figure 8.- Continued.

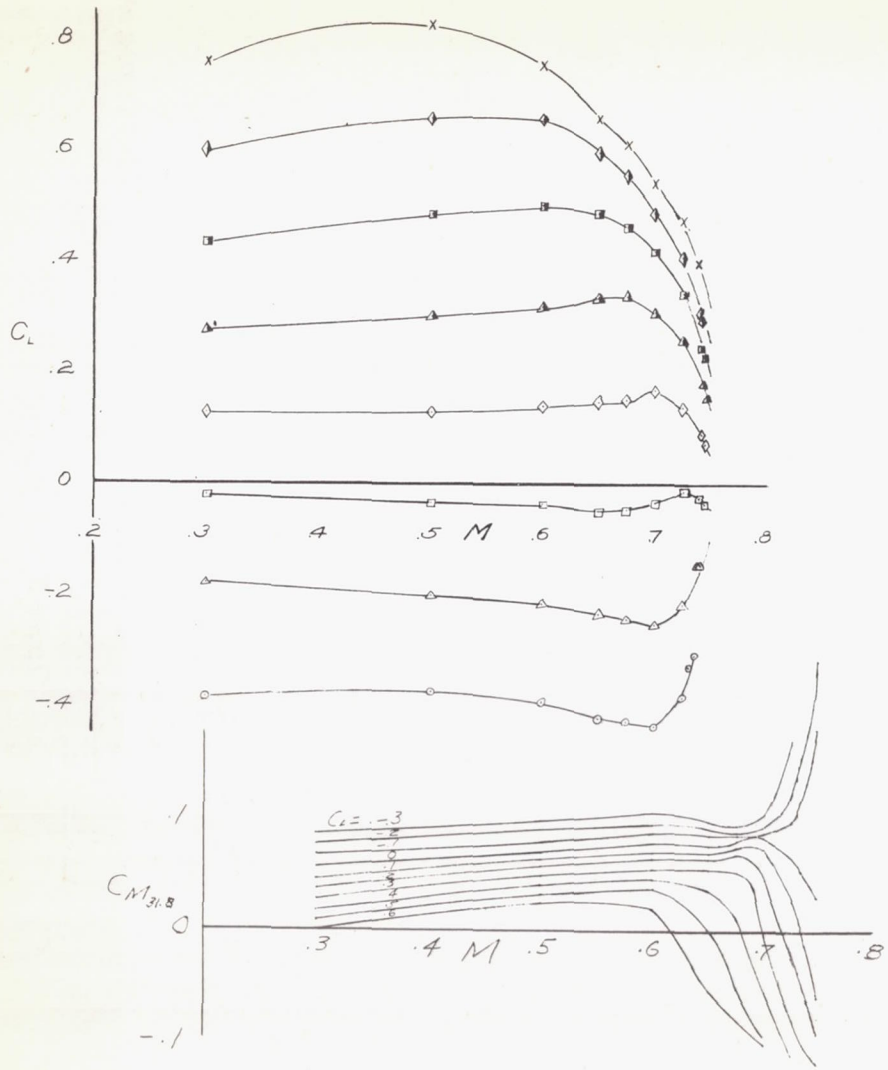

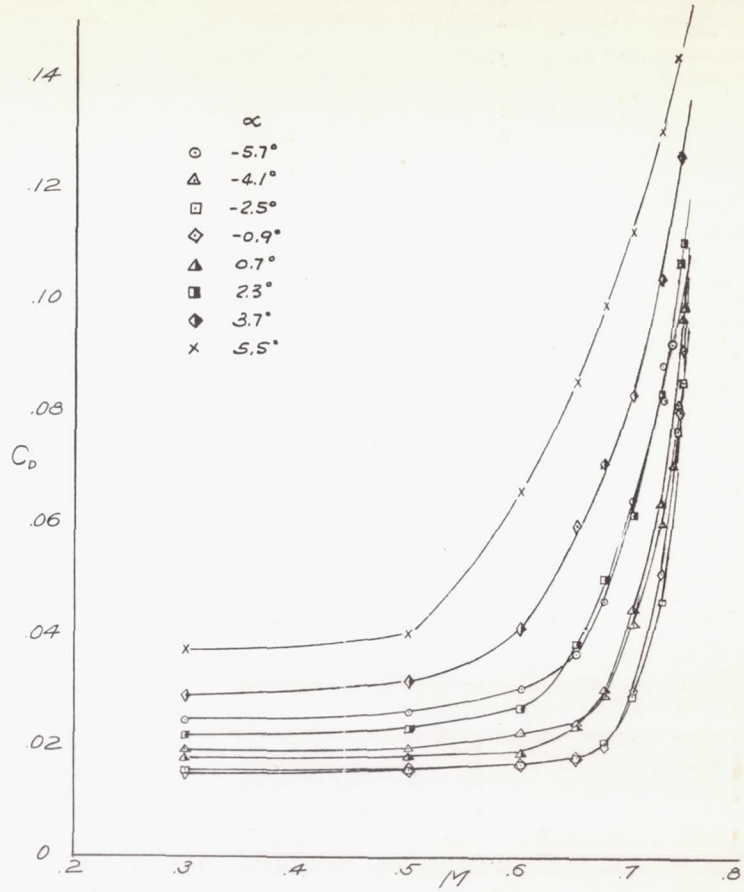

(c) Variation of C_L, C_D, and C_M with Mach number.

Figure 8.– Continued.

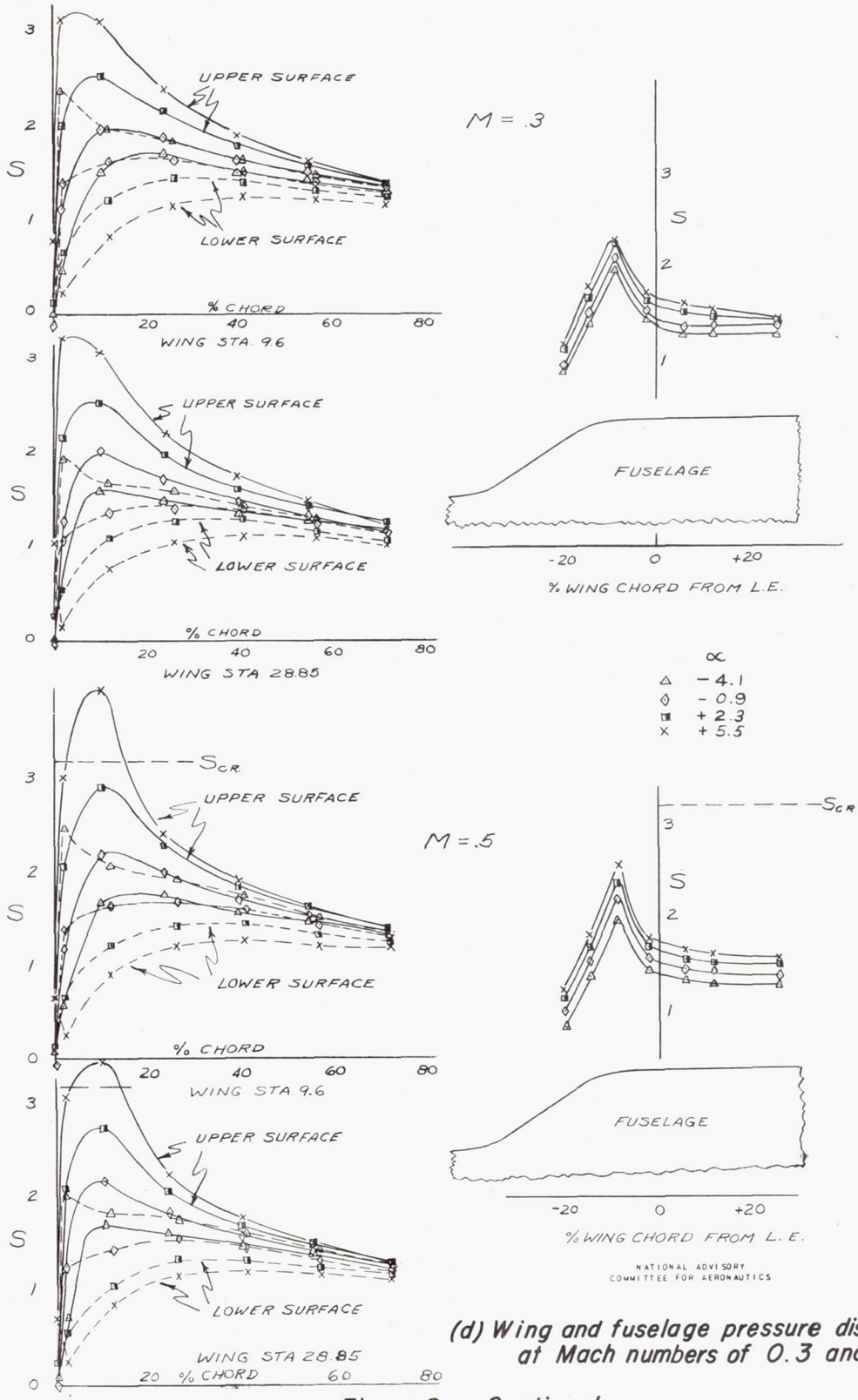

(d) Wing and fuselage pressure distribution at Mach numbers of 0.3 and 0.5.

Figure 8.– Continued.

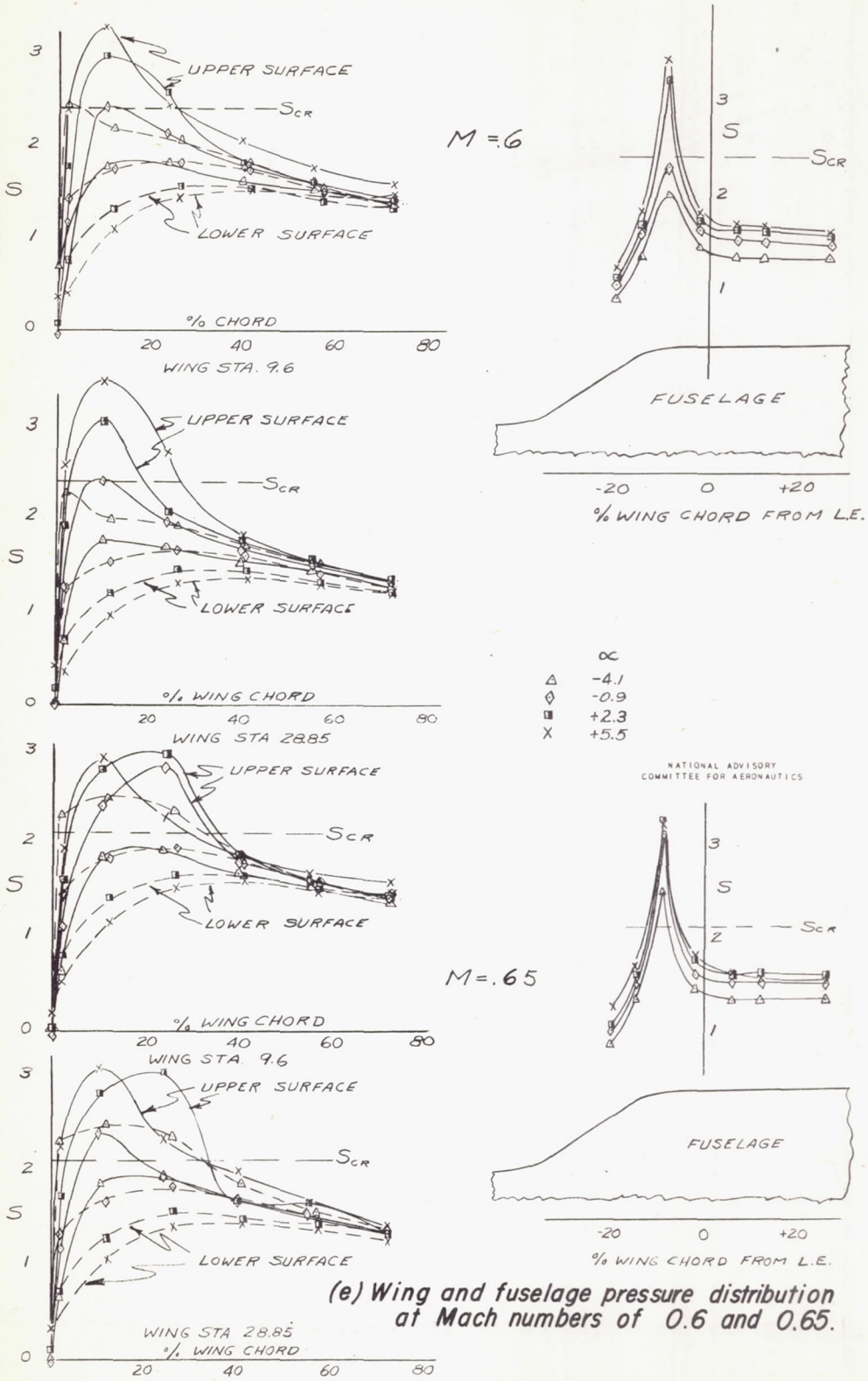

(e) Wing and fuselage pressure distribution at Mach numbers of 0.6 and 0.65.

Figure 8. – Continued

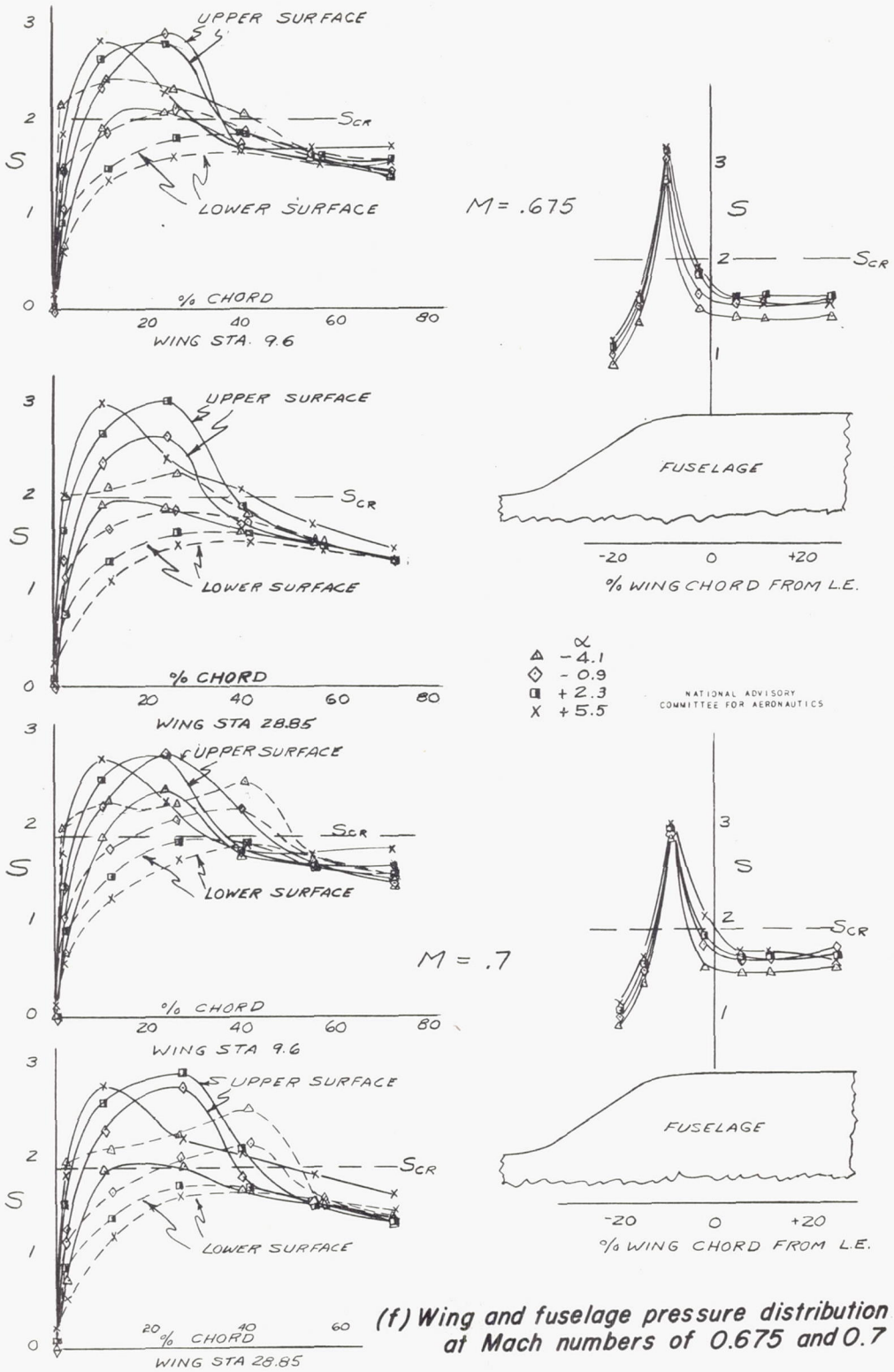

(f) Wing and fuselage pressure distribution at Mach numbers of 0.675 and 0.7

Figure 8.- Continued.

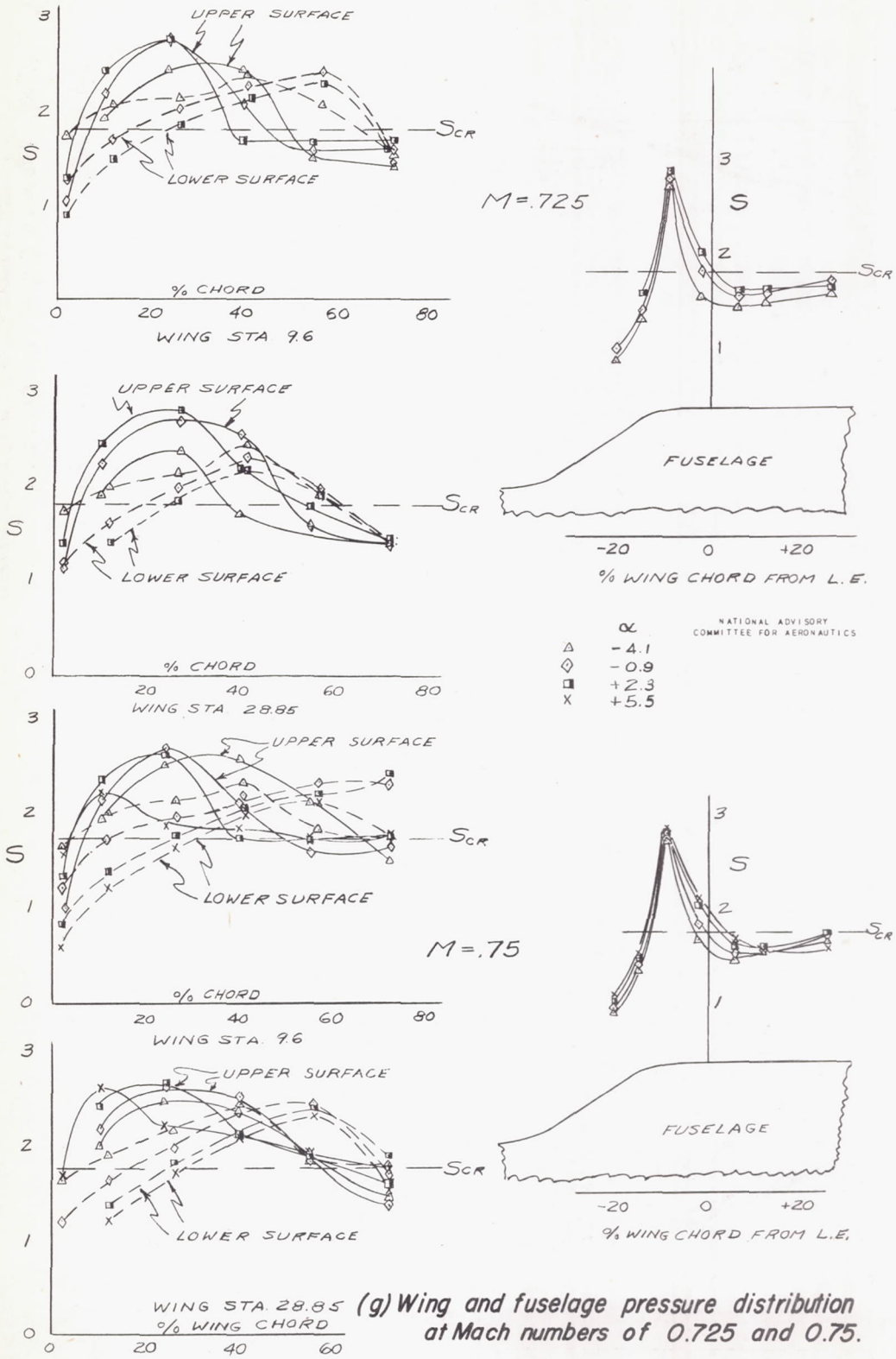

(g) Wing and fuselage pressure distribution at Mach numbers of 0.725 and 0.75.

Figure 8.– Concluded.

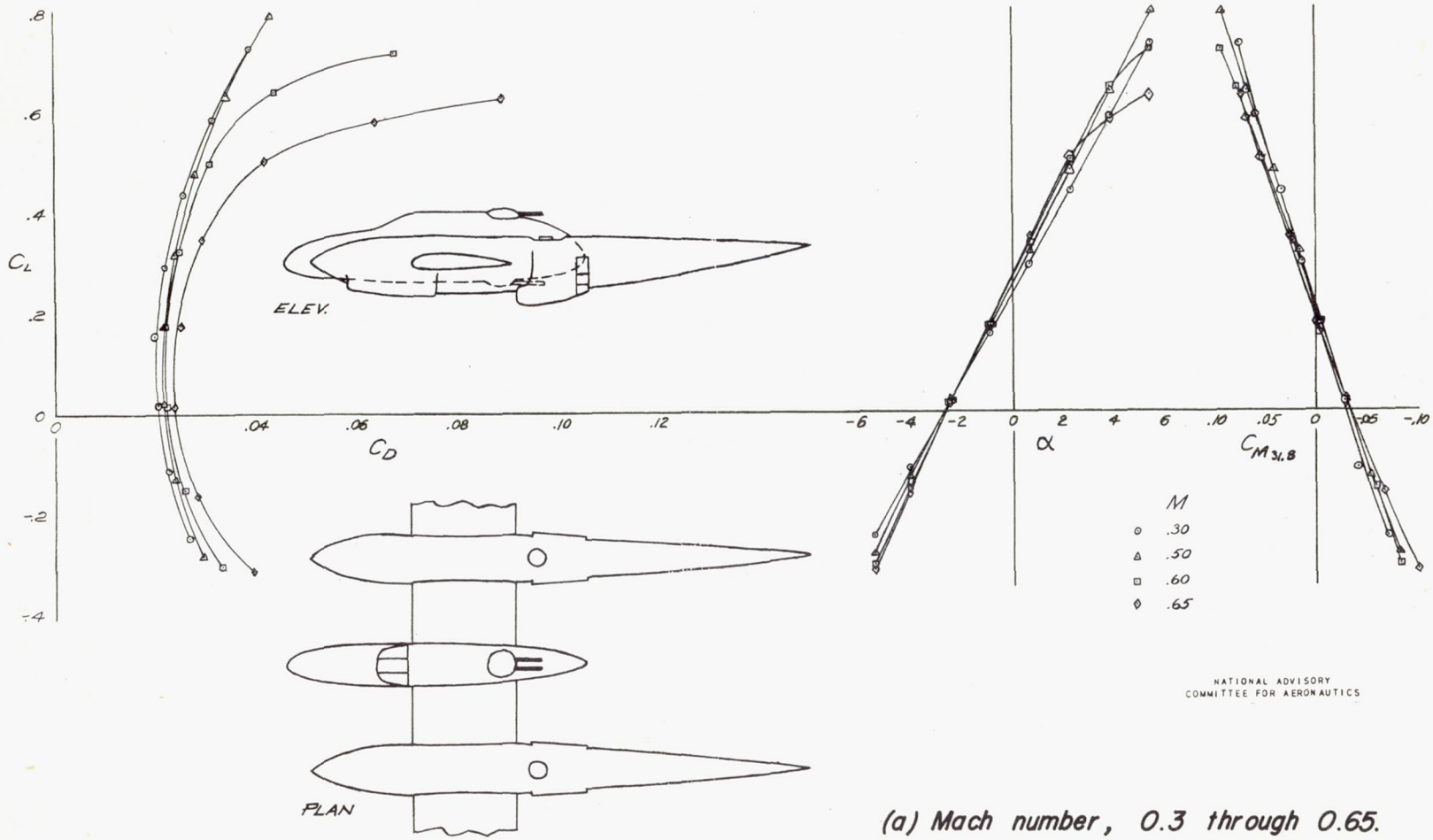

(a) Mach number, 0.3 through 0.65.

Figure 9.- Characteristics with 230 wing, large booms, fuselage, all accessories.

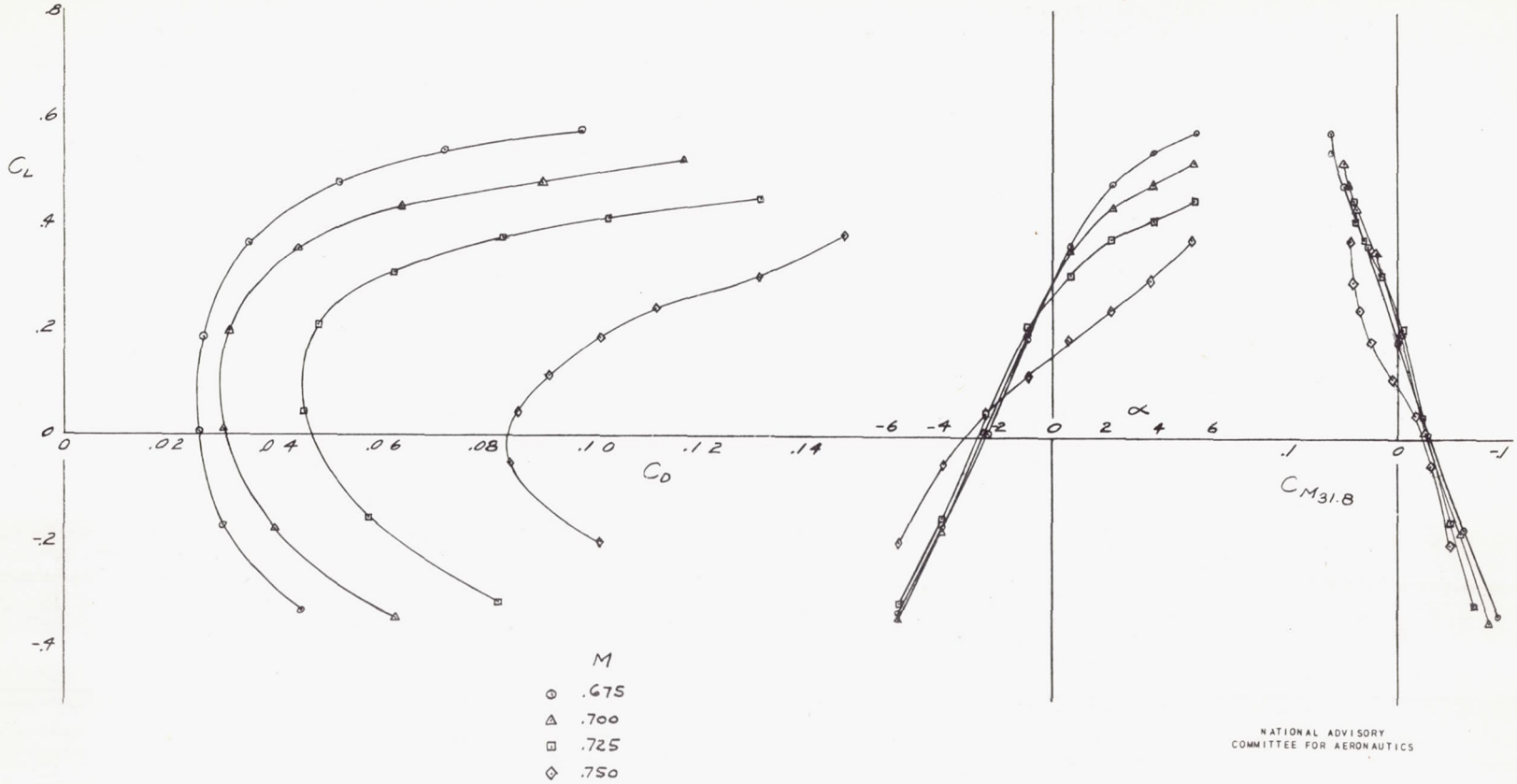

(b) Mach number, 0.675 through 0.75.

Figure 9.- Continued.

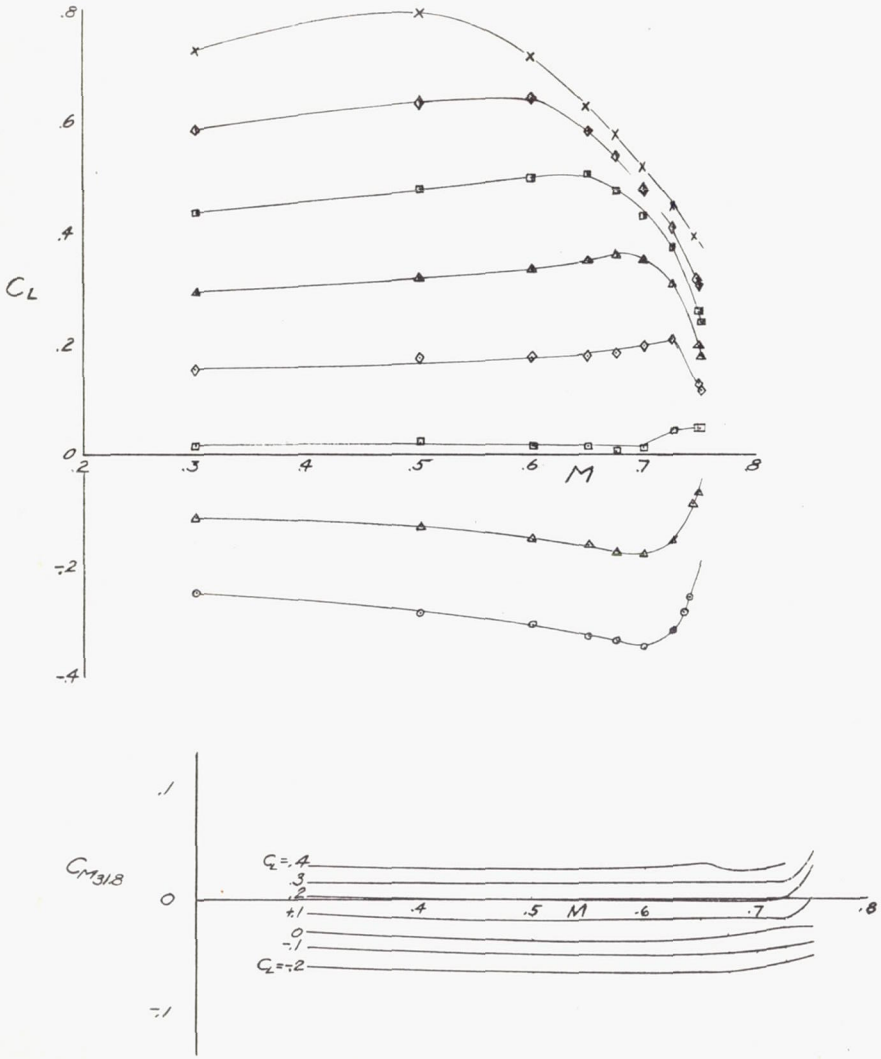

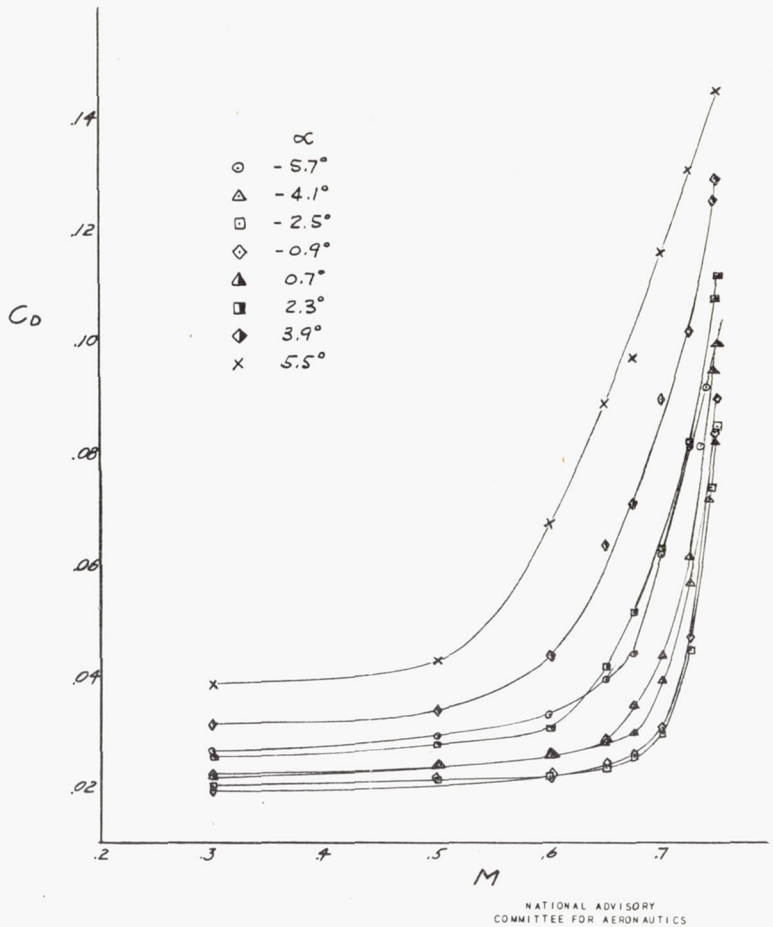

(c) Variation of C_L, C_D, and C_M with Mach number.

Figure 9.- Concluded.

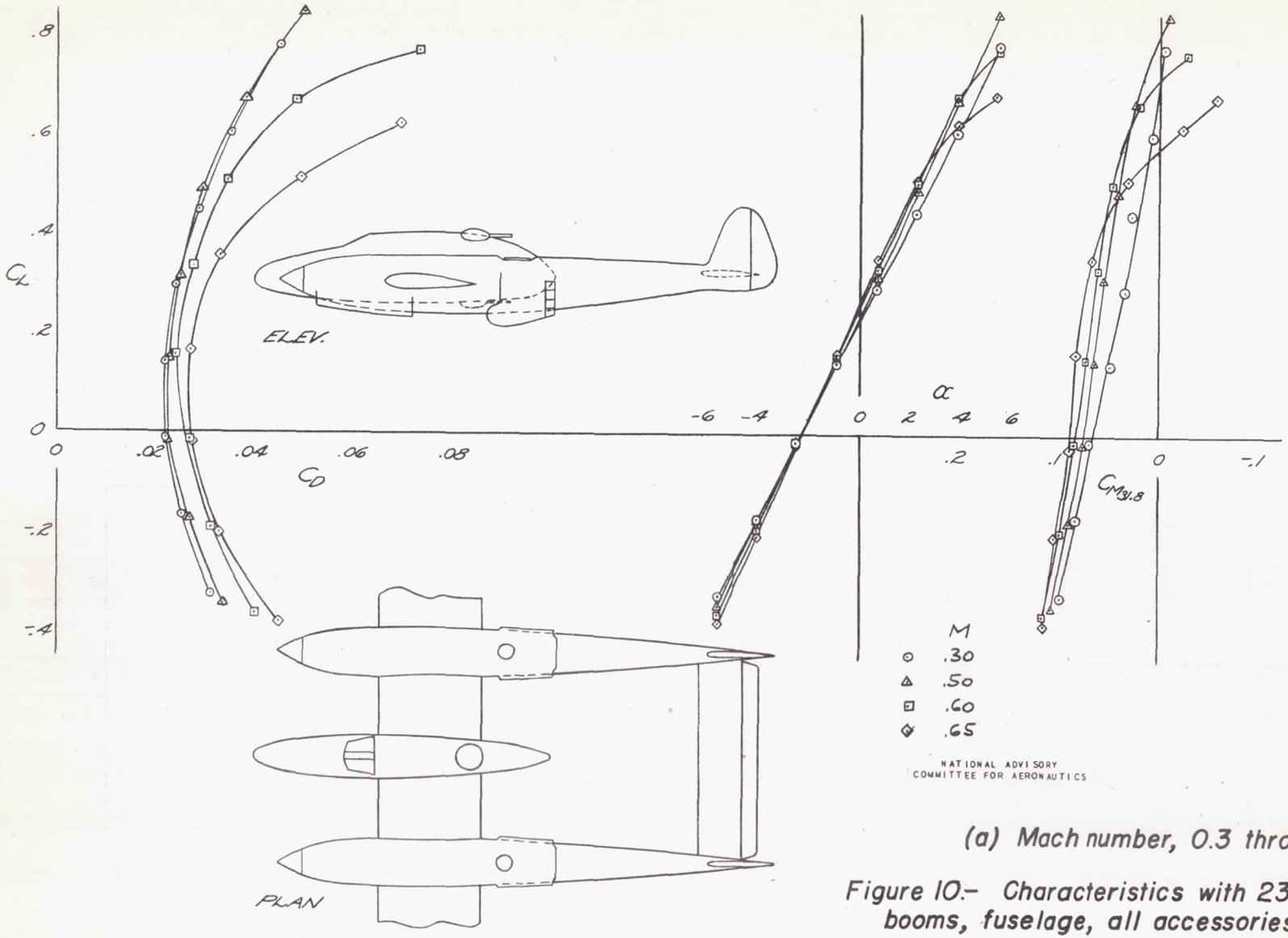

(a) Mach number, 0.3 through 0.65.

Figure 10.- Characteristics with 230 wing, large booms, fuselage, all accessories, tail.

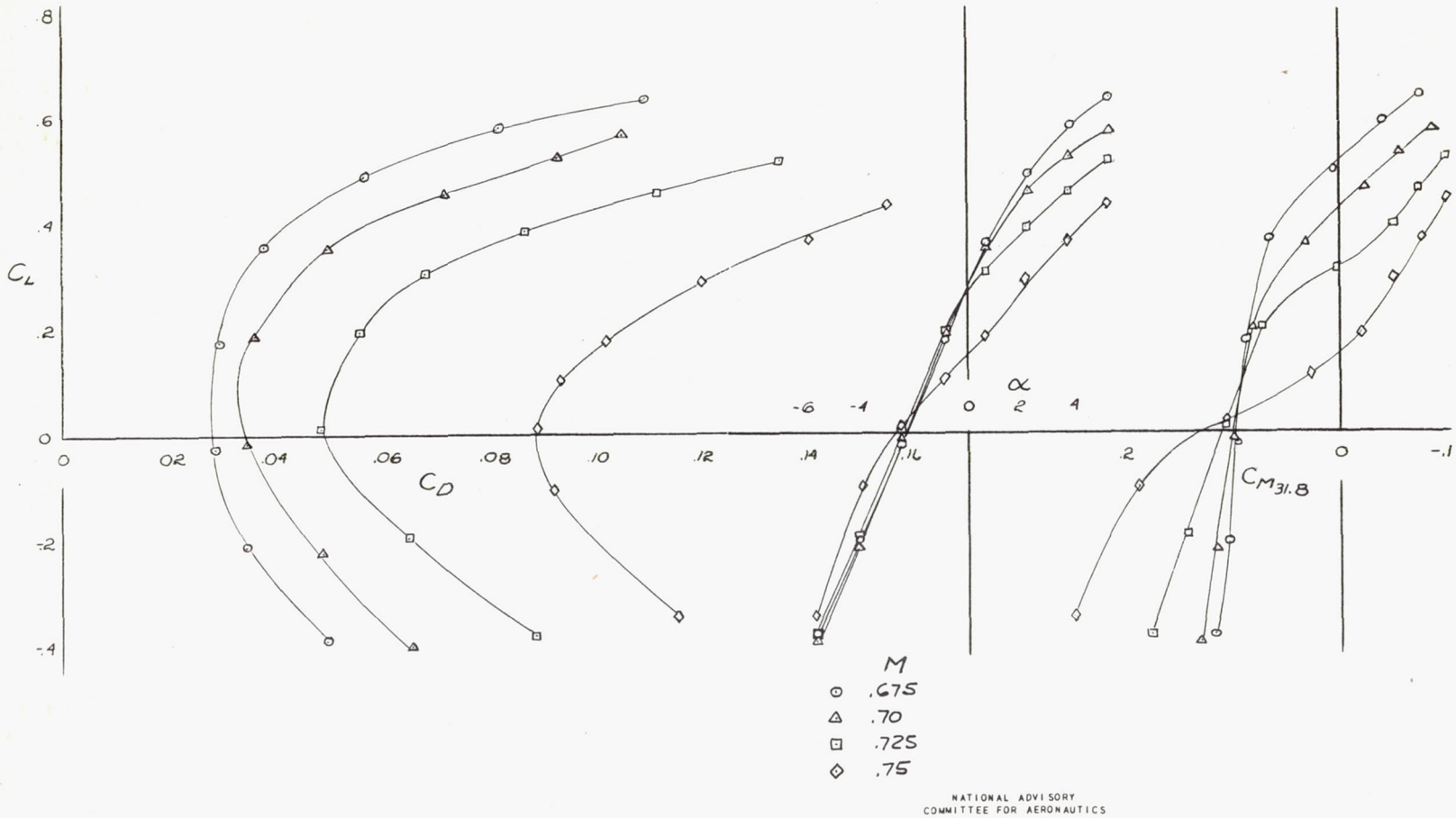

(b) Mach number, 0.675 through 0.75.

Figure 10.– Continued.

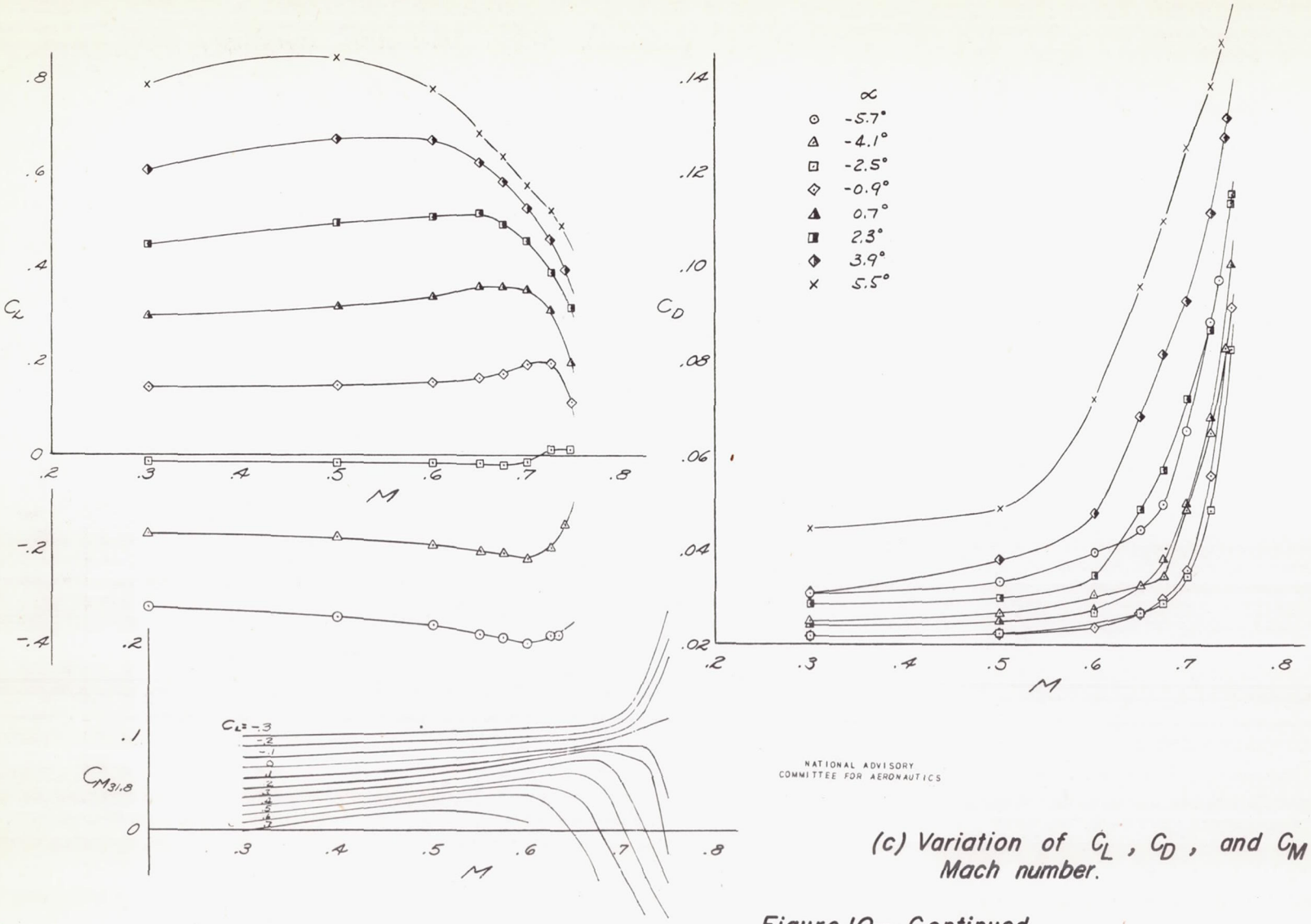

(c) Variation of C_L, C_D, and C_M with Mach number.

Figure 10.- Continued.

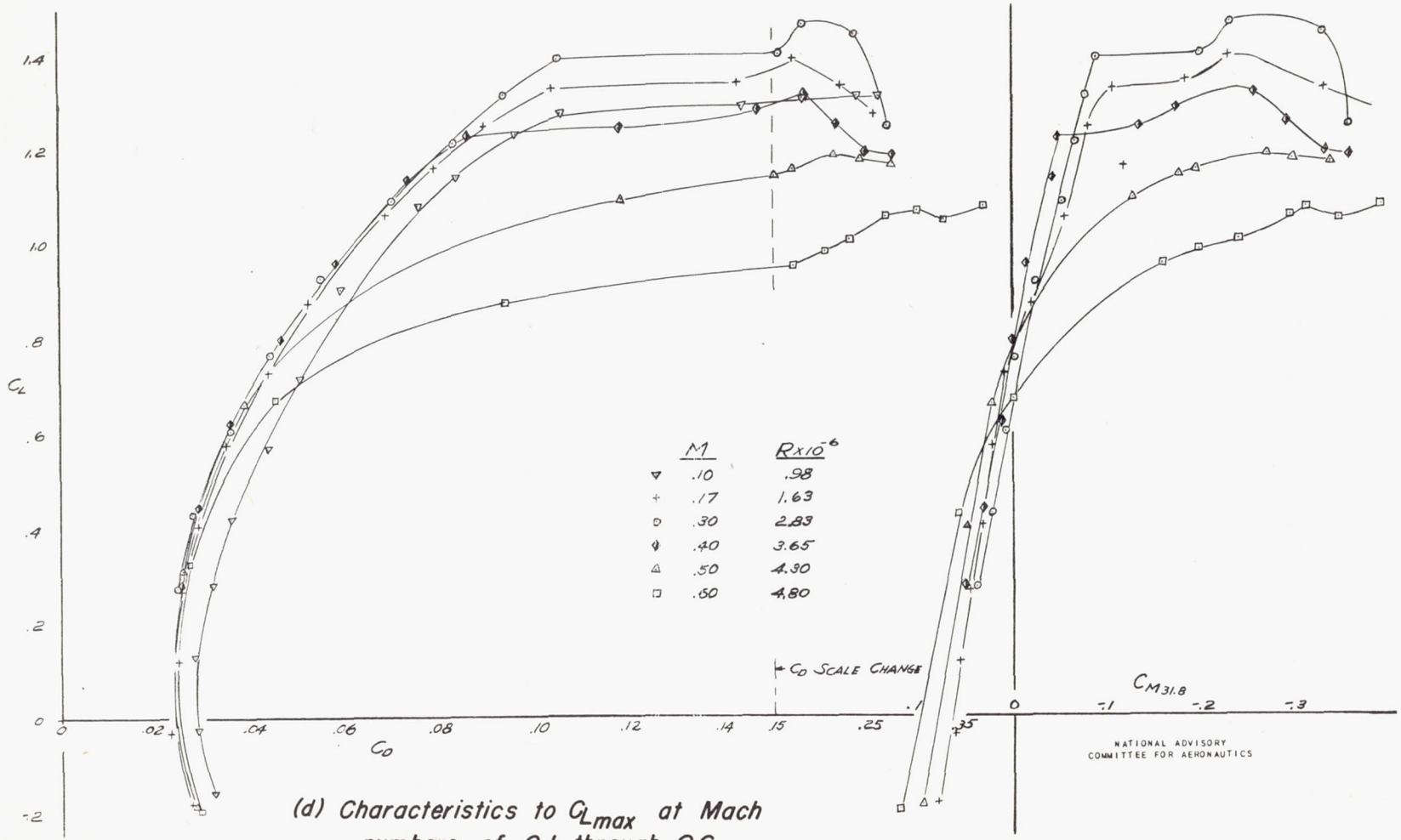

(d) Characteristics to $C_{L_{max}}$ at Mach numbers of 0.1 through 0.6.

Figure 10.– Continued.

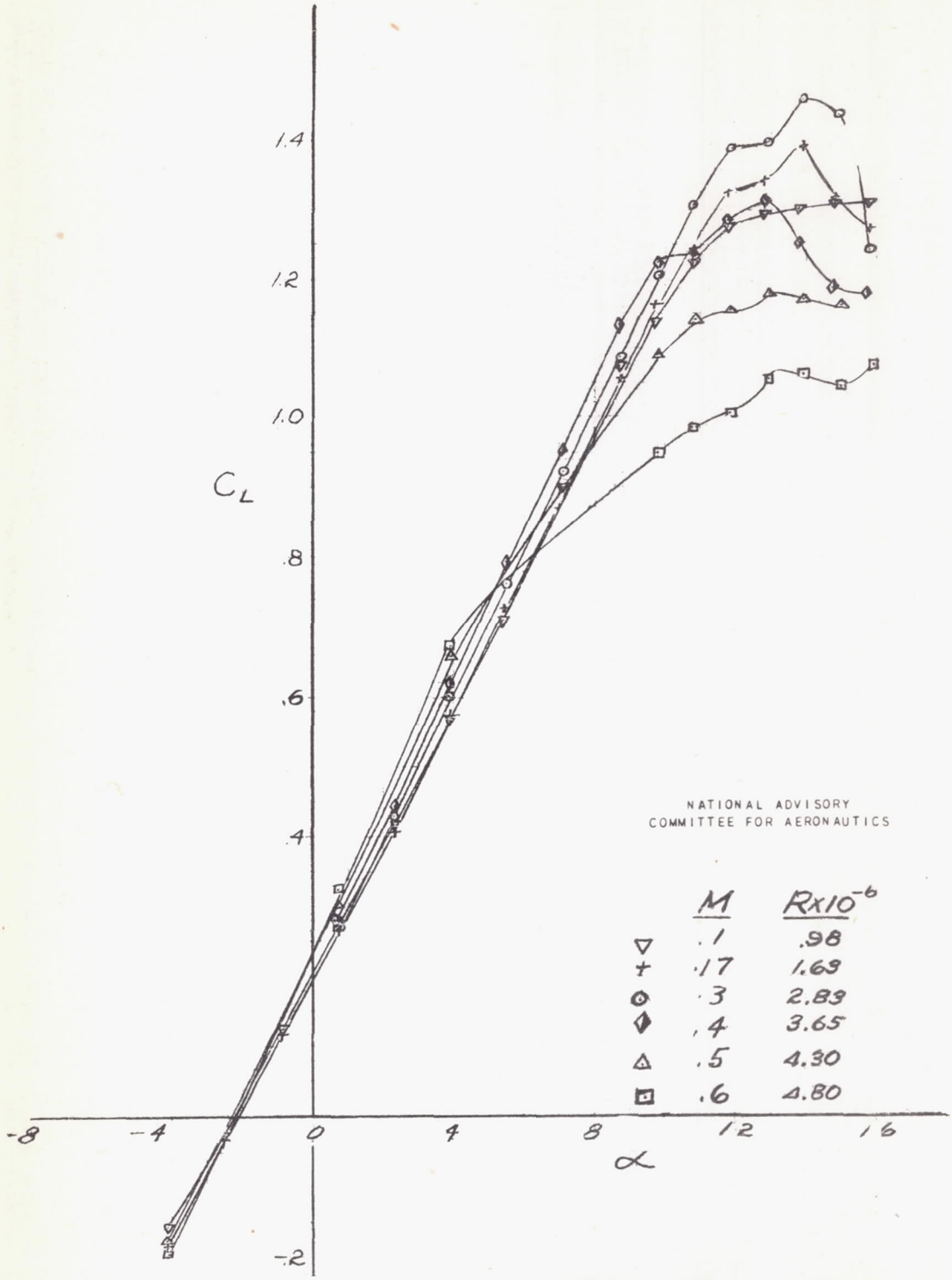

(e) Variations of C_L with angle of attack at Mach numbers of 0.1 through 0.6.

Figure 10.- Concluded.

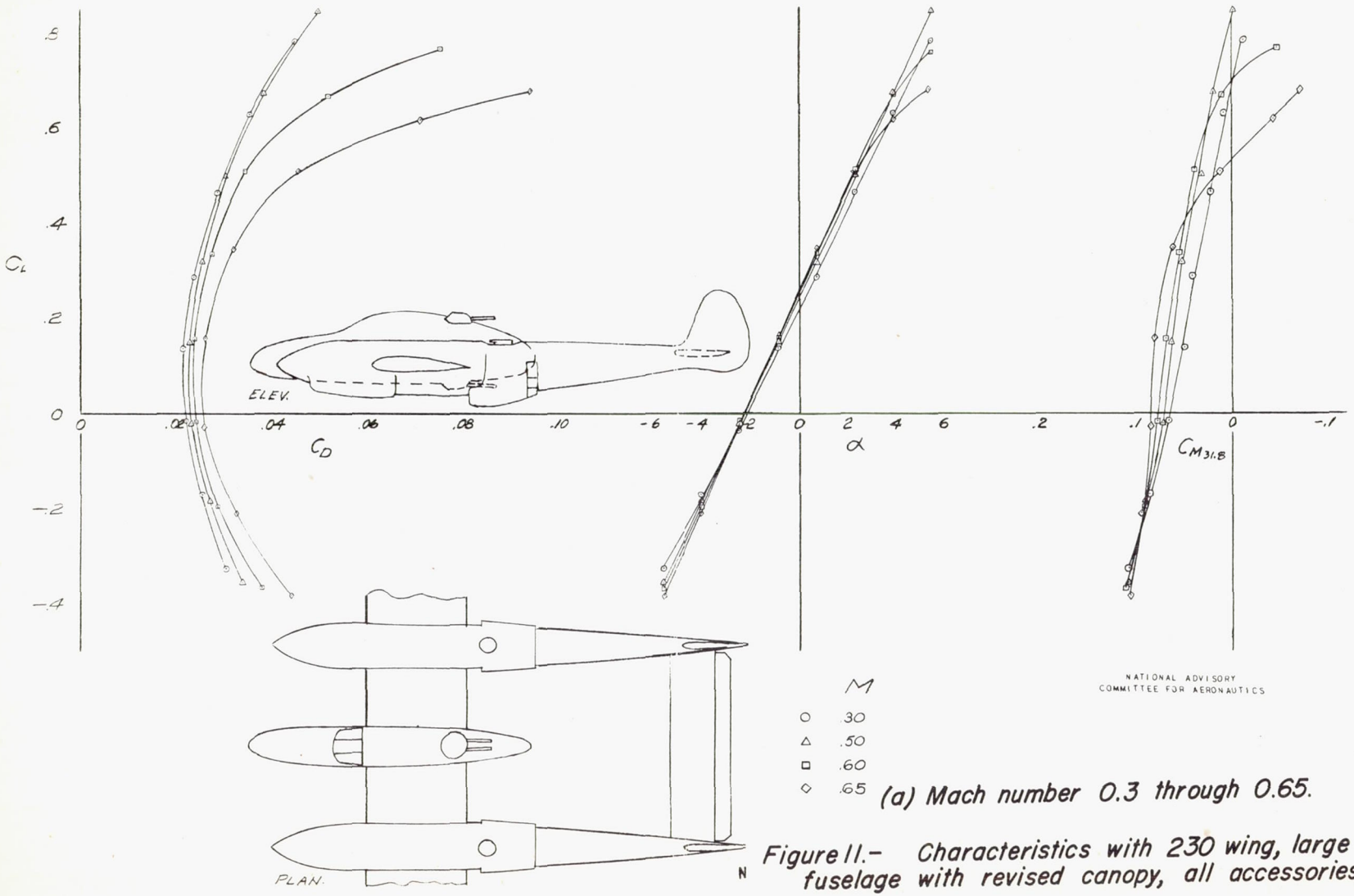

(a) Mach number 0.3 through 0.65.

Figure 11.- Characteristics with 230 wing, large booms, fuselage with revised canopy, all accessories, tail.

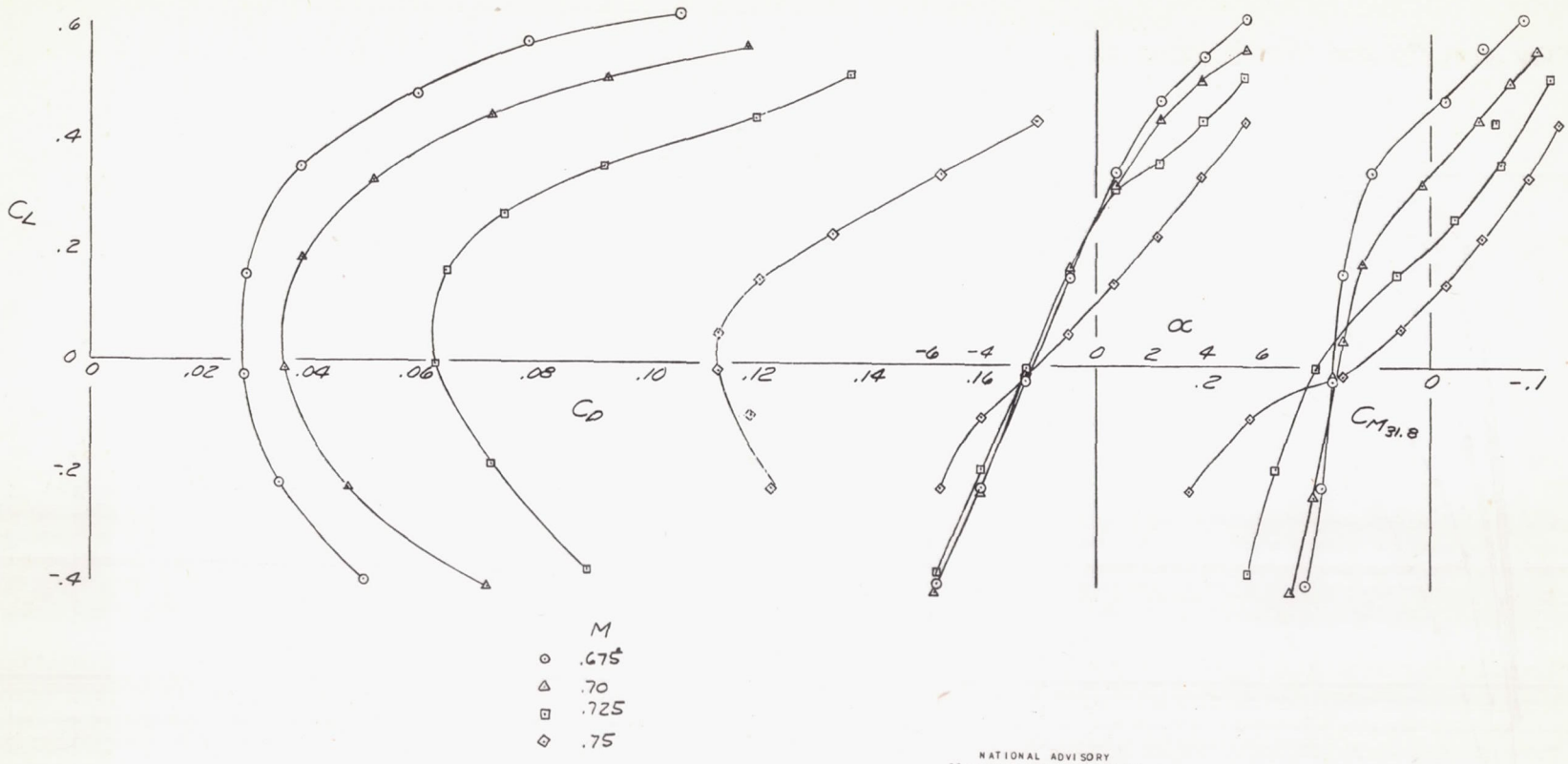

NATIONAL ADVISORY
COMMITTEE FOR AERONAUTICS

(b) Mach number 0.675 through 0.75.

Figure 11.- Continued.

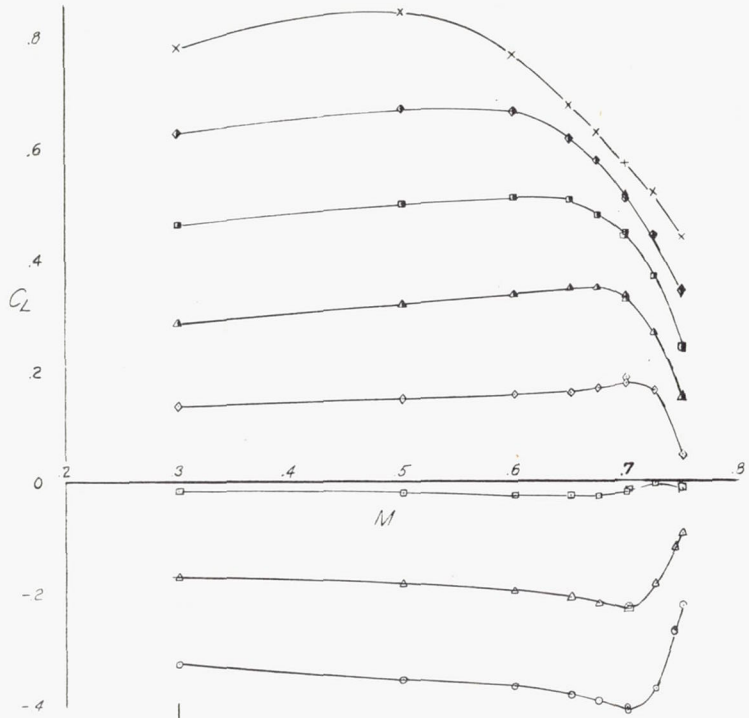

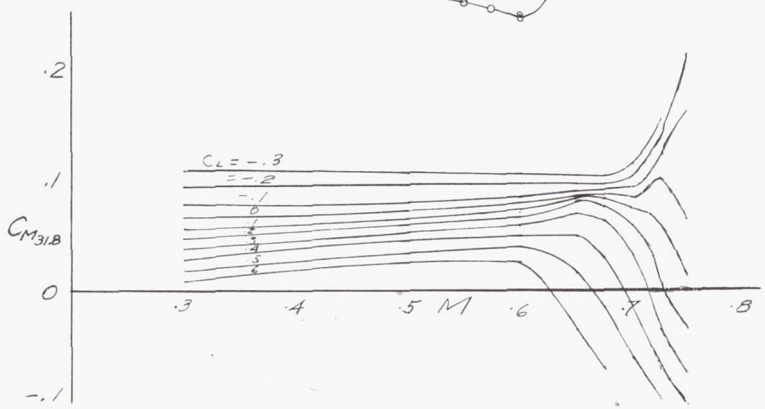

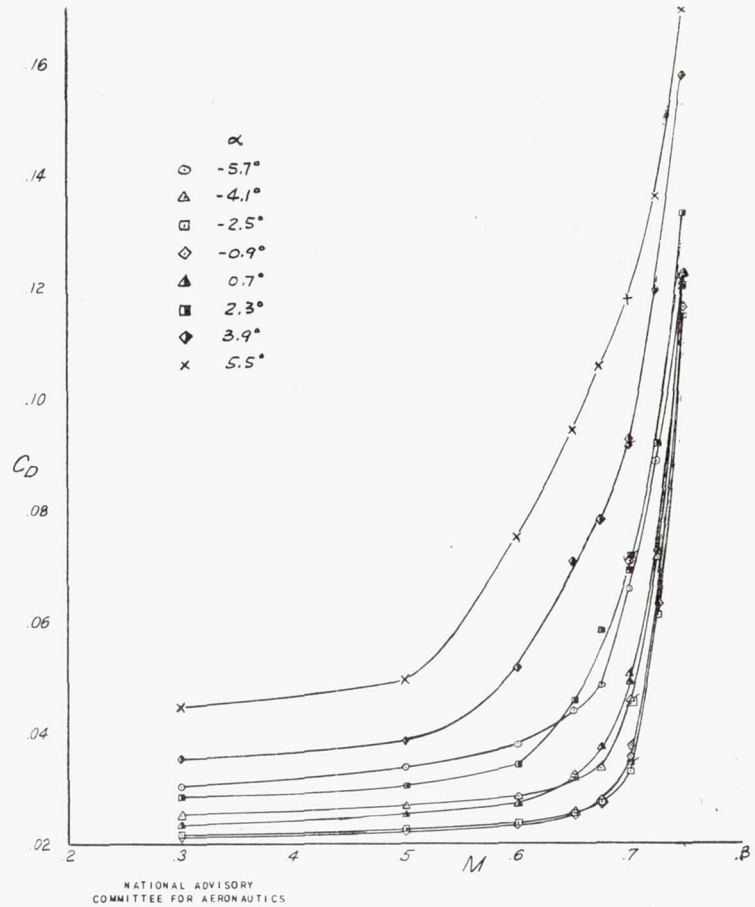

(c) Variation of C_L, C_D, and C_M with Mach number.

Figure 11.– Concluded.

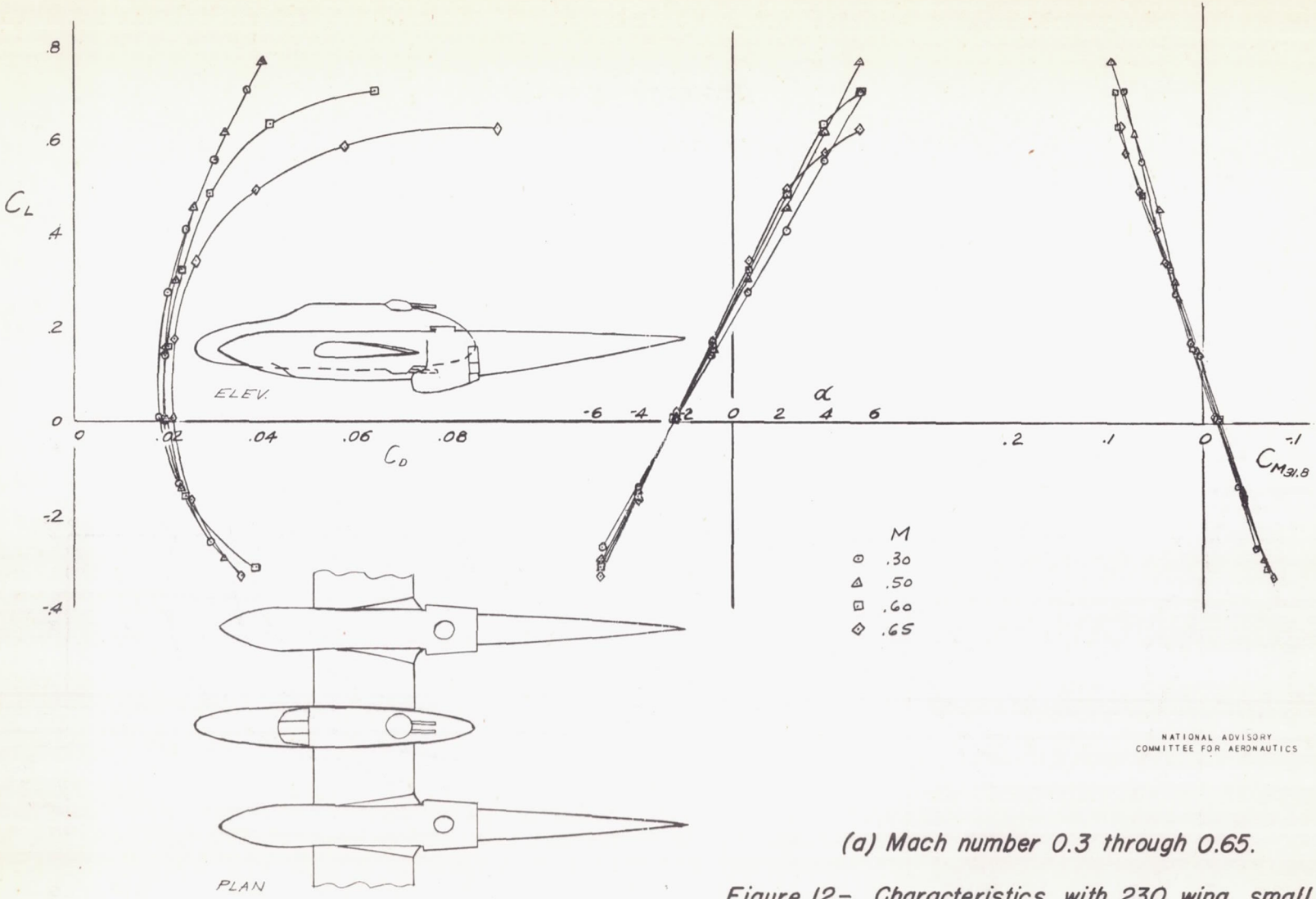

NATIONAL ADVISORY
COMMITTEE FOR AERONAUTICS

(a) Mach number 0.3 through 0.65.

Figure 12.- Characteristics with 230 wing, small booms, fuselage, all accessories.

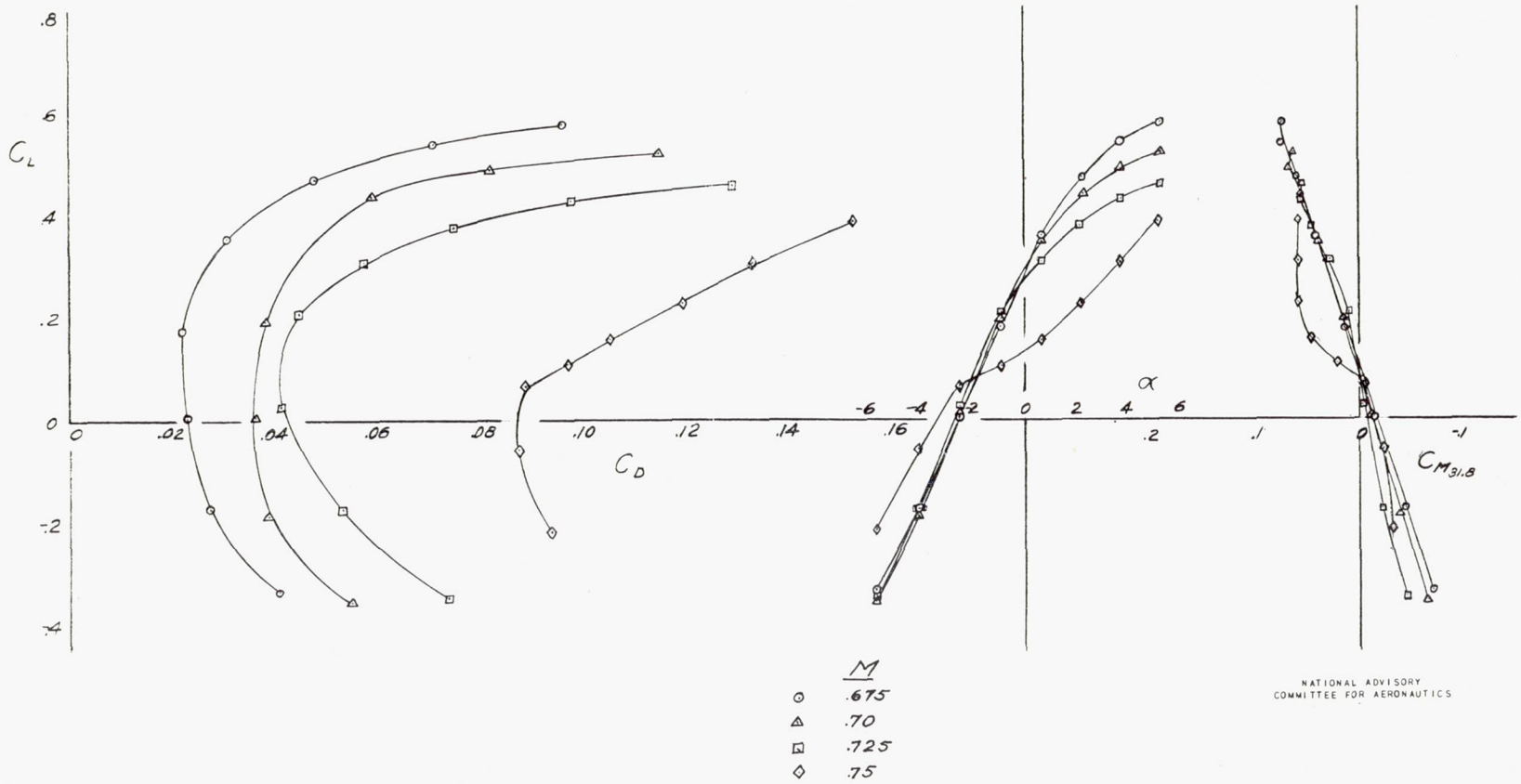

(b) Mach number 0.675 through 0.75.

Figure 12.- Continued.

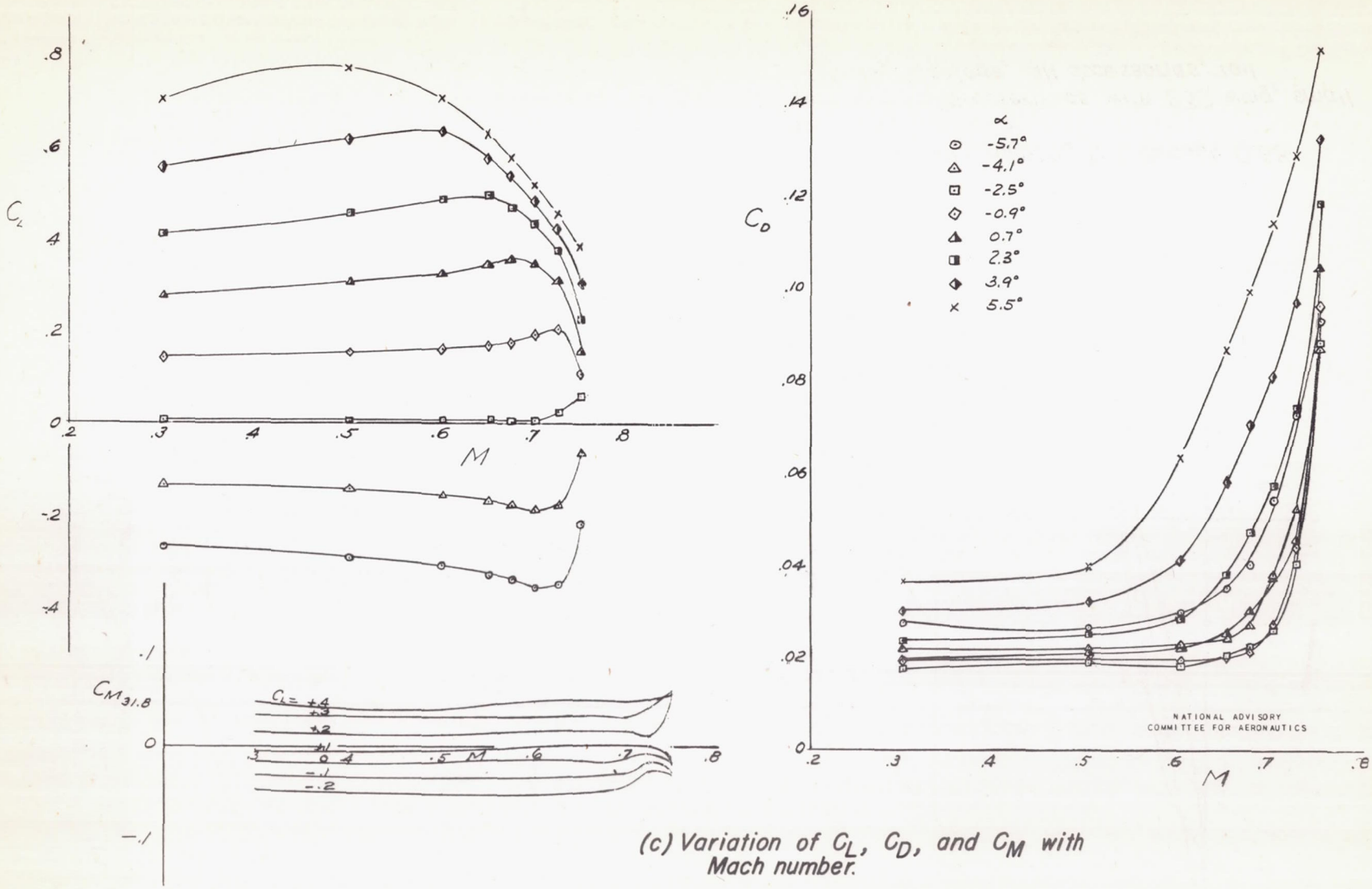

(c) Variation of C_L, C_D, and C_M with Mach number.

Figure 12.- Concluded.

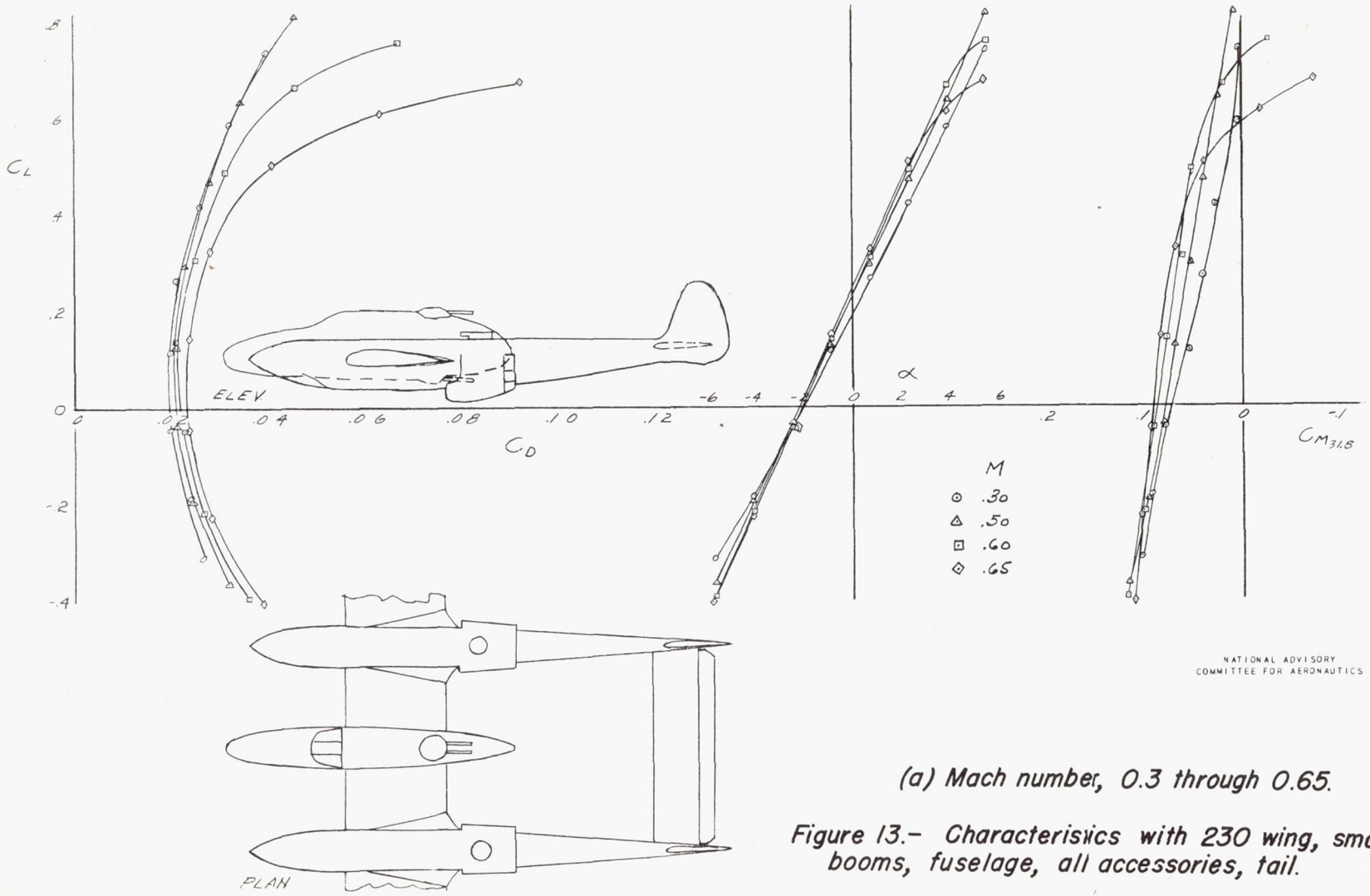

NATIONAL ADVISORY
COMMITTEE FOR AERONAUTICS

(a) Mach number, 0.3 through 0.65.

Figure 13.- Characteristics with 230 wing, small booms, fuselage, all accessories, tail.

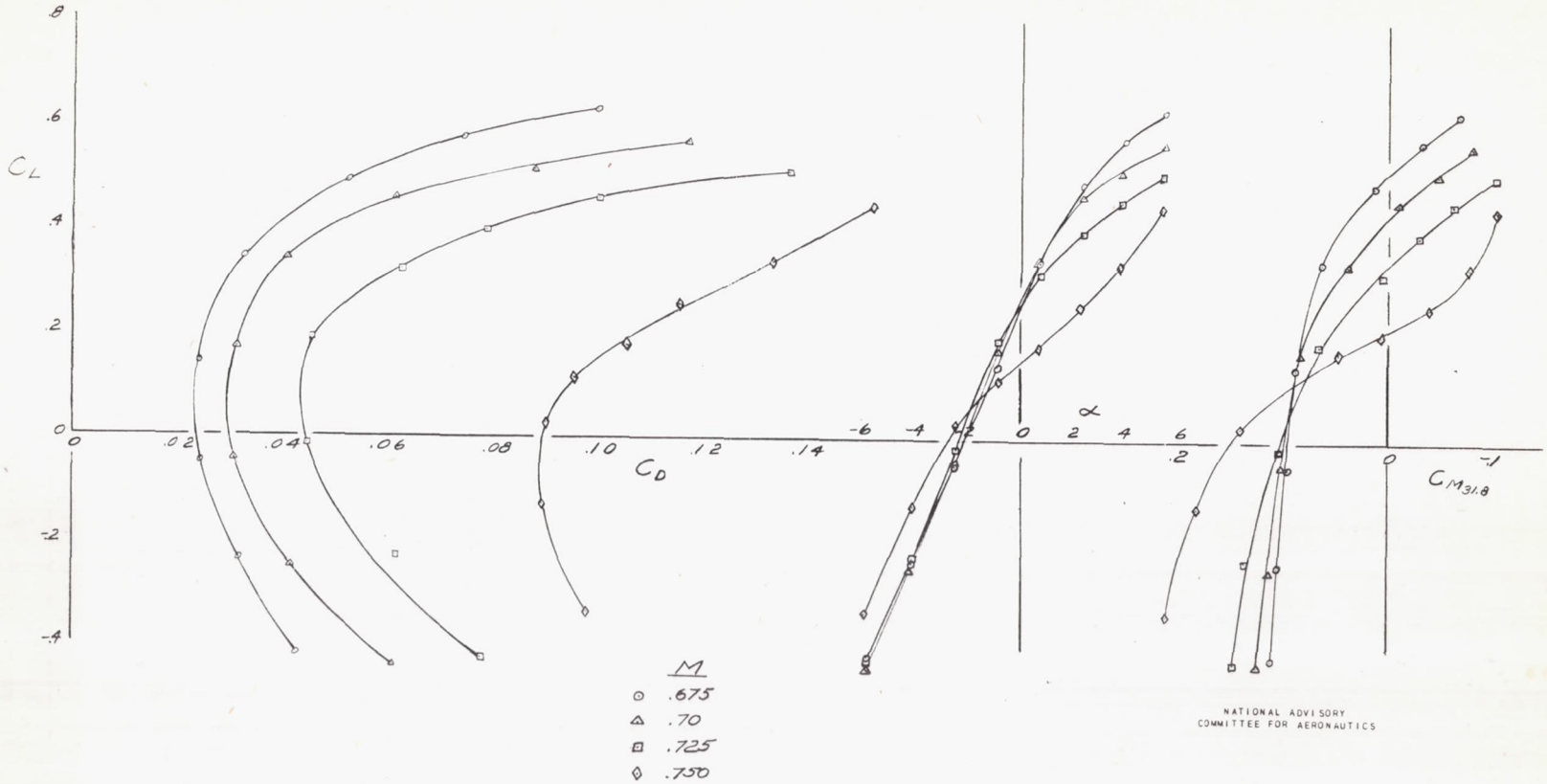

(b) Mach number 0.675 through 0.75.

Figure 13.– Continued.

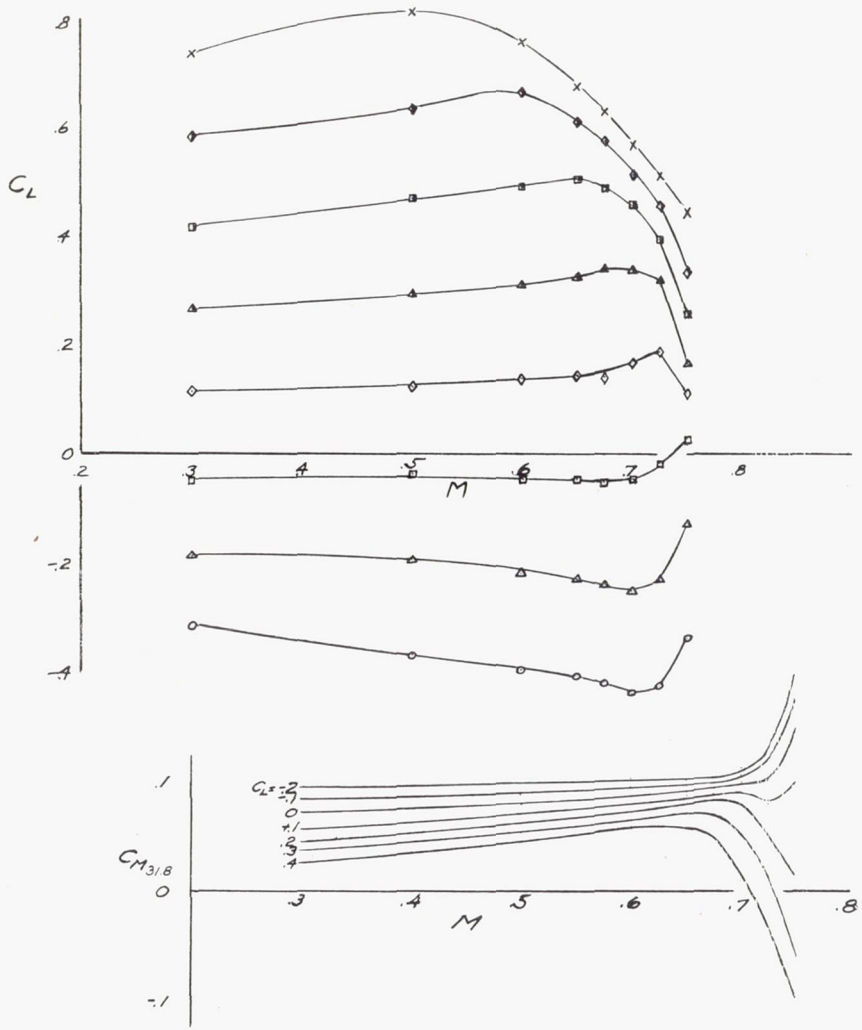

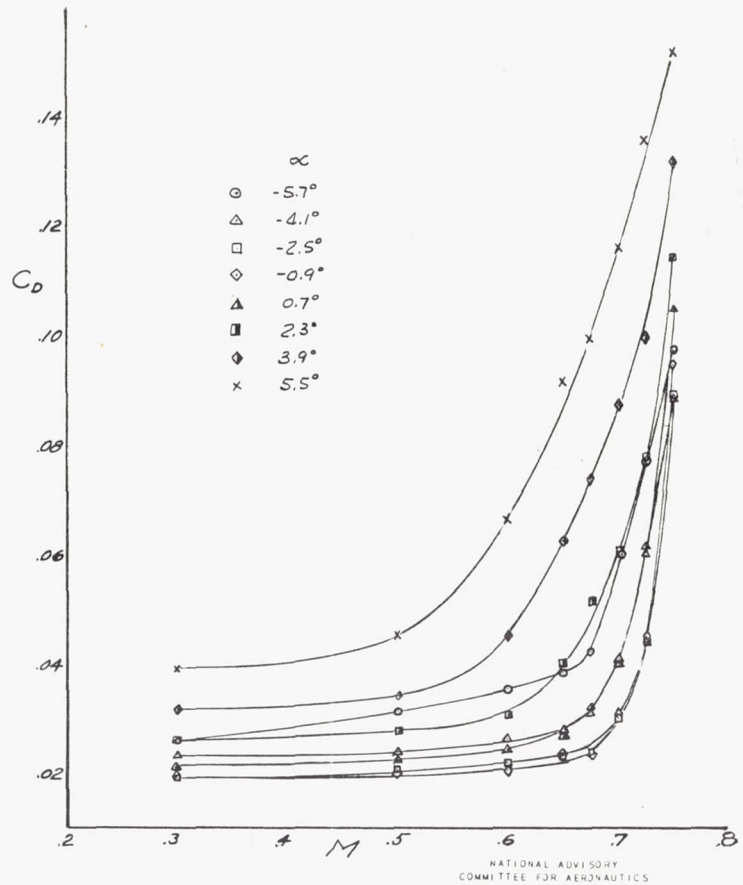

(c) Variation of C_L, C_D, and C_M with Mach number.

Figure 13.- Concluded.

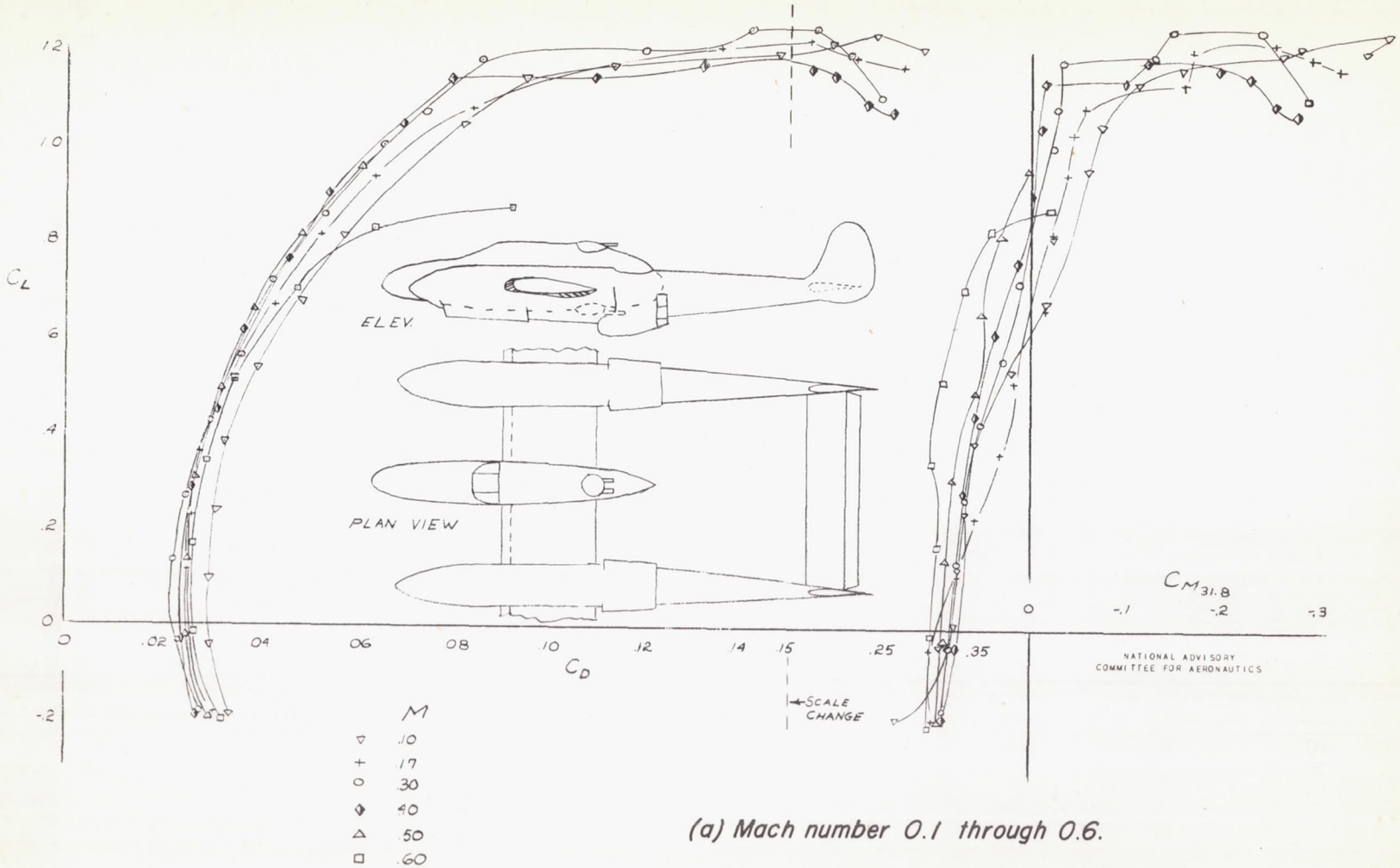

(a) Mach number 0.1 through 0.6.

Figure 14.- Characteristics with modified 230 wing, large booms, fuselage, all accessories, tail.

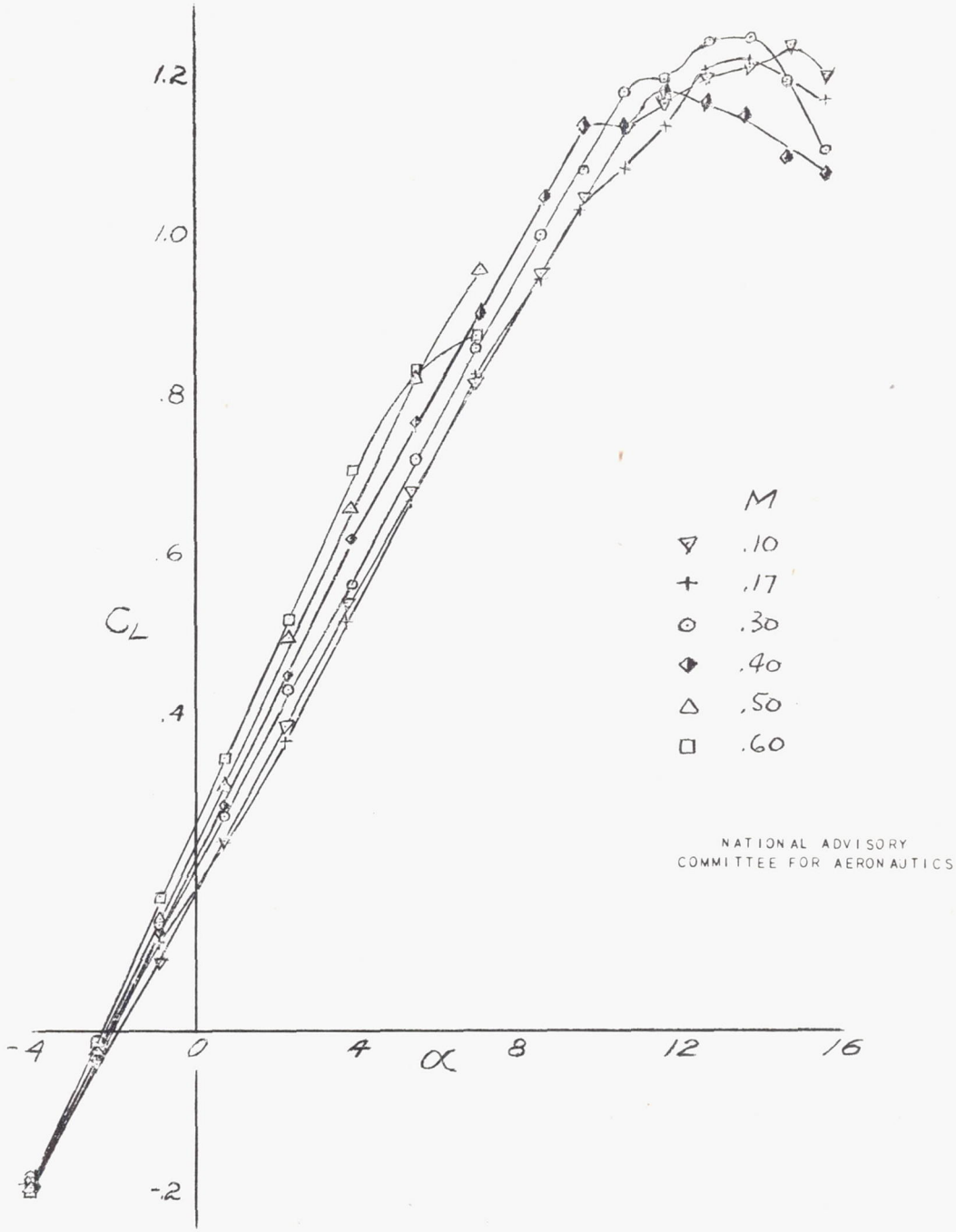

(b) Variation of C_L with angle of attack at Mach numbers of 0.1 through 0.6.

Figure 14.- Continued.

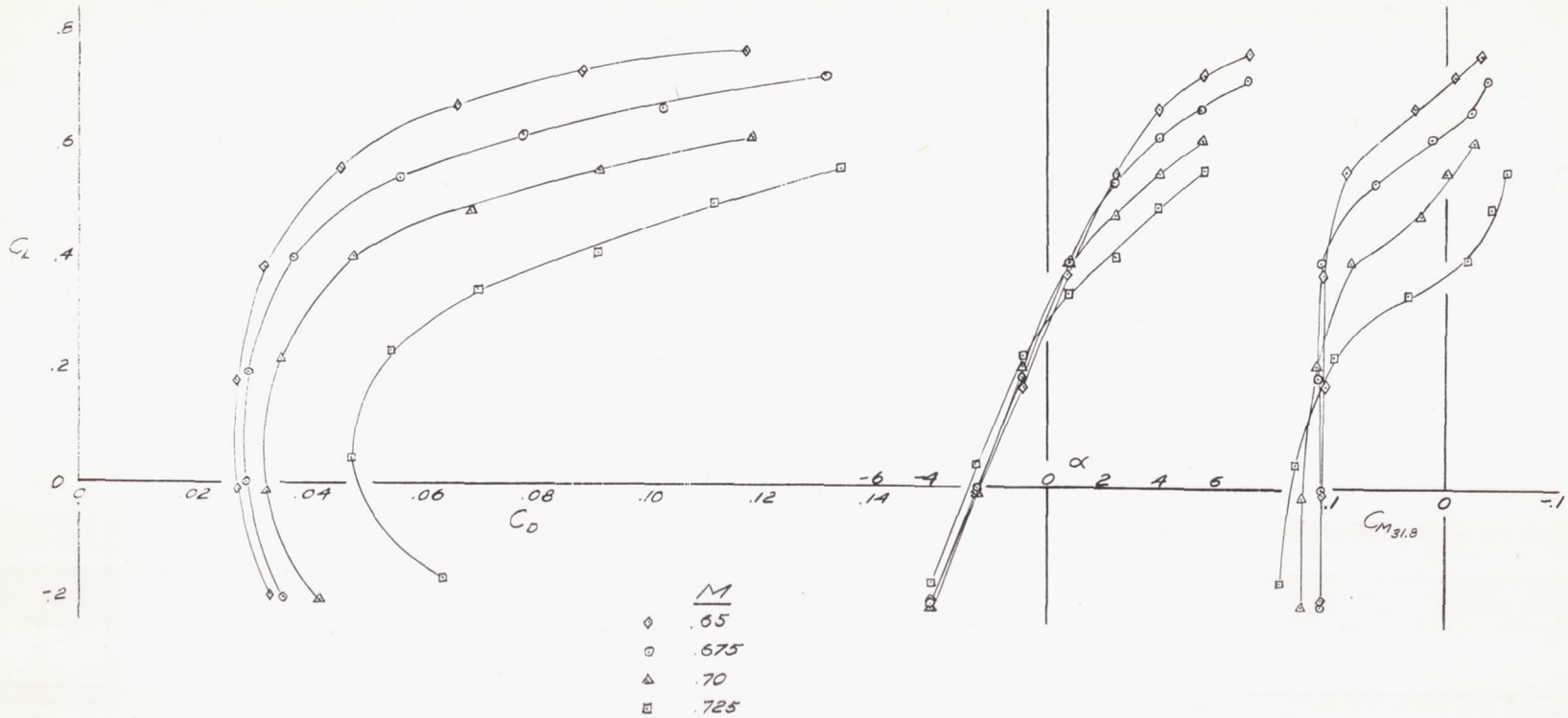

NATIONAL ADVISORY
COMMITTEE FOR AERONAUTICS

(c) Mach number 0.65 through 0.725.

Figure 14.- Continued.

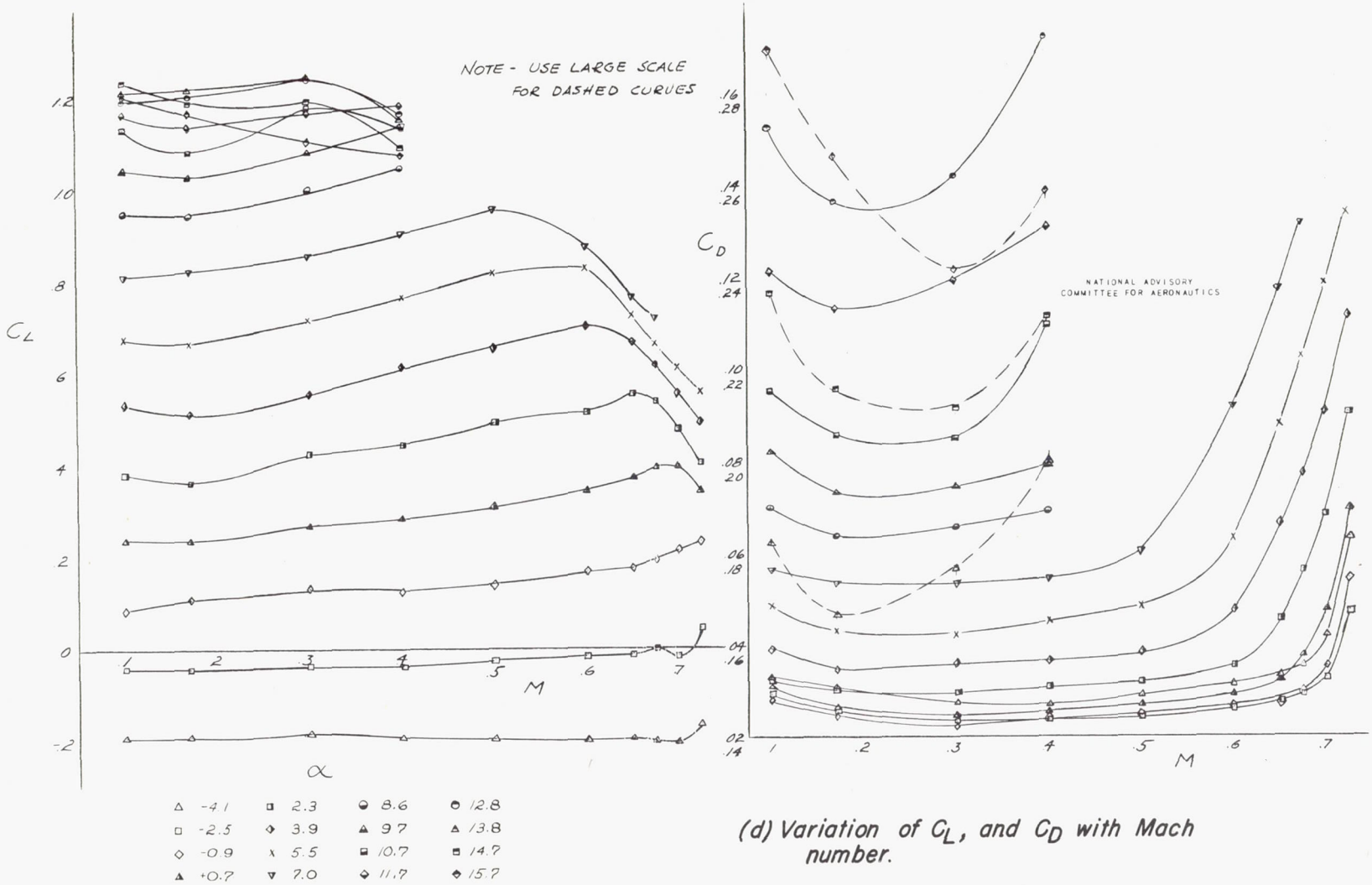

(d) Variation of C_L, and C_D with Mach number.

Figure 14.– Continued.

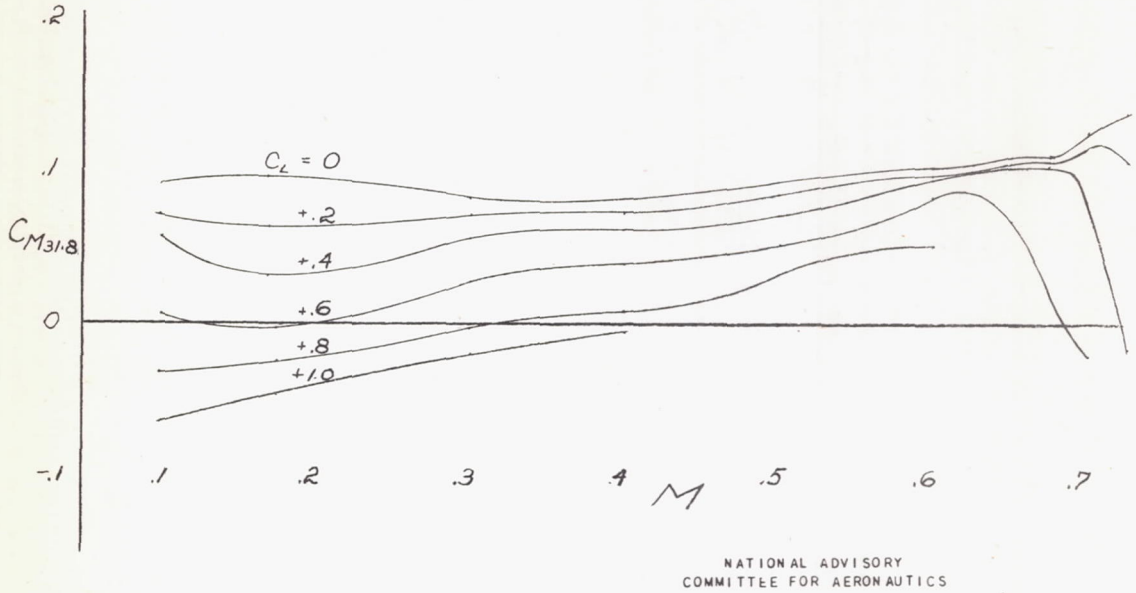

(e) Variation of C_M with Mach number.

Figure 14.- Continued.

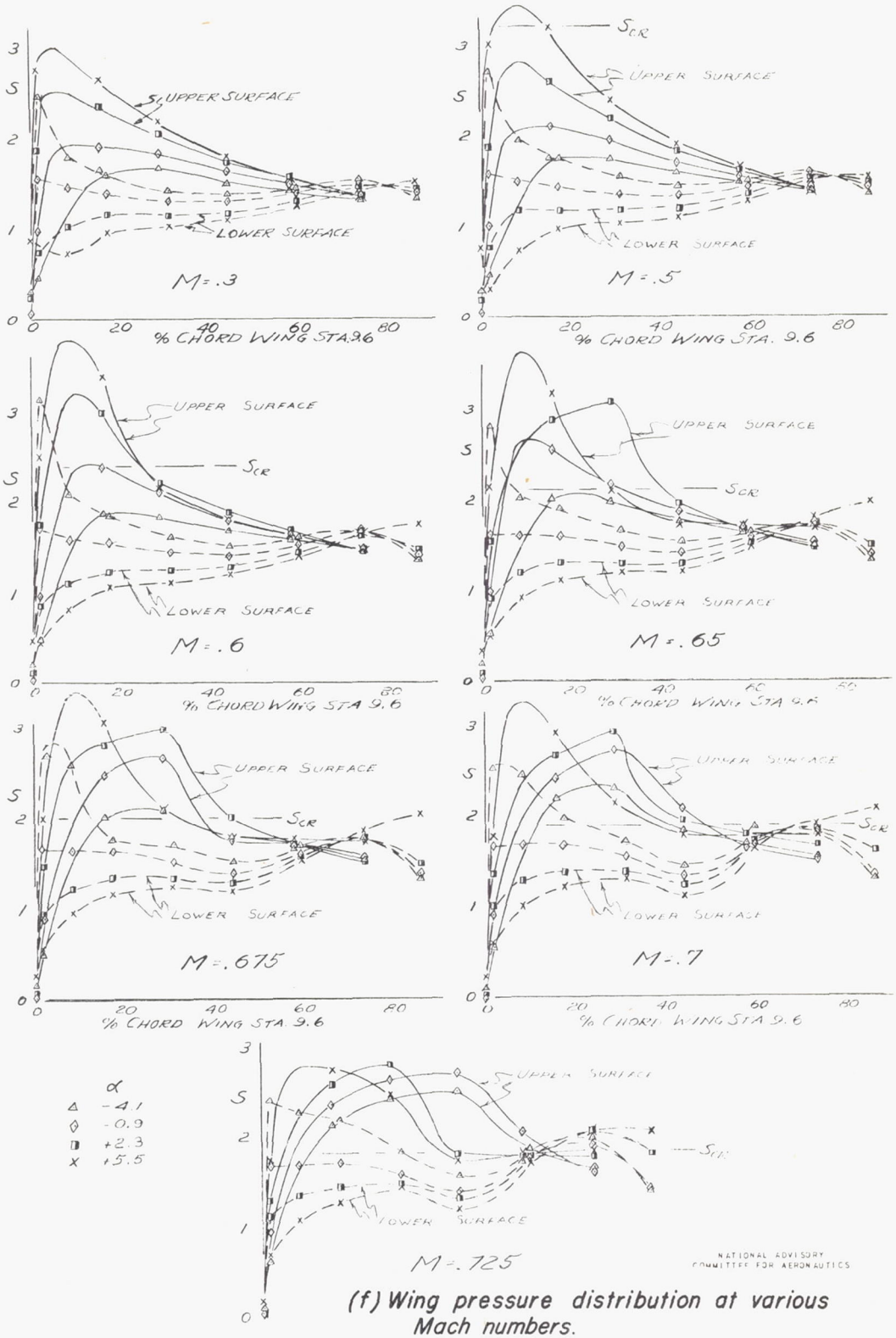

(f) Wing pressure distribution at various Mach numbers.

Figure 14.– Concluded.

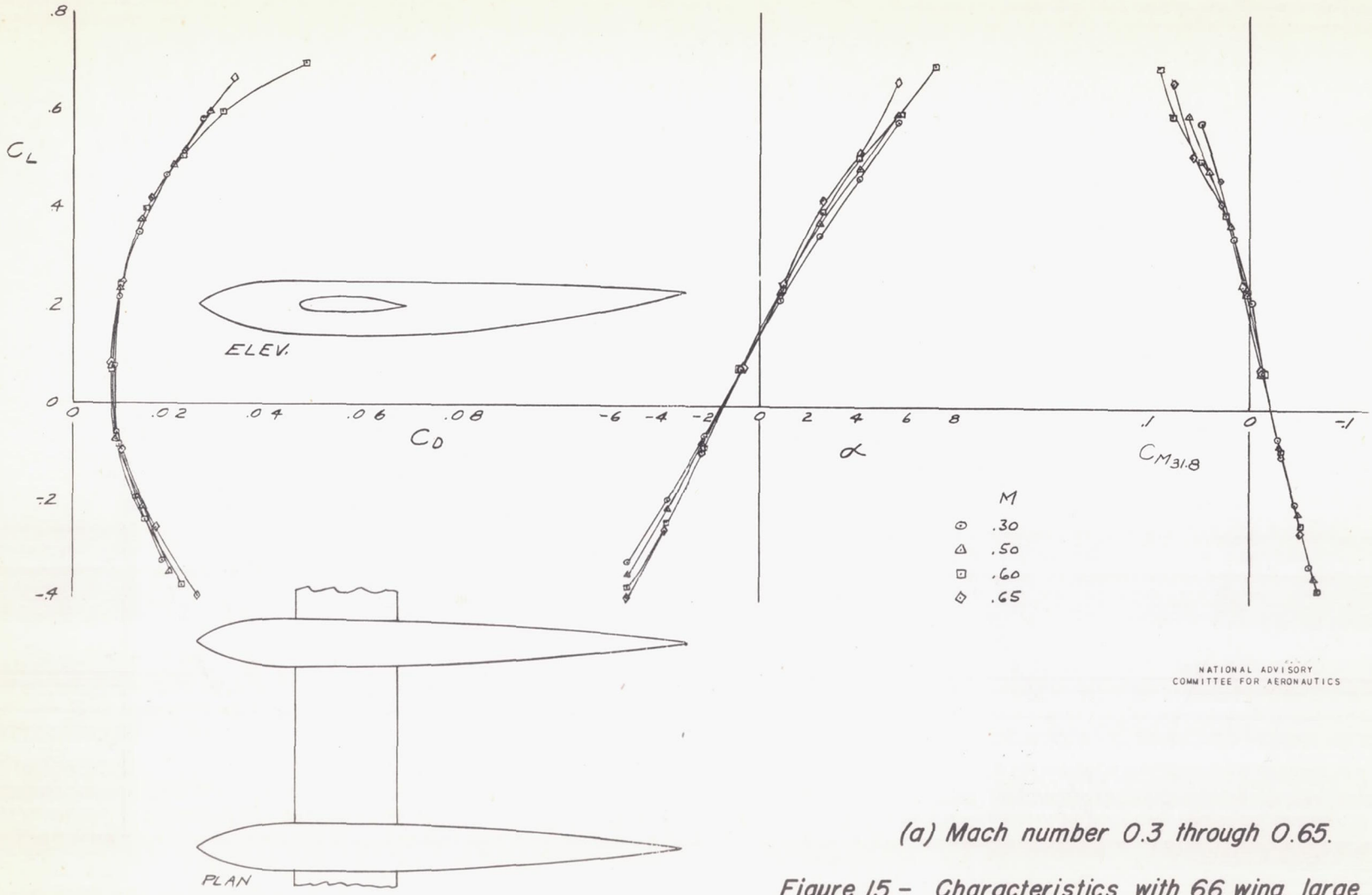

NATIONAL ADVISORY
COMMITTEE FOR AERONAUTICS

(a) Mach number 0.3 through 0.65.

Figure 15.- Characteristics with 66 wing, large booms.

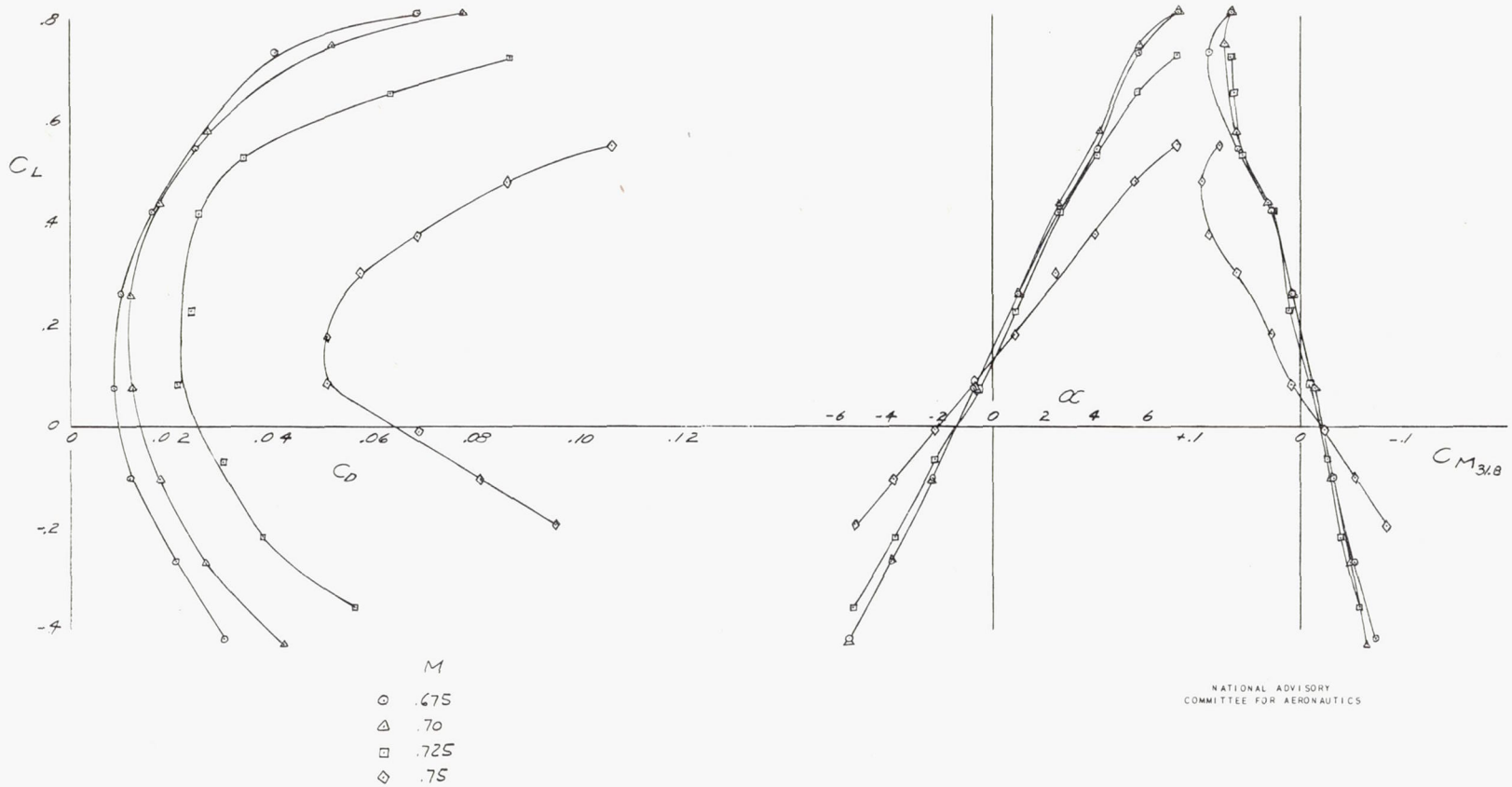

(b) Mach number 0.675 through 0.75.

Figure 15.- Continued.

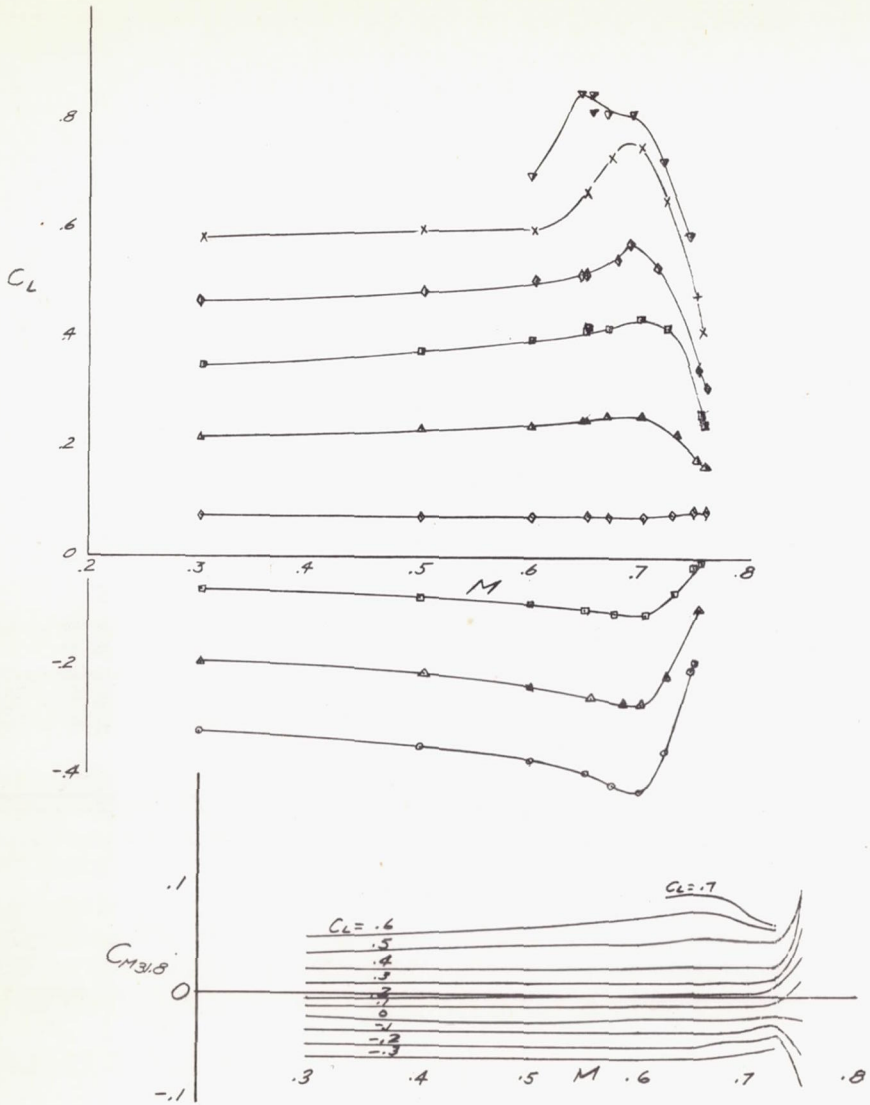

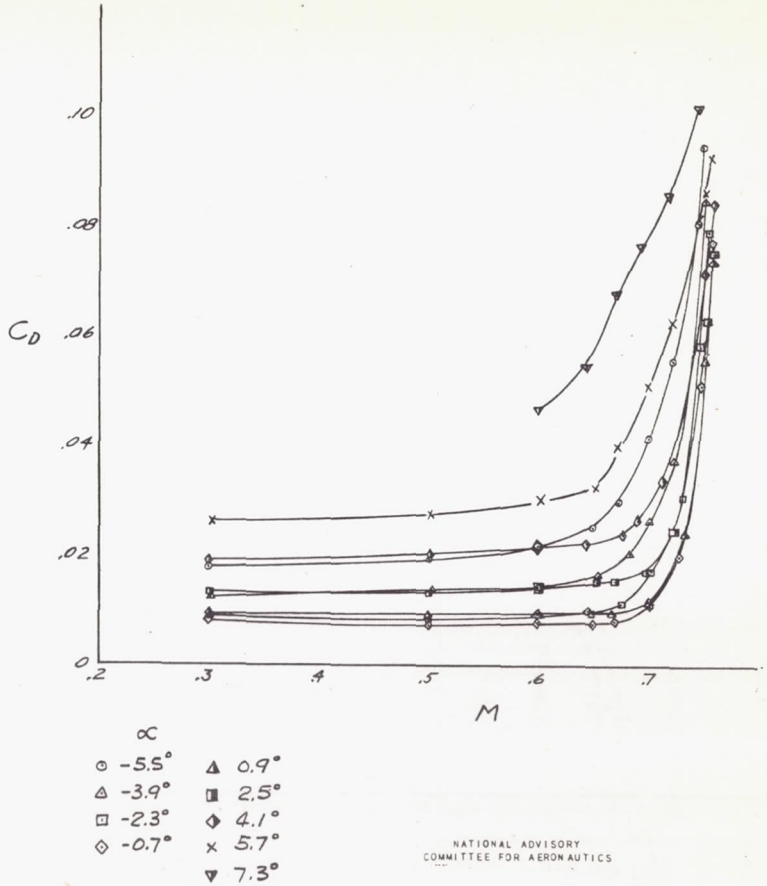

NATIONAL ADVISORY COMMITTEE FOR AERONAUTICS

(c) Variation of C_L, C_D, and C_M with Mach number.

Figure 15.- Continued.

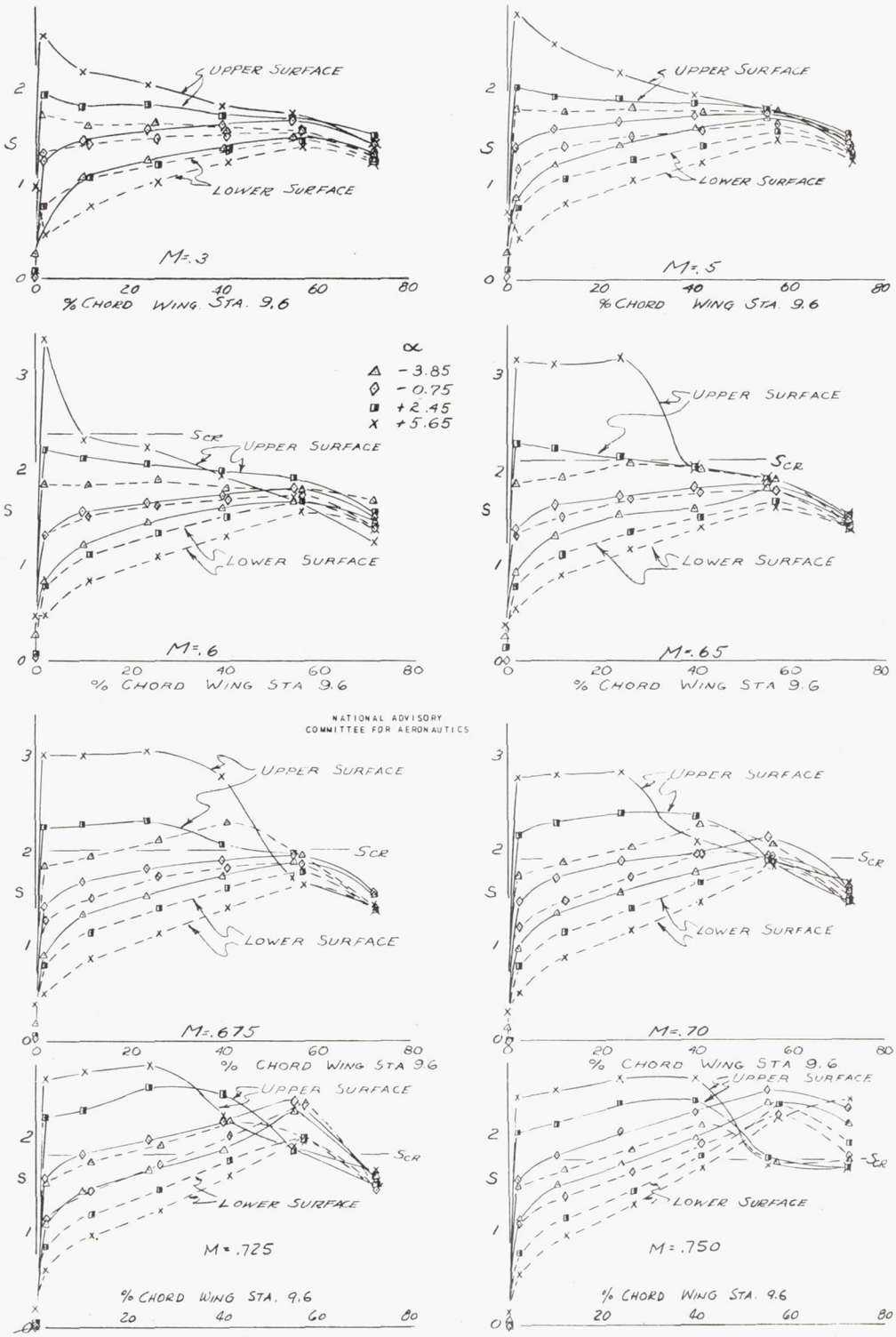

(d) Wing pressure distribution at various Mach numbers.

Figure 15.- Concluded.

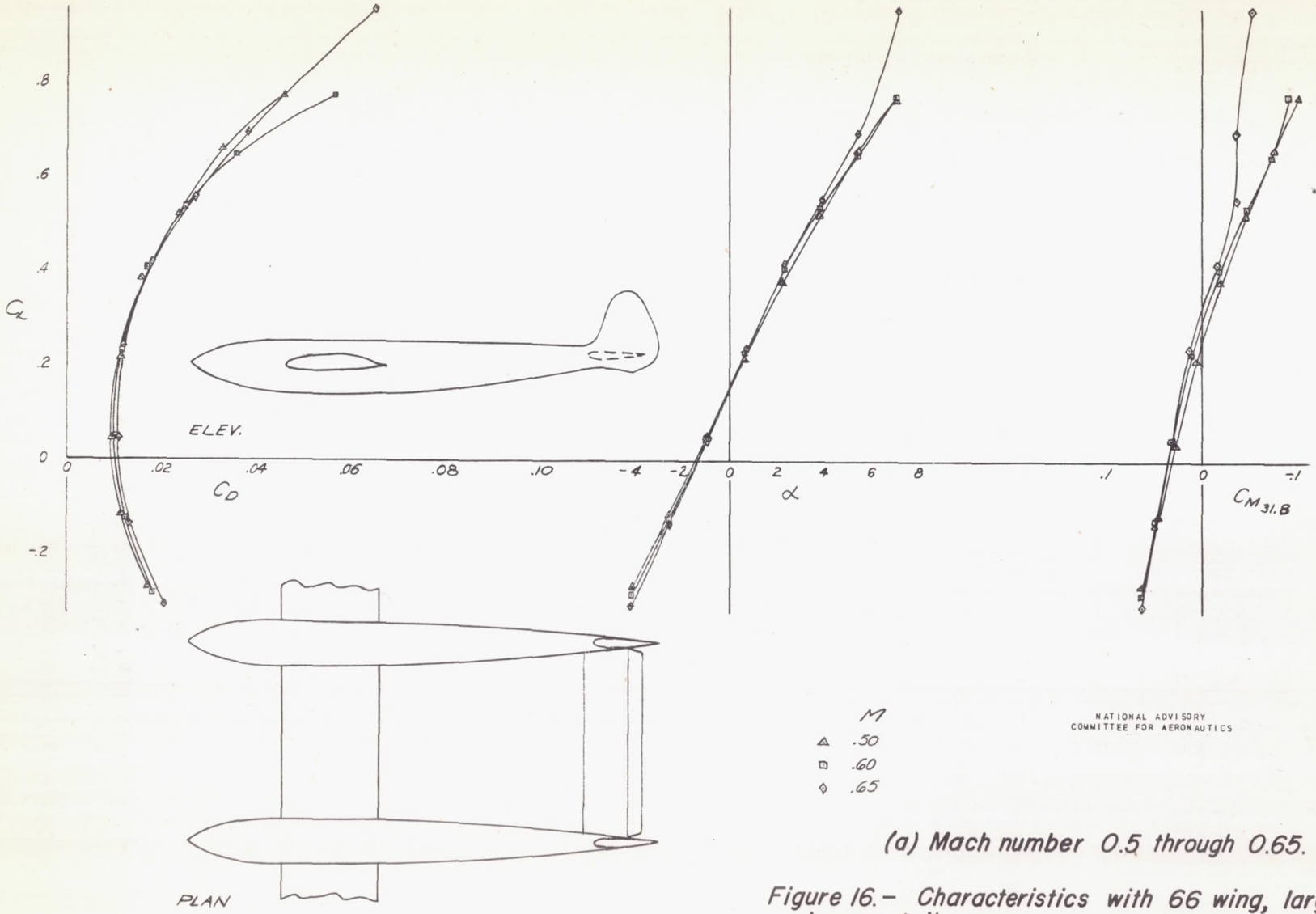

NATIONAL ADVISORY
COMMITTEE FOR AERONAUTICS

(a) Mach number 0.5 through 0.65.

Figure 16.- Characteristics with 66 wing, large booms, tail.

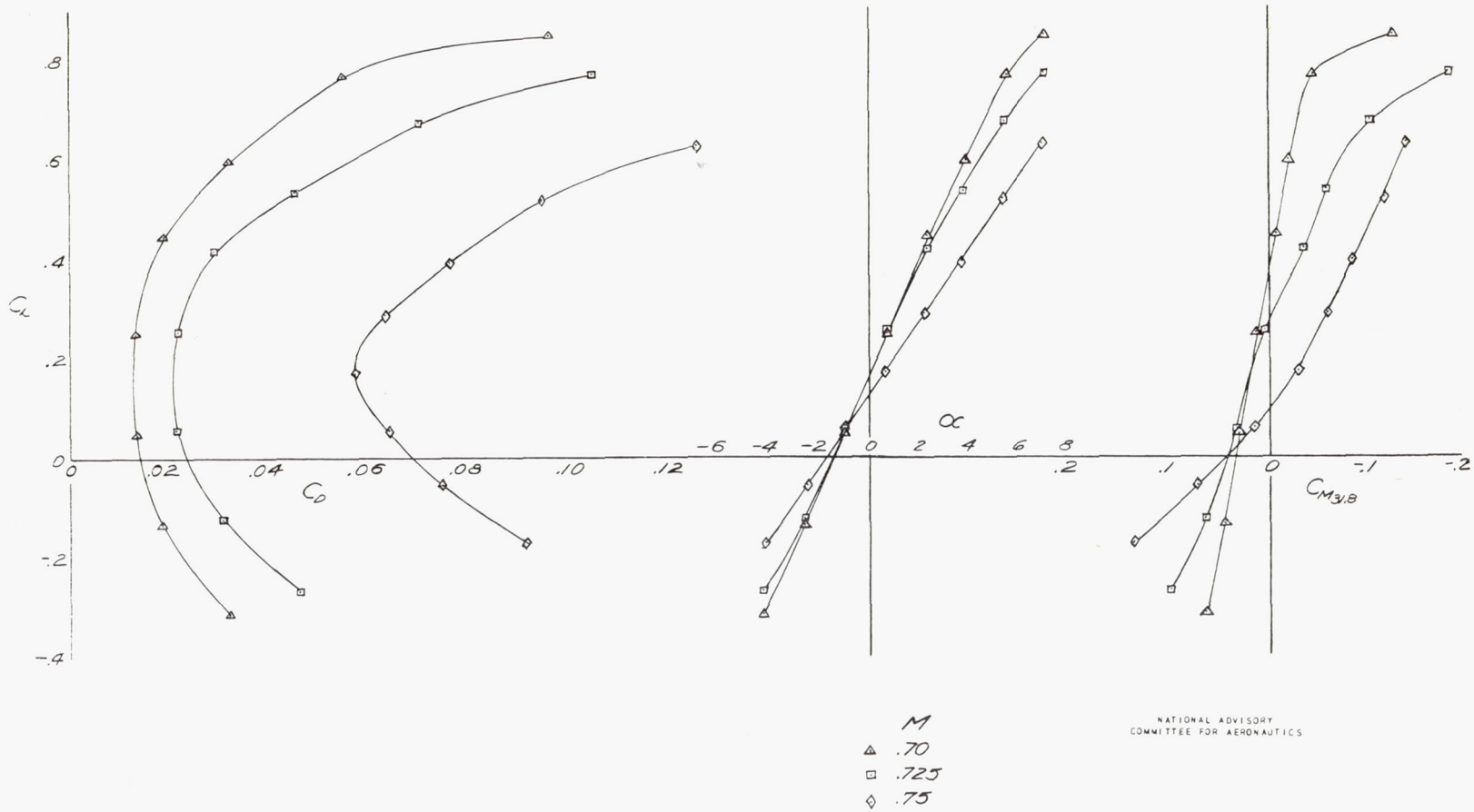

(b) Mach number 0.7 through 0.75.

Figure 16.- Continued.

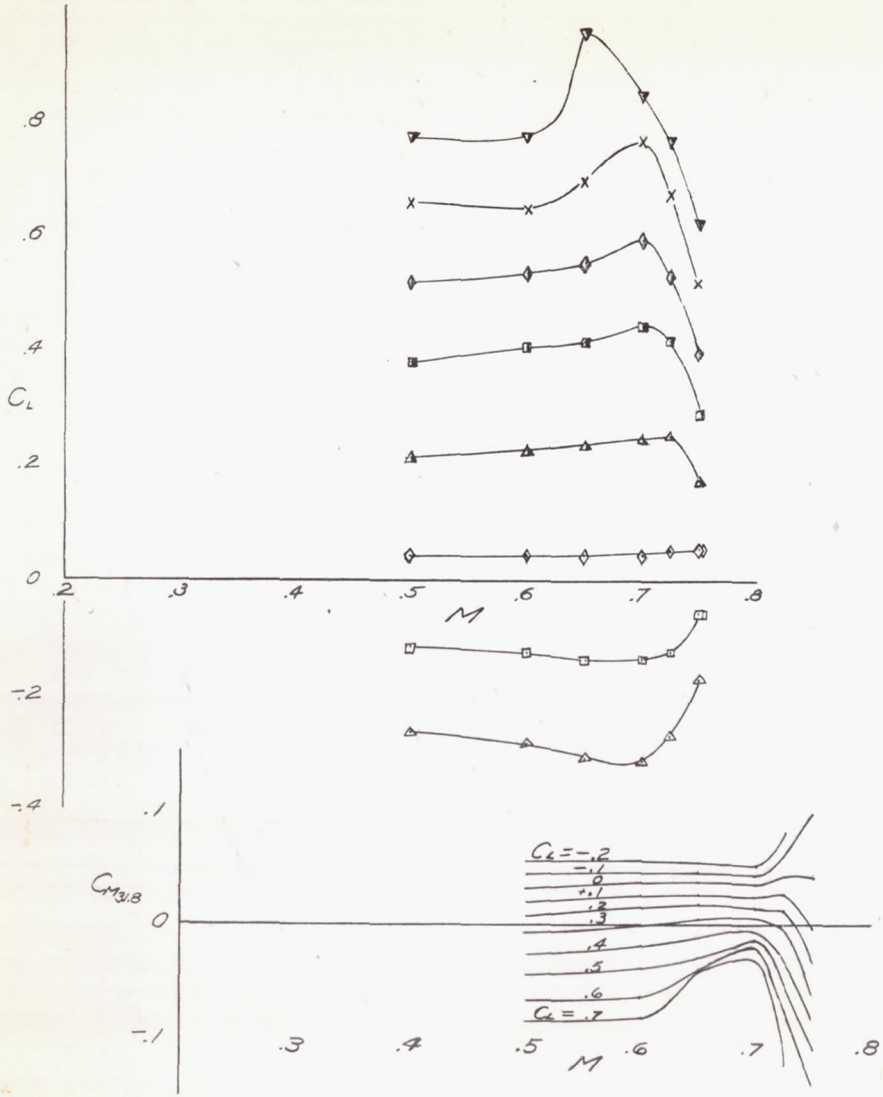

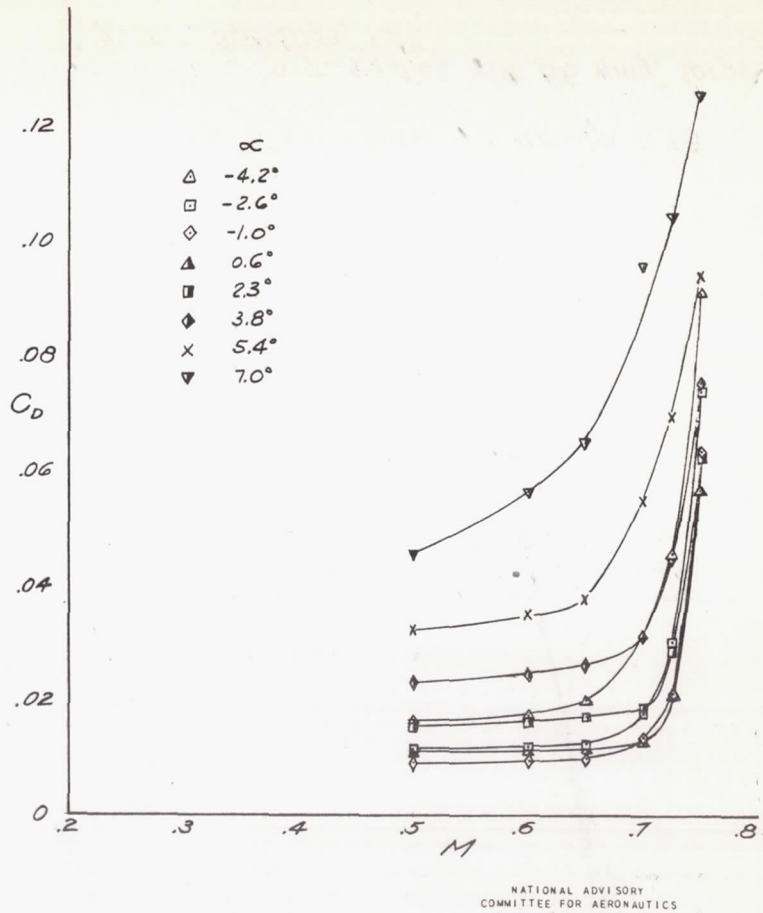

(c) Variation of C_L, C_D, and C_M with Mach number.

Figure 16.– Concluded.

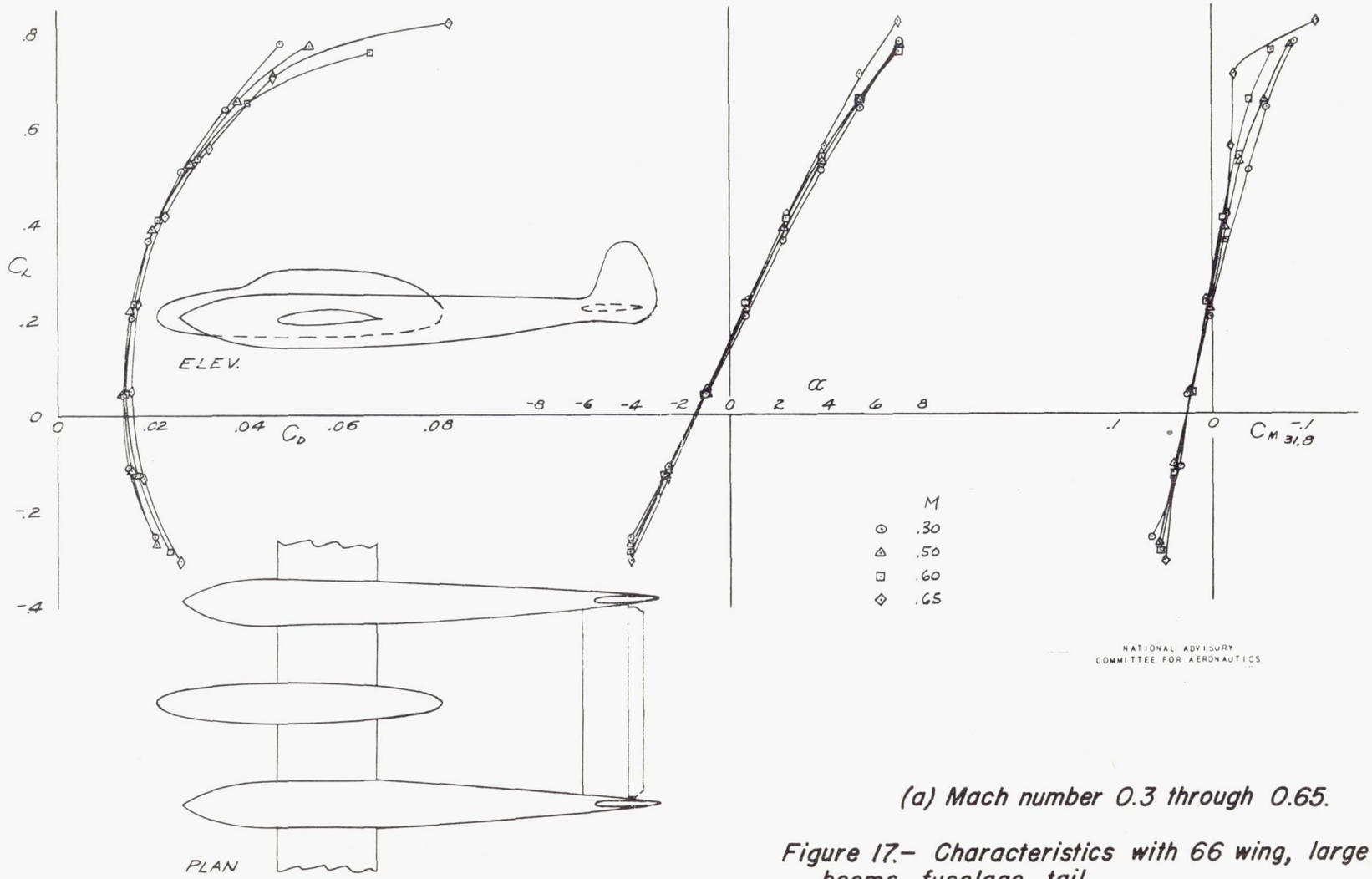

(a) Mach number 0.3 through 0.65.

Figure 17.- Characteristics with 66 wing, large booms, fuselage, tail.

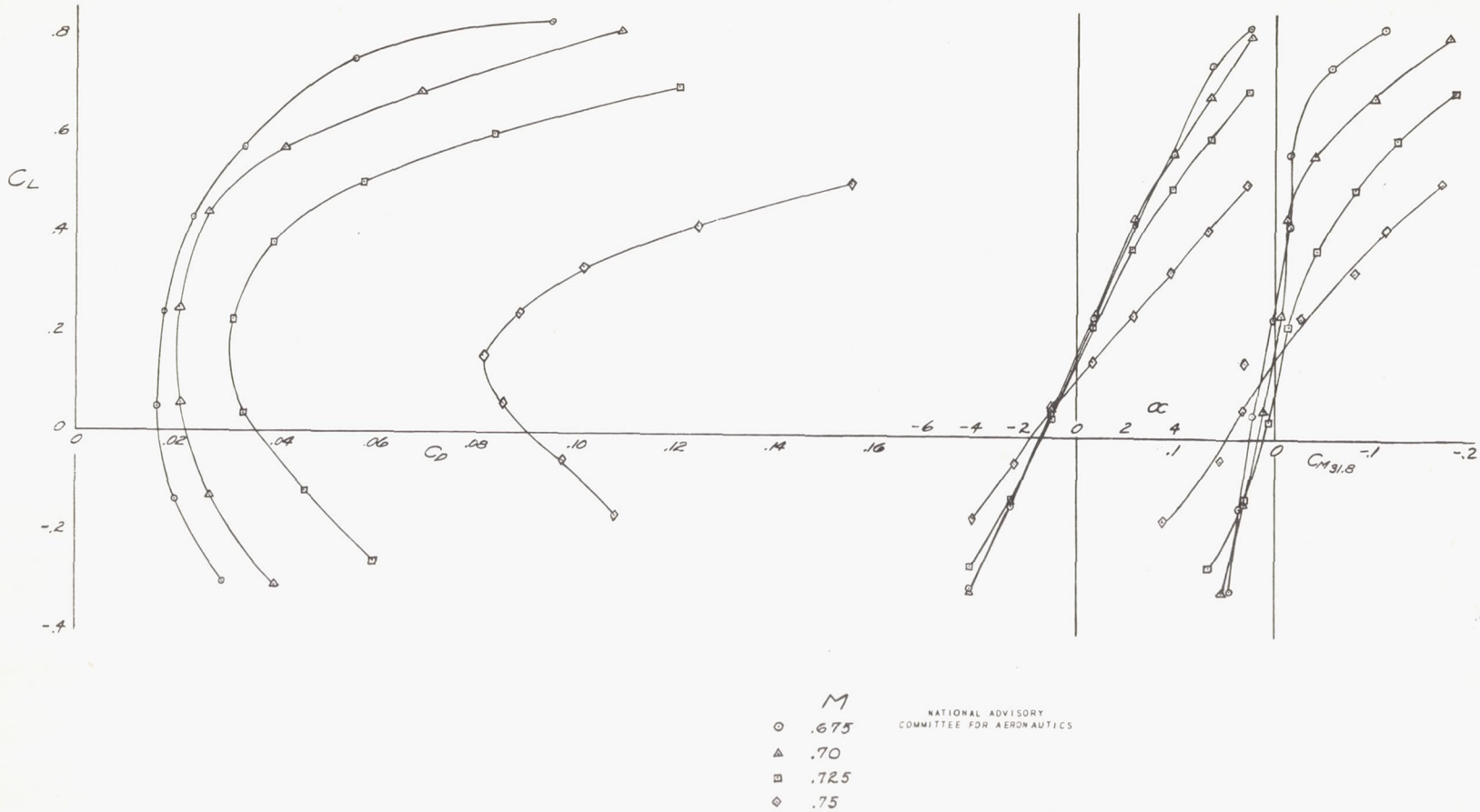

(b) Mach number 0.675 through 0.75.

Figure 17.- Continued.

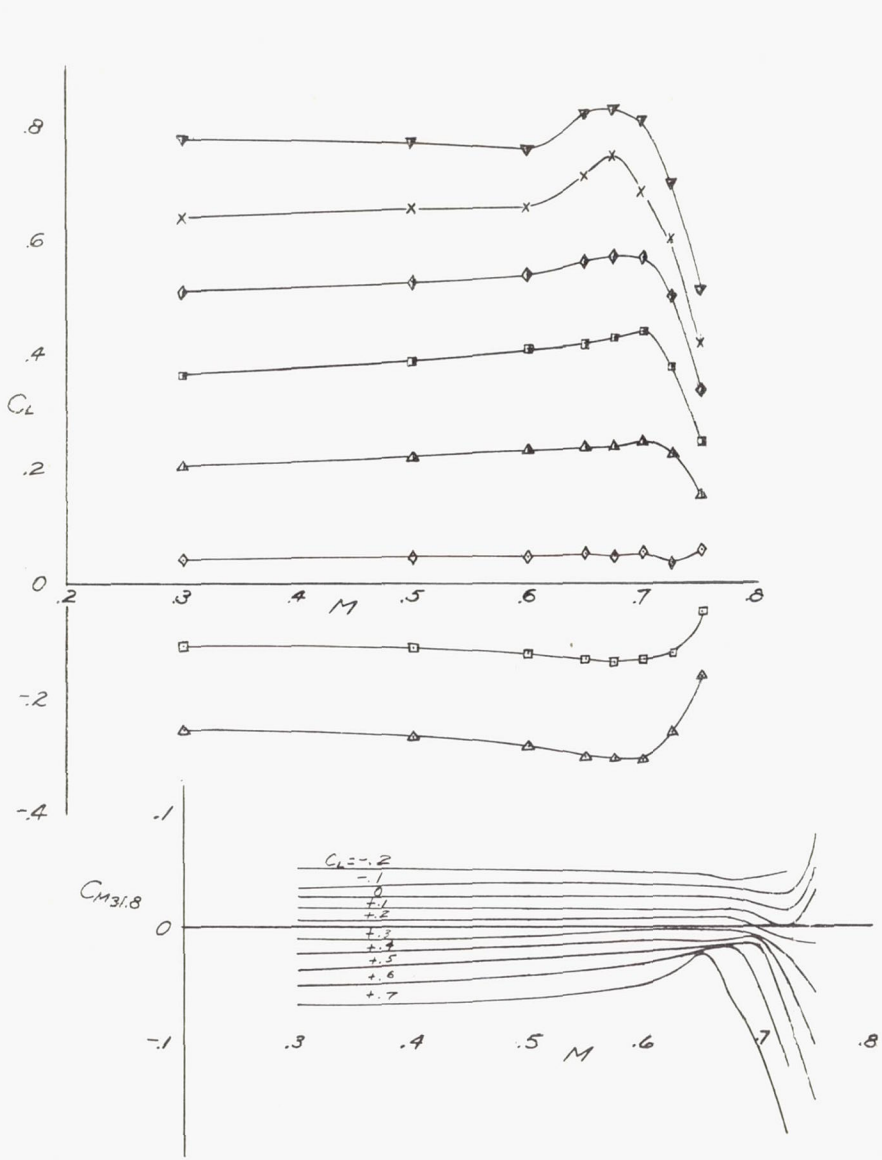

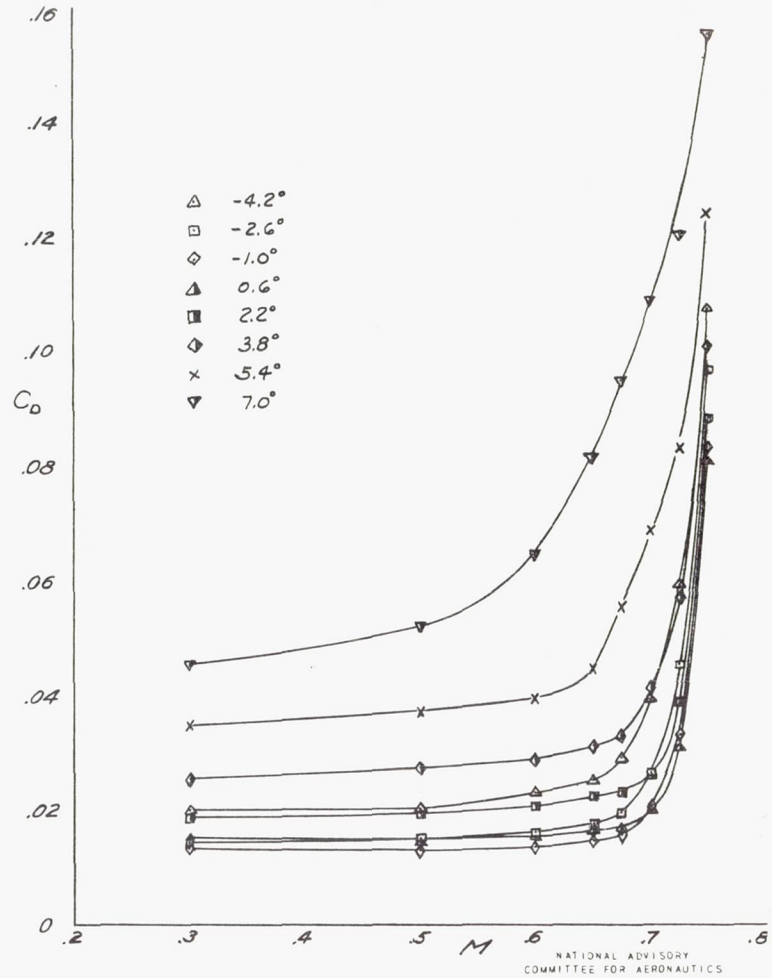

(c) Variation of C_L, C_D, and C_M with Mach number.

Figure 17.– Continued.

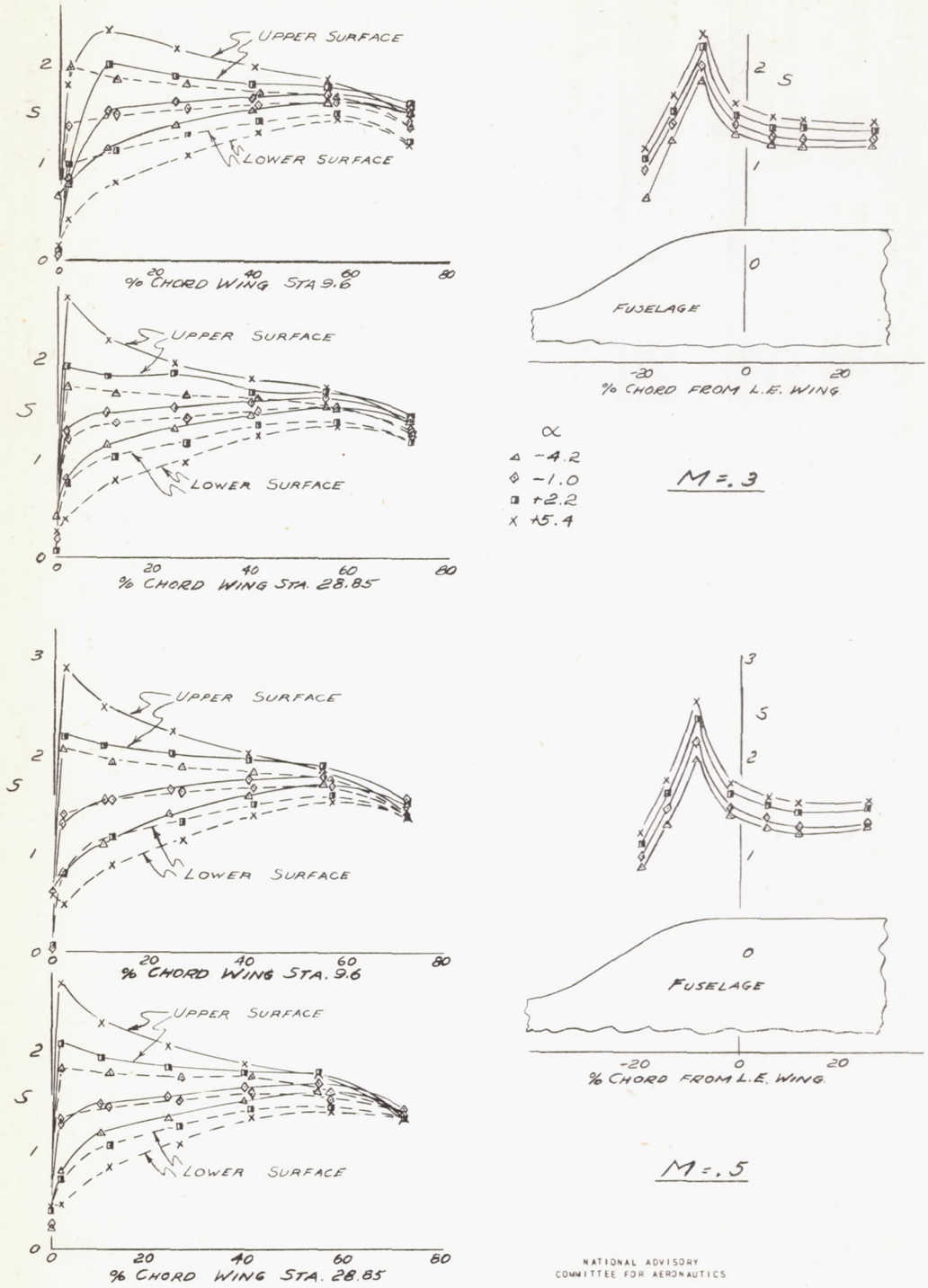

(d) Wing and fuselage pressure distribution at Mach numbers 0.3 and 0.5.

Figure 17.– Continued.

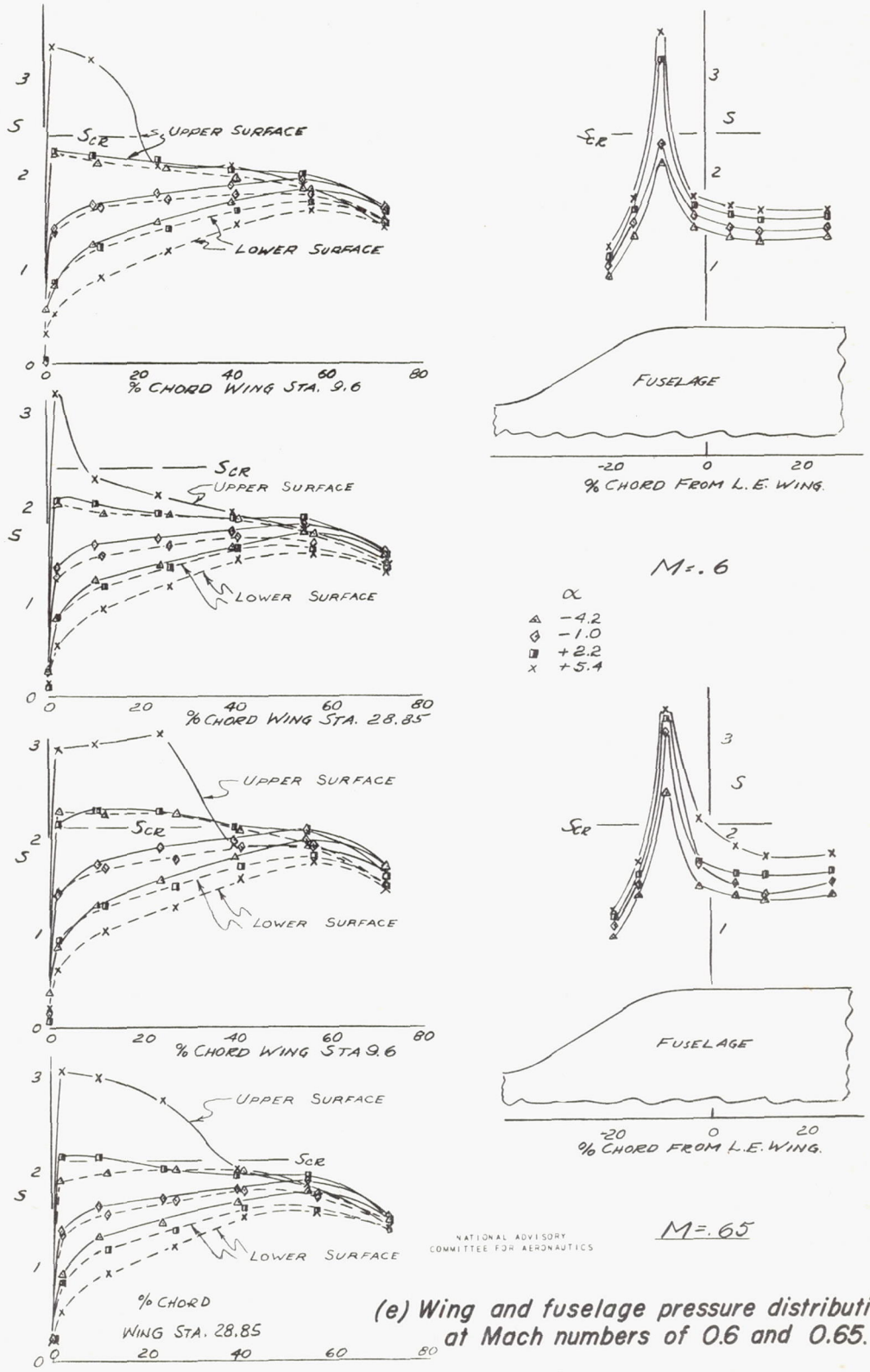

(e) Wing and fuselage pressure distribution at Mach numbers of 0.6 and 0.65.

Figure 17.- Continued.

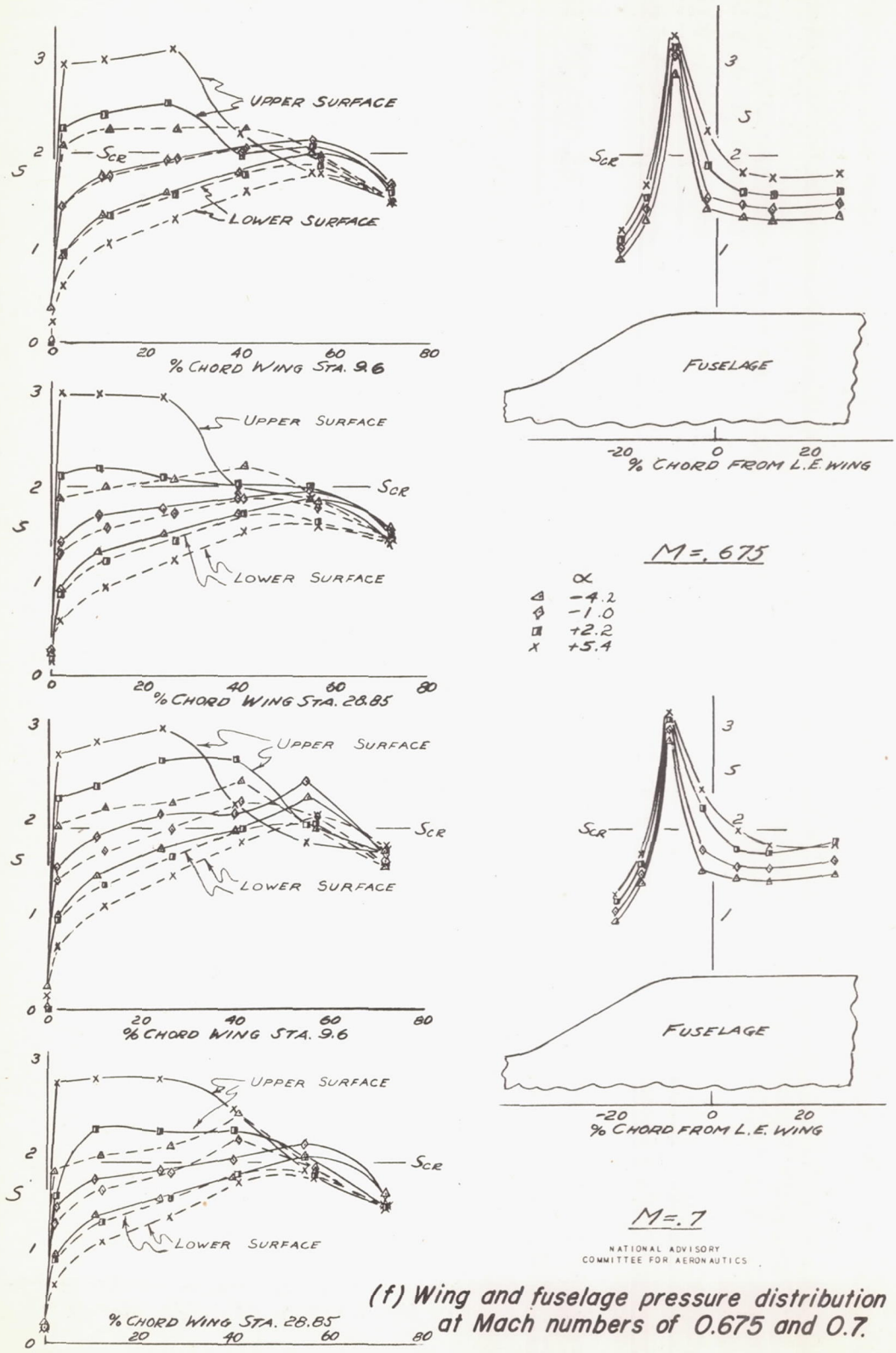

NATIONAL ADVISORY COMMITTEE FOR AERONAUTICS

(f) Wing and fuselage pressure distribution at Mach numbers of 0.675 and 0.7.

Figure 17.- Continued.

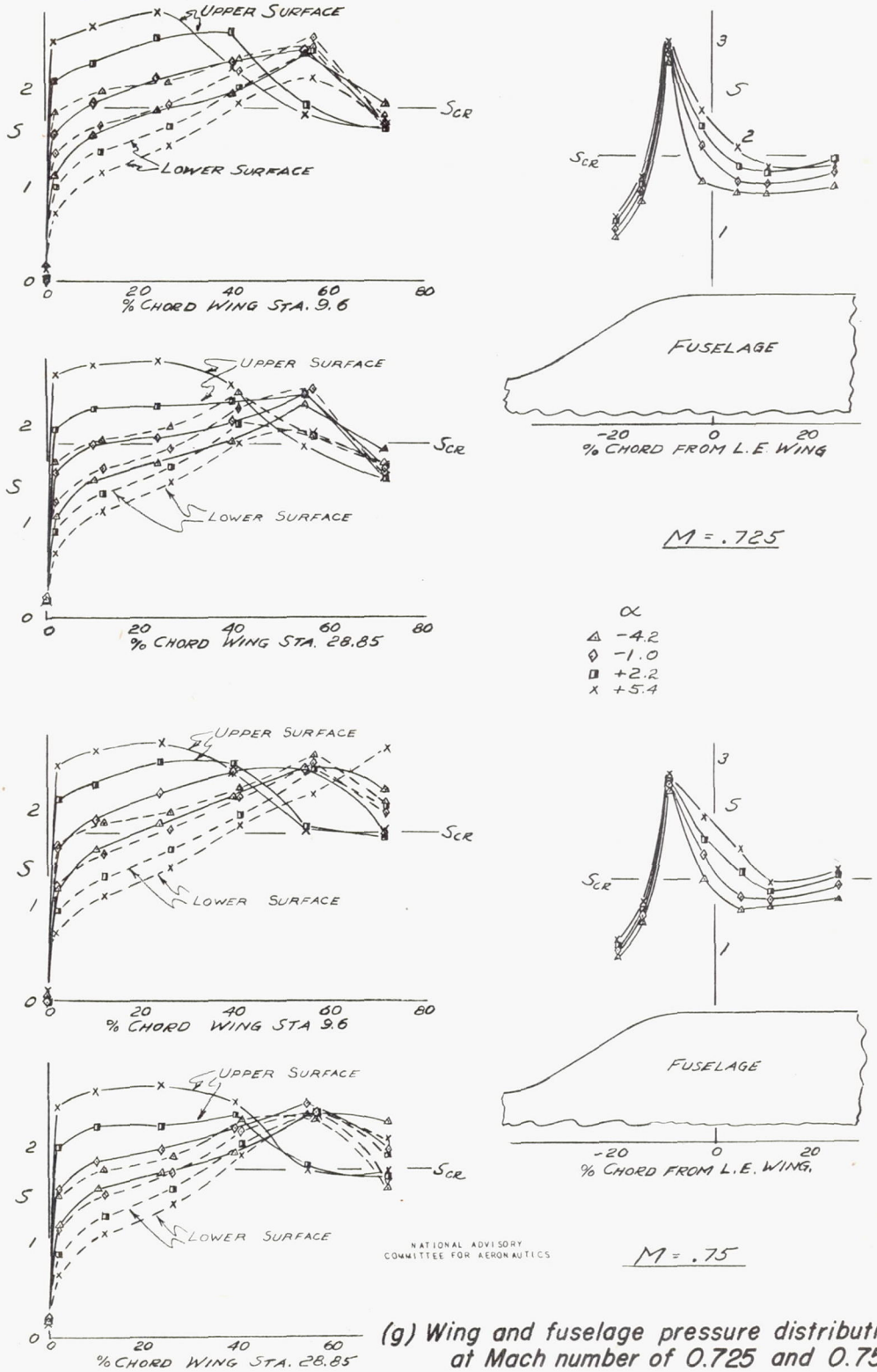

(g) Wing and fuselage pressure distribution at Mach number of 0.725 and 0.75

Figure 17.- Concluded.

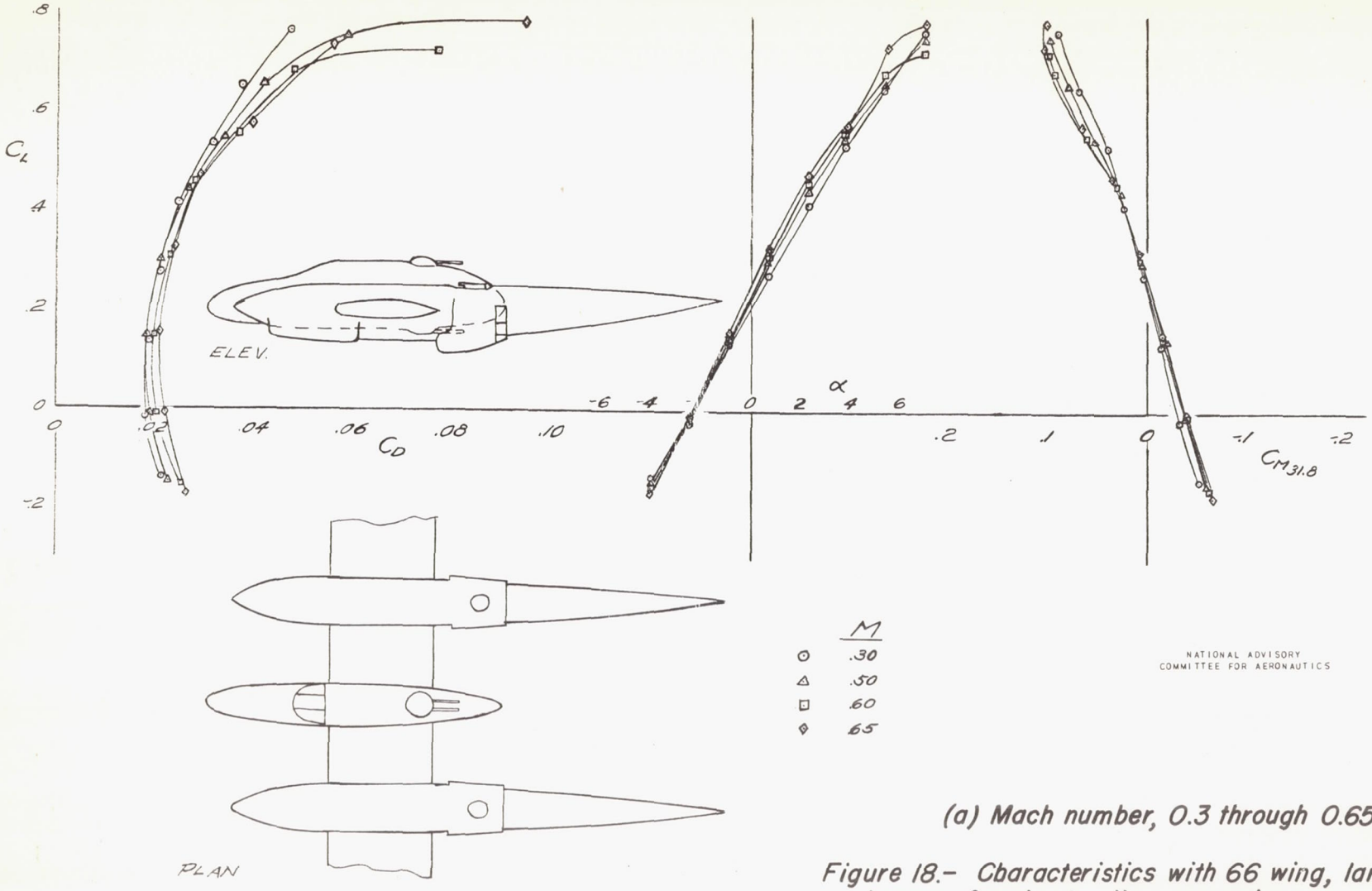

NATIONAL ADVISORY
COMMITTEE FOR AERONAUTICS

(a) Mach number, 0.3 through 0.65.

Figure 18.- Characteristics with 66 wing, large booms, fuselage, all accessories.

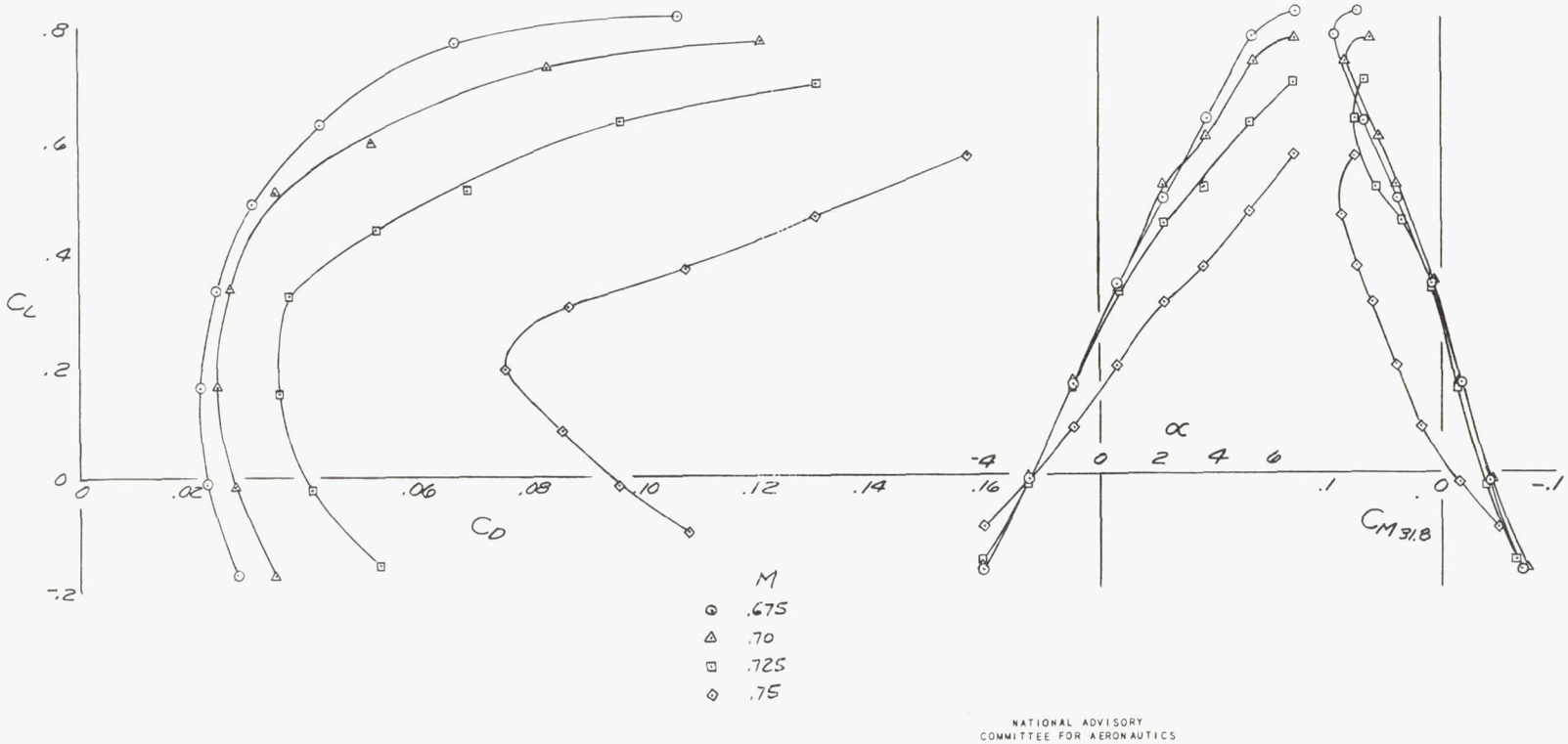

(b) Mach number, 0.675 through 0.75.

Figure 18.– Continued.

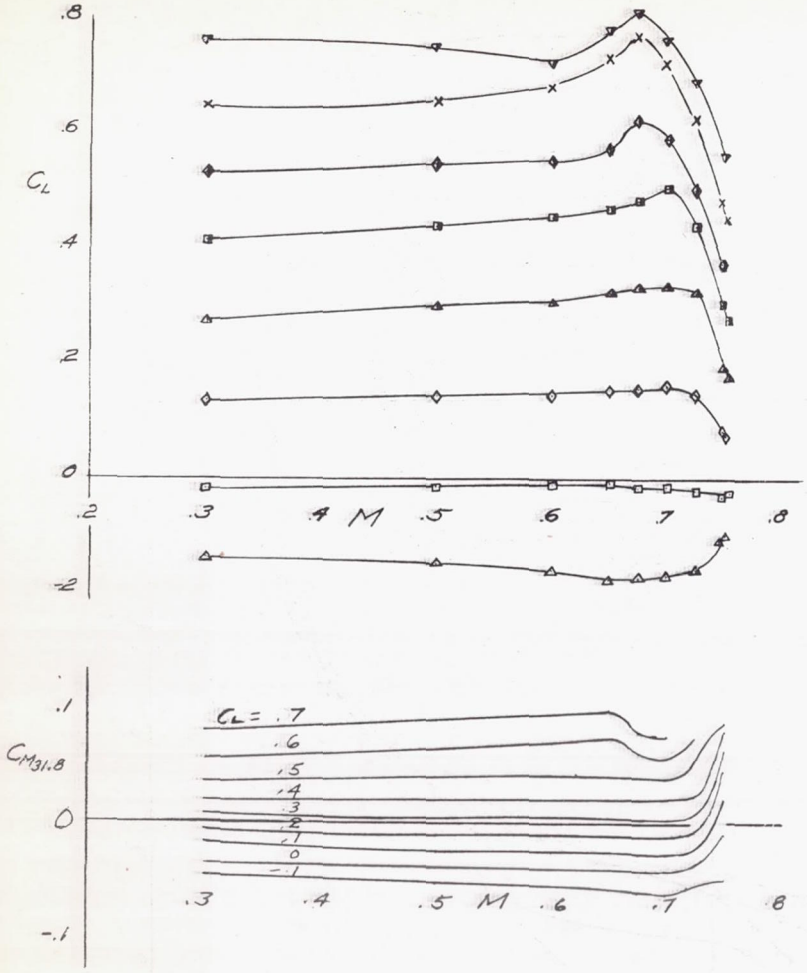

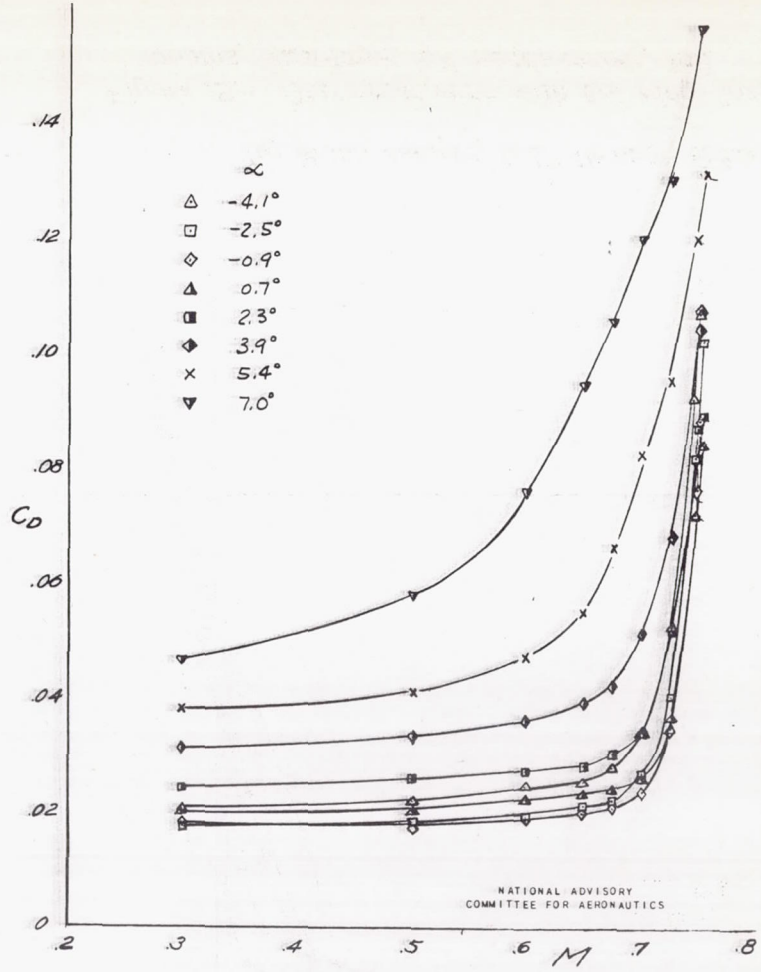

(c) Variation of C_L, C_D, and C_M with Mach number.

Figure 18.– Concluded.

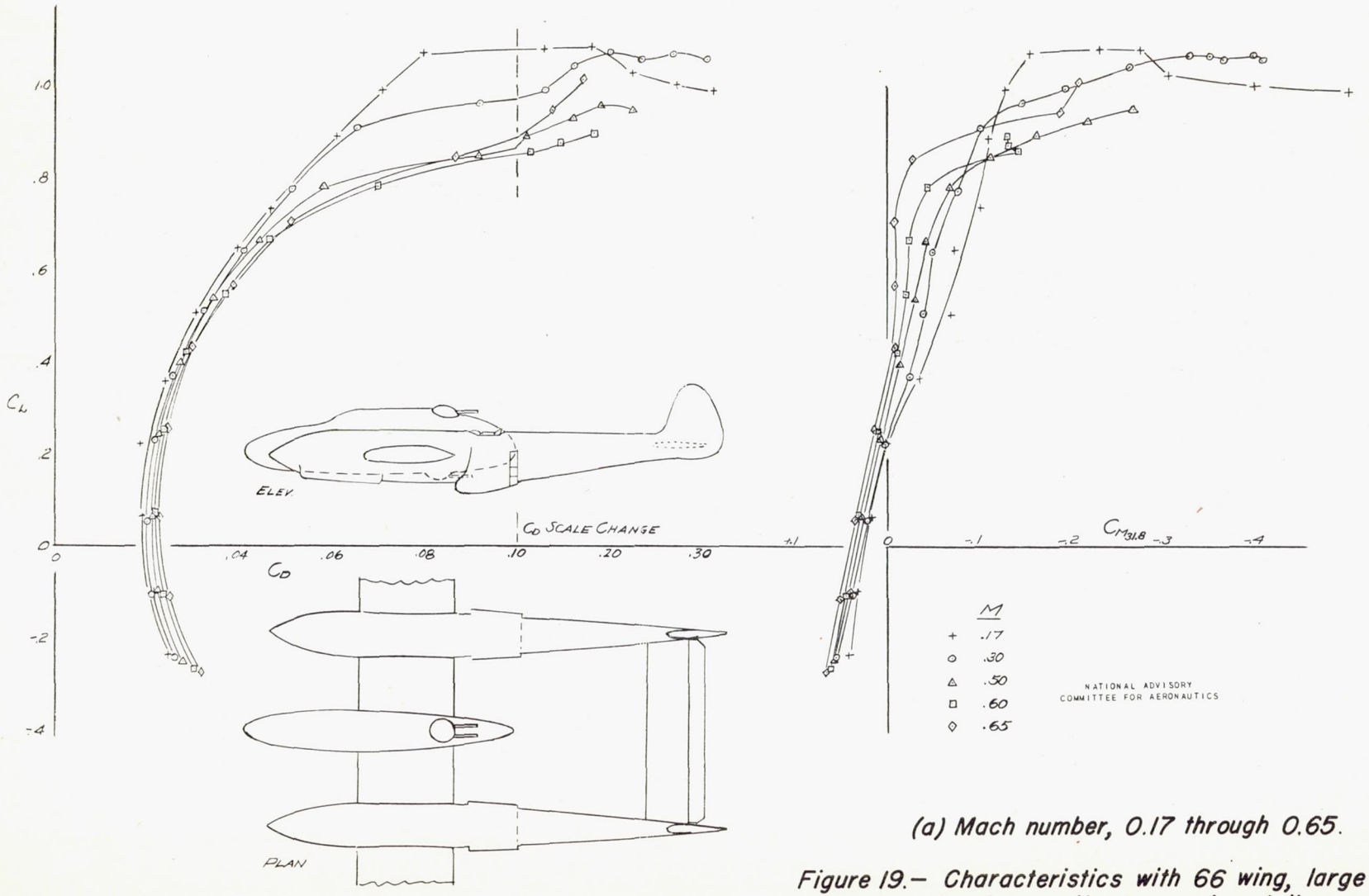

(a) Mach number, 0.17 through 0.65.

Figure 19.– Characteristics with 66 wing, large booms, fuselage, all accessories, tail.

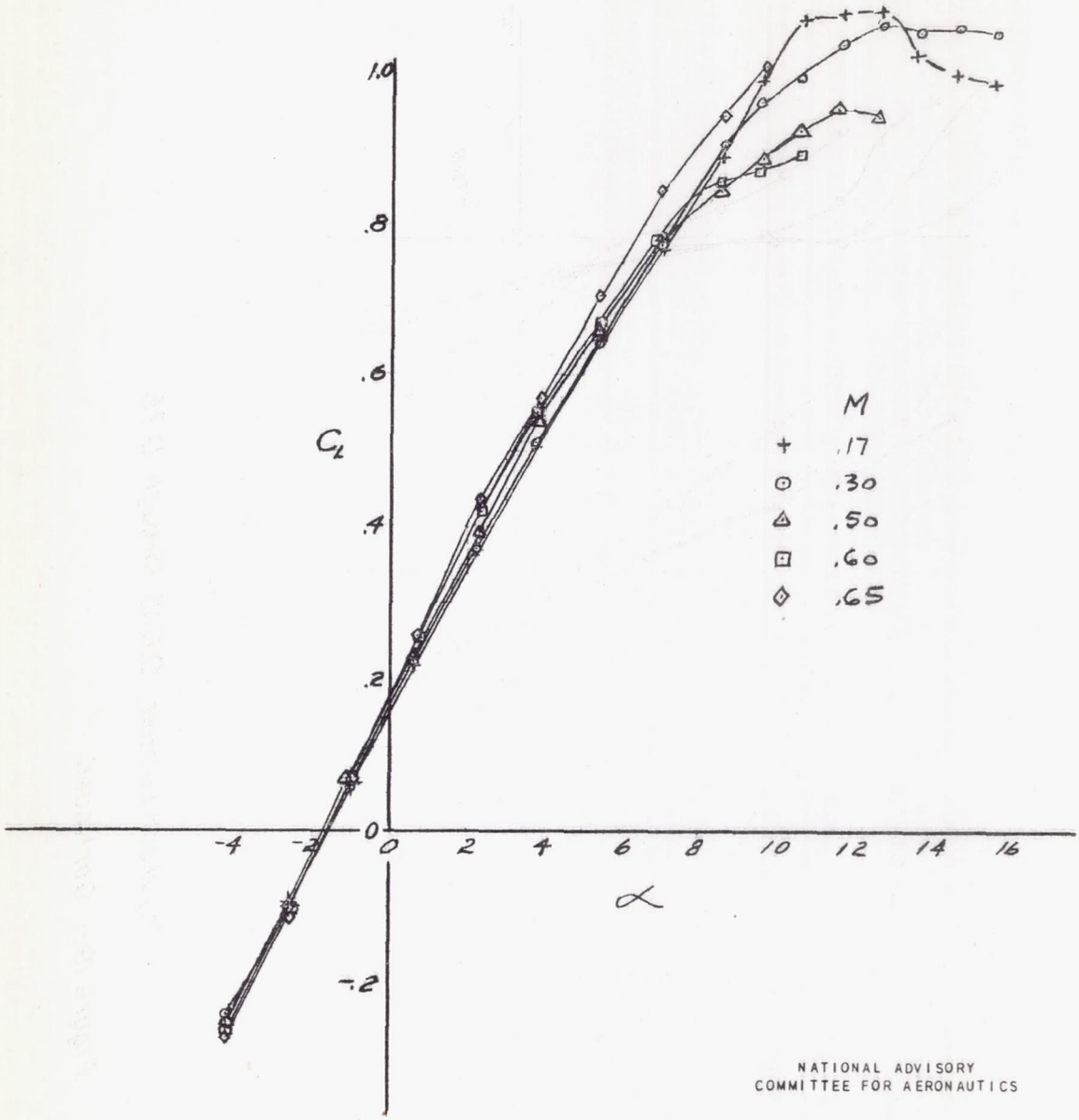

(b) Variation of C_L with angle of attack at Mach numbers of 0.17 through 0.65.

Figure 19.- Continued.

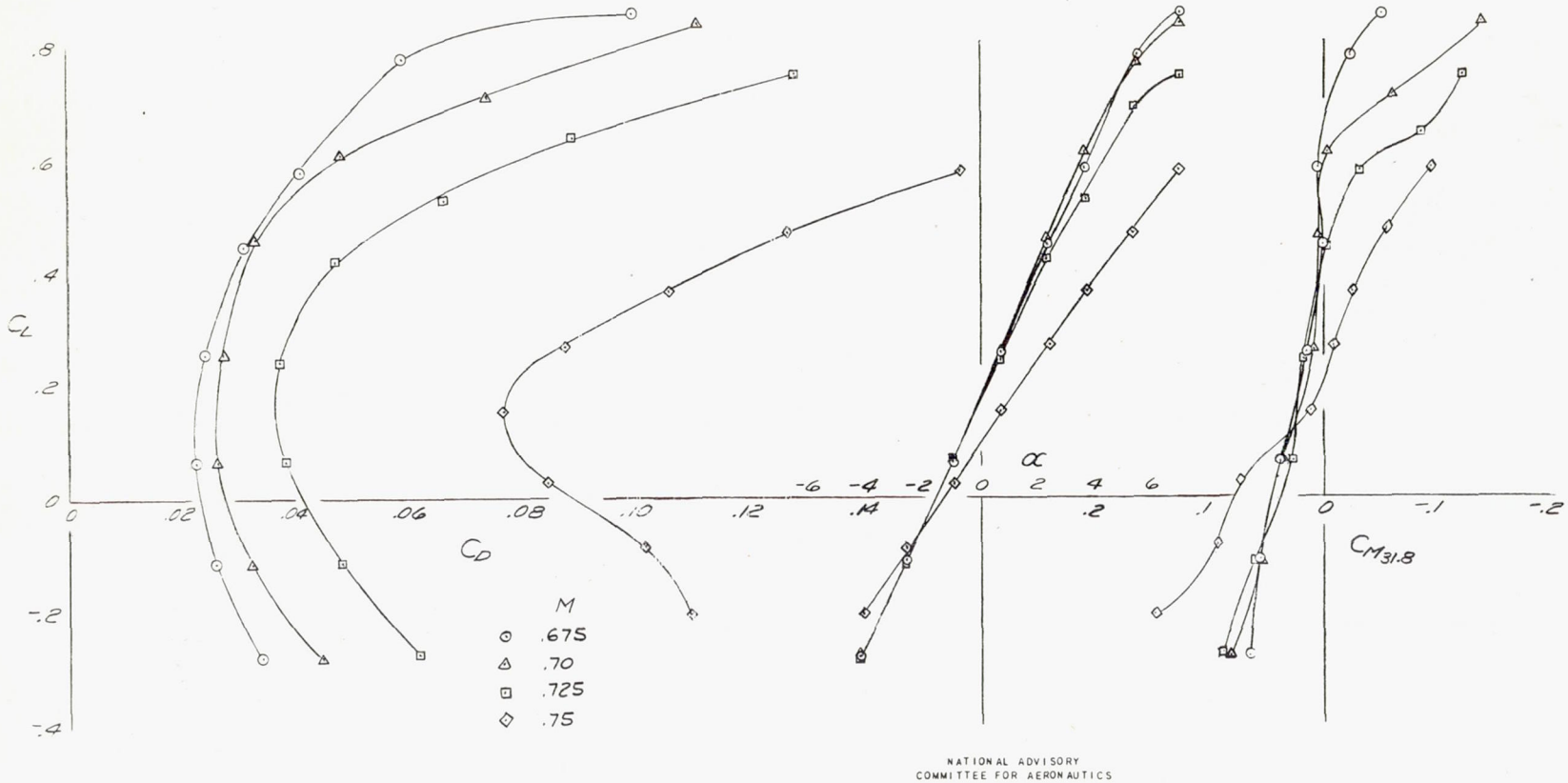

(c) Mach number, 0.675 through 0.75.

Figure 19.- Continued.

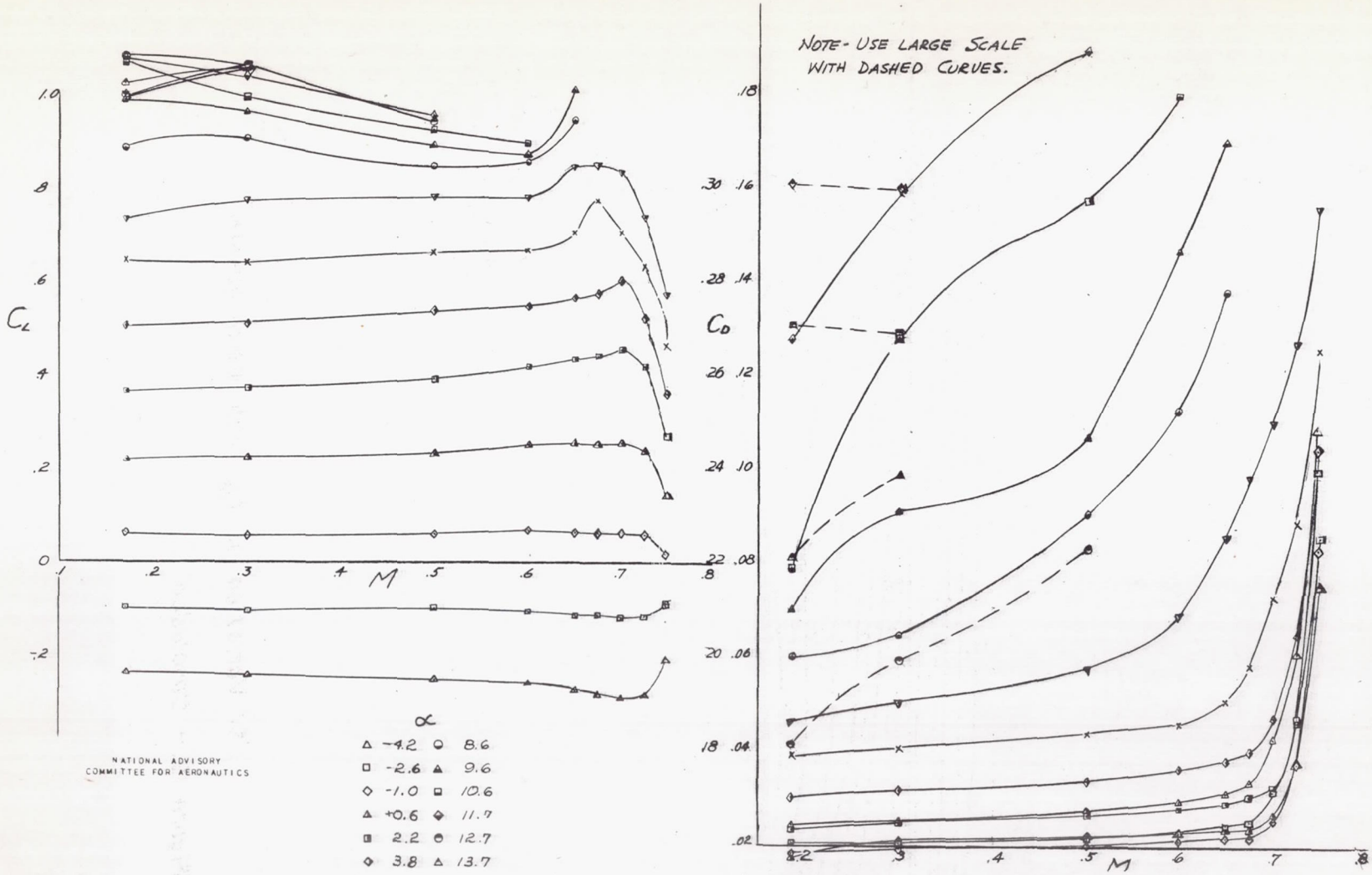

(d) Variation of C_L, and C_D with Mach number.

Figure 19.- Continued.

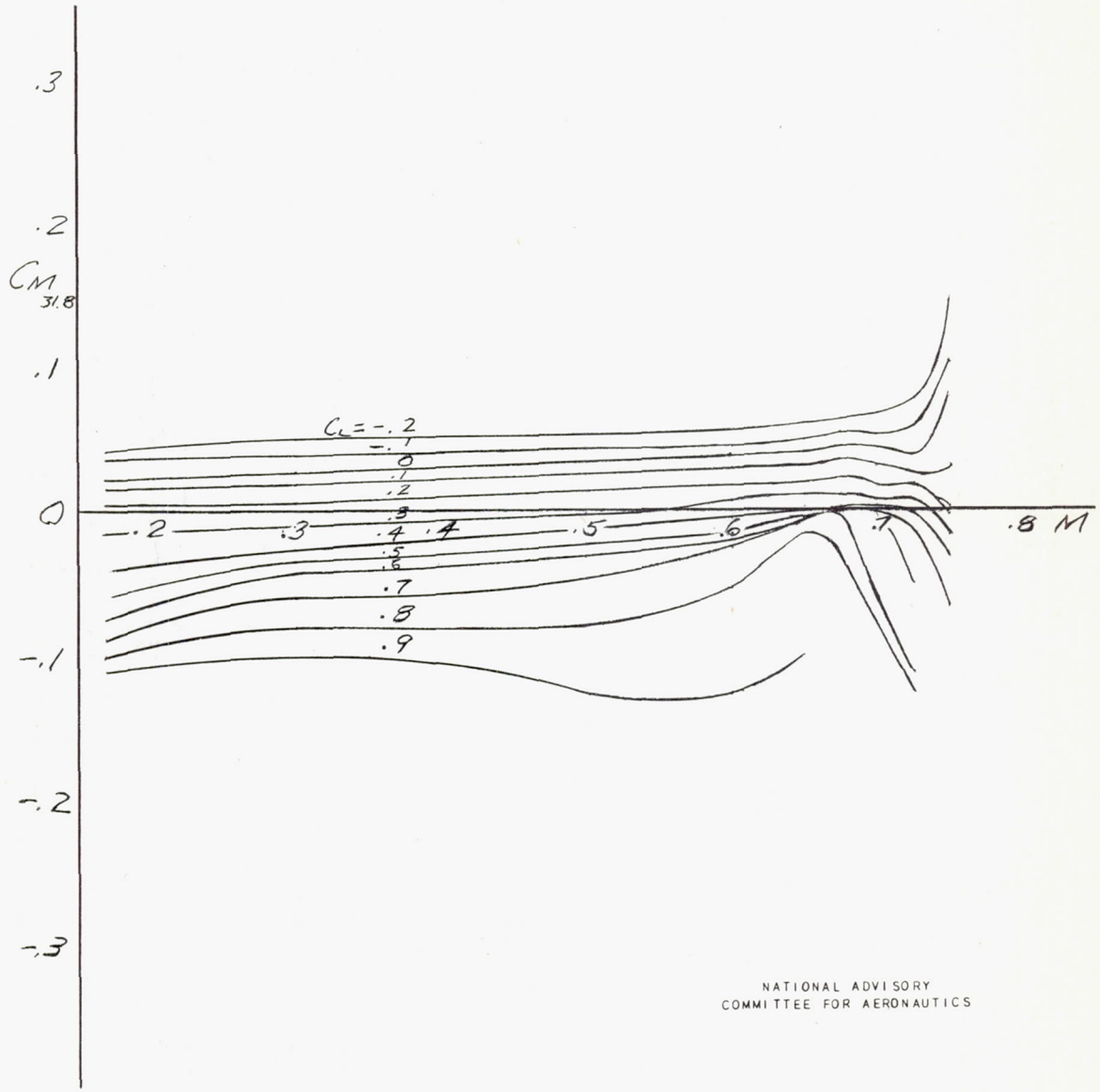

(e) Variation of C_M with Mach number.

Figure 19.- Concluded.

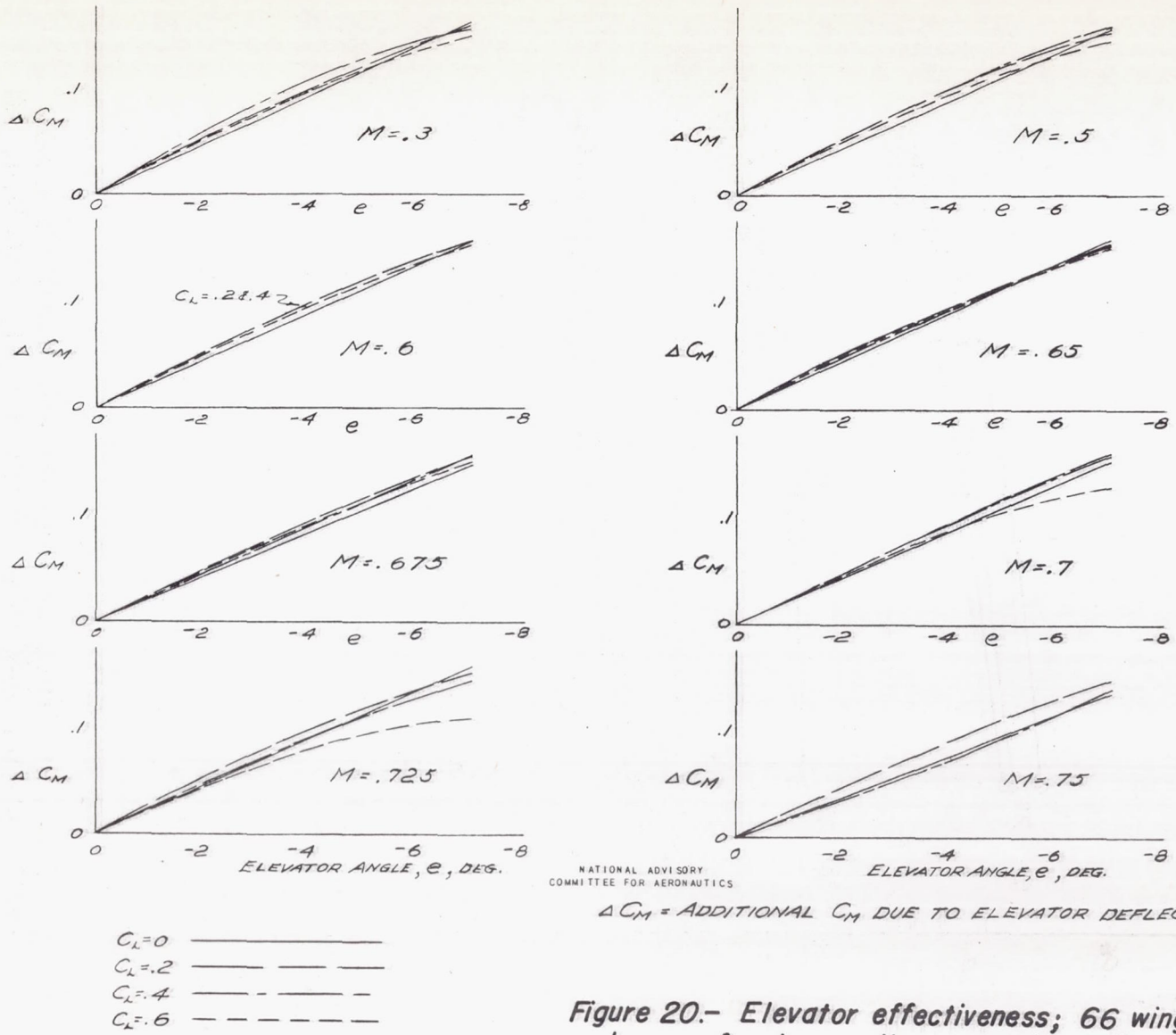

Figure 20.- Elevator effectiveness; 66 wing, large booms, fuselage, all accessories, tail.

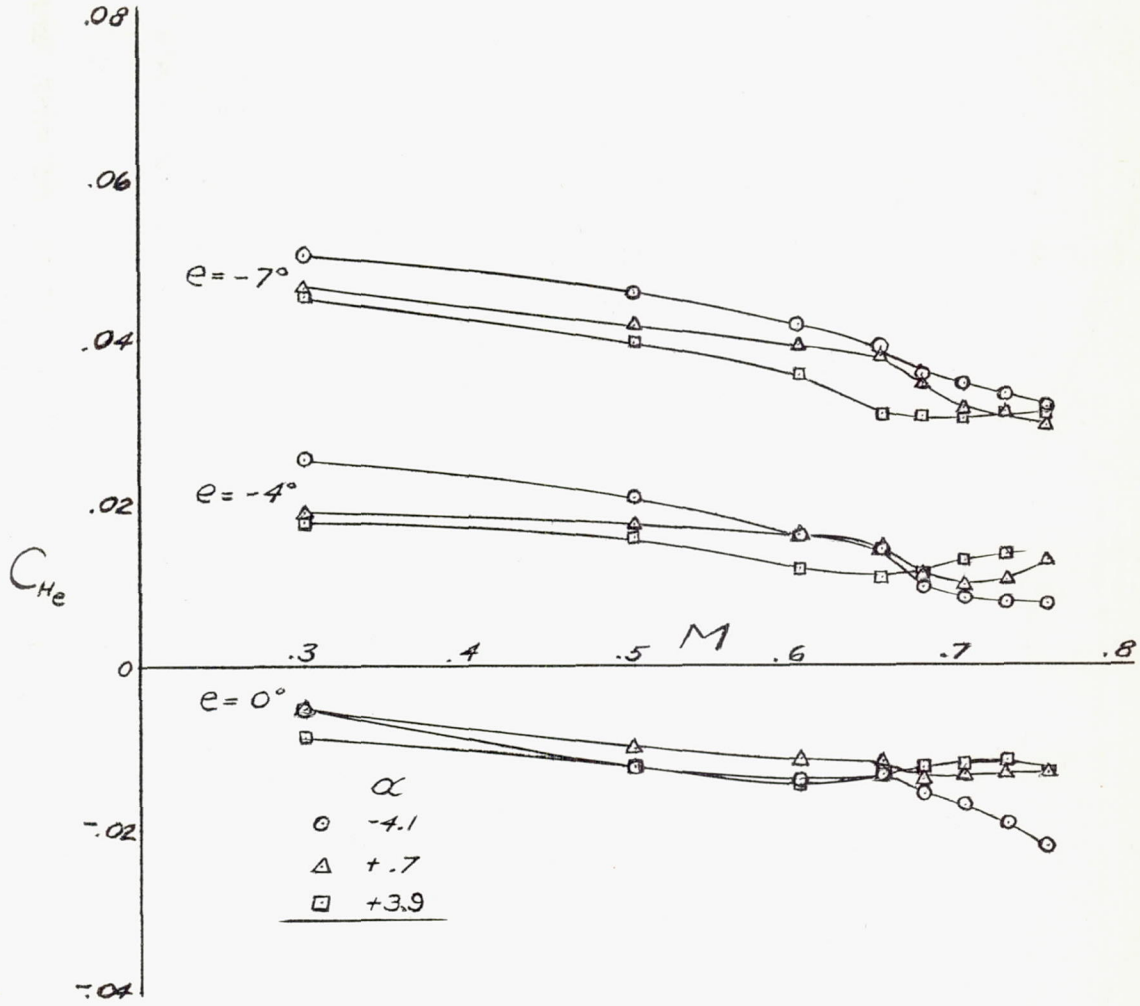

NATIONAL ADVISORY
COMMITTEE FOR AERONAUTICS

Figure 21.- Variation of hinge-moment coefficient with Mach number; 230 wing, large booms, fuselage, all accessories, tail.

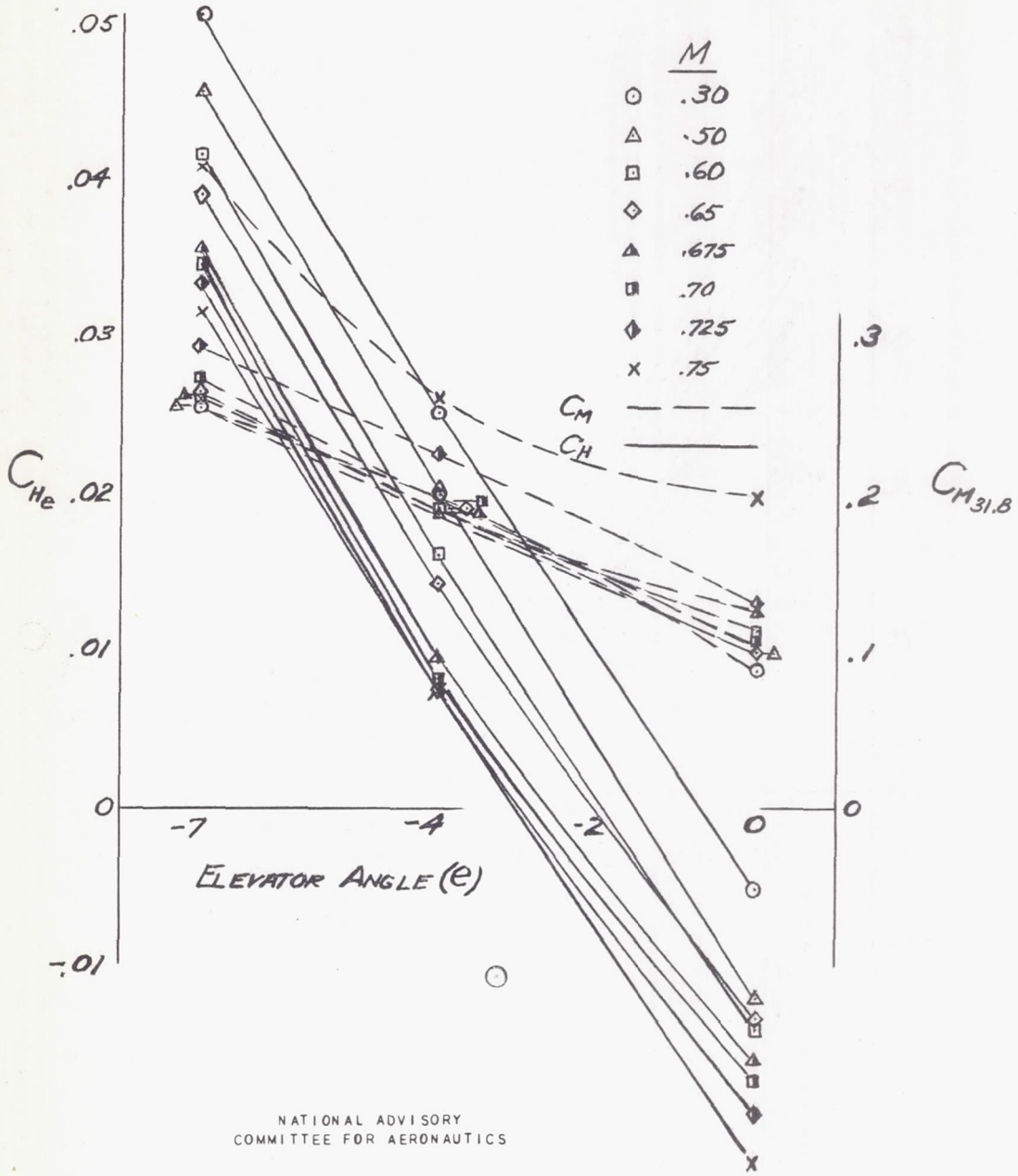

(a) Angle of attack, -4.1°.

Figure 22.- Variation of pitching moment and elevator hinge moment with elevator angle; 230 wing, large booms, fuselage, all accessories, tail.

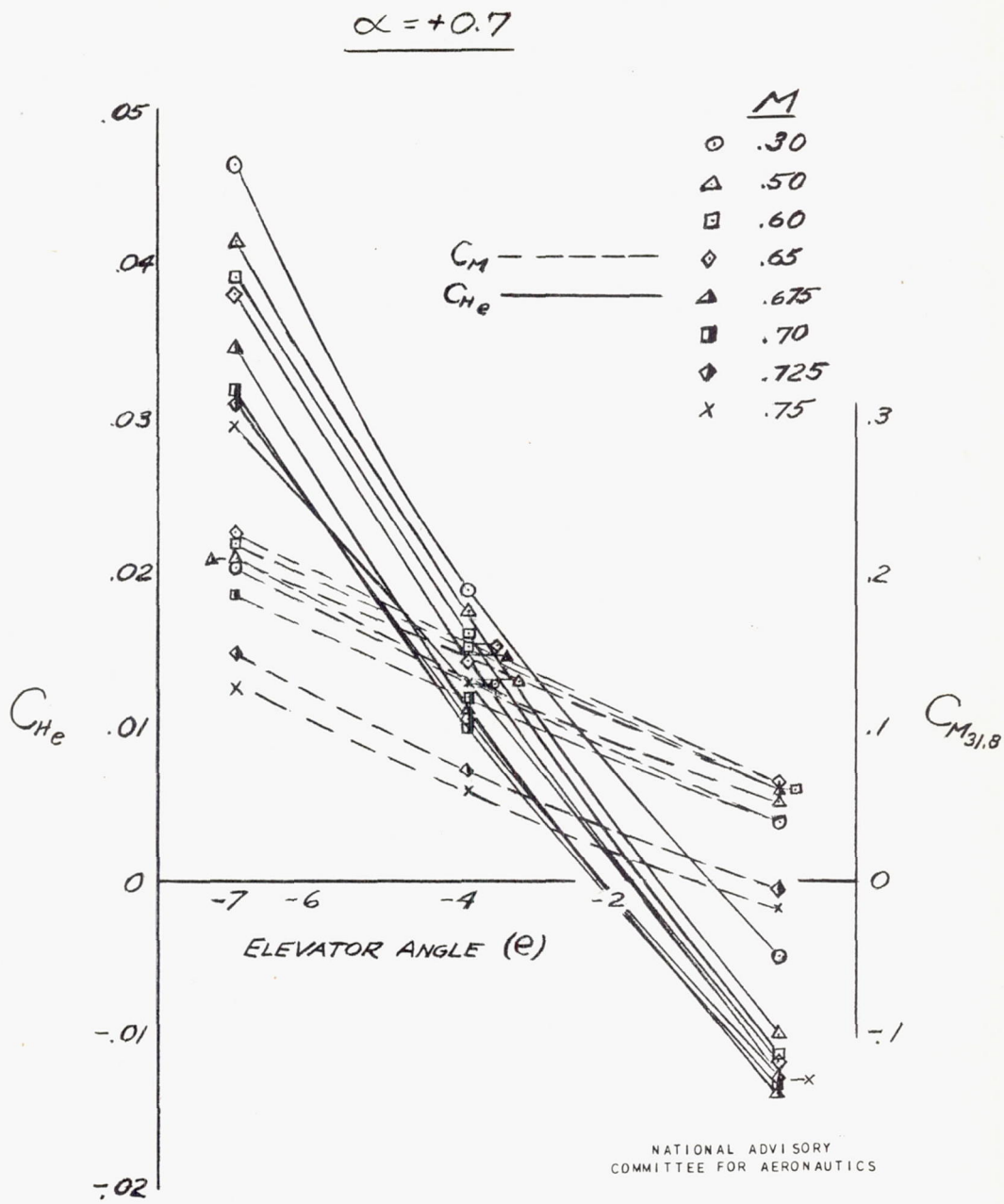

(b) Angle of attack, 0.7°.

Figure 22.– Continued.

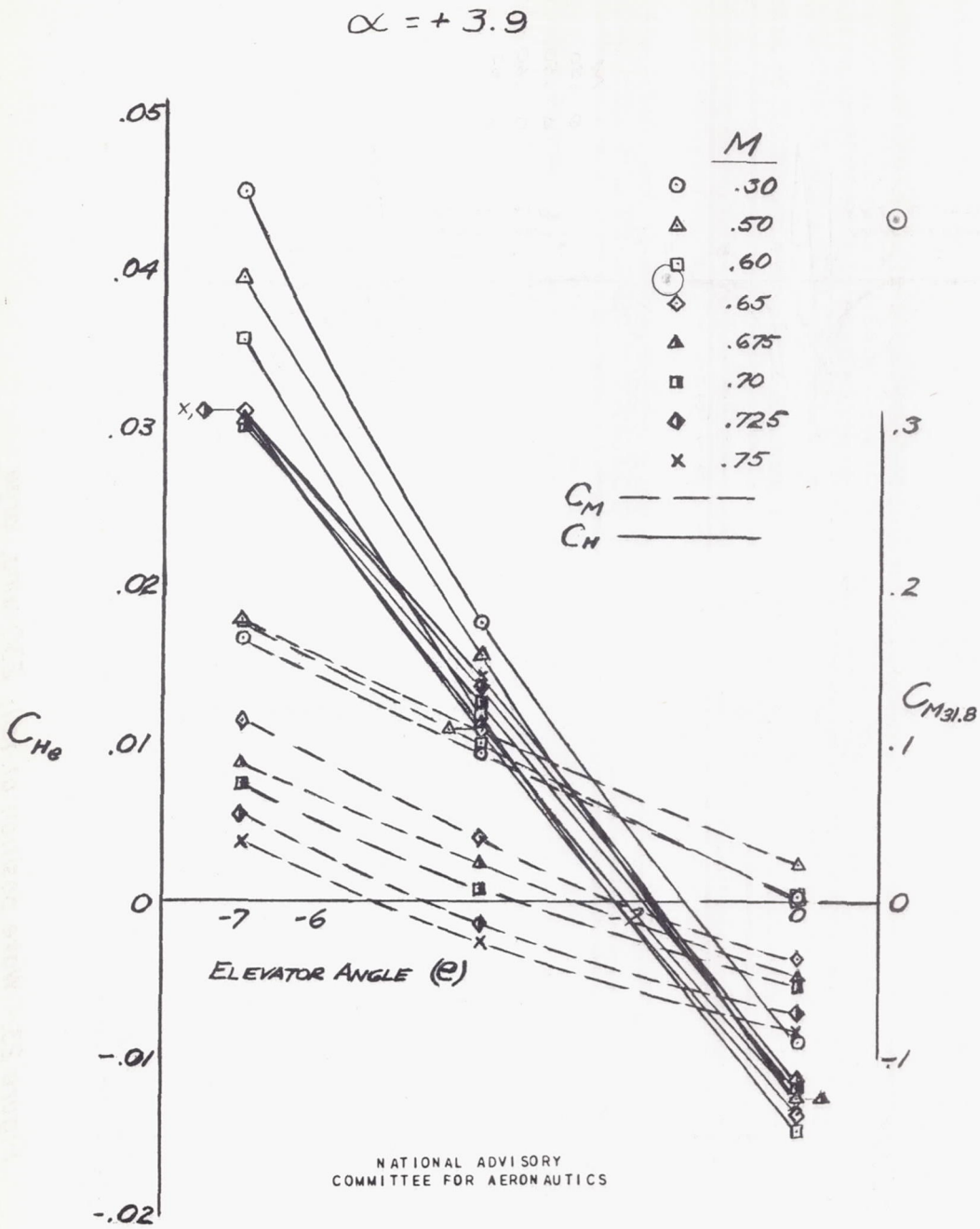

(c) Angle of attack, 3.9°.

Figure 22.- Concluded.

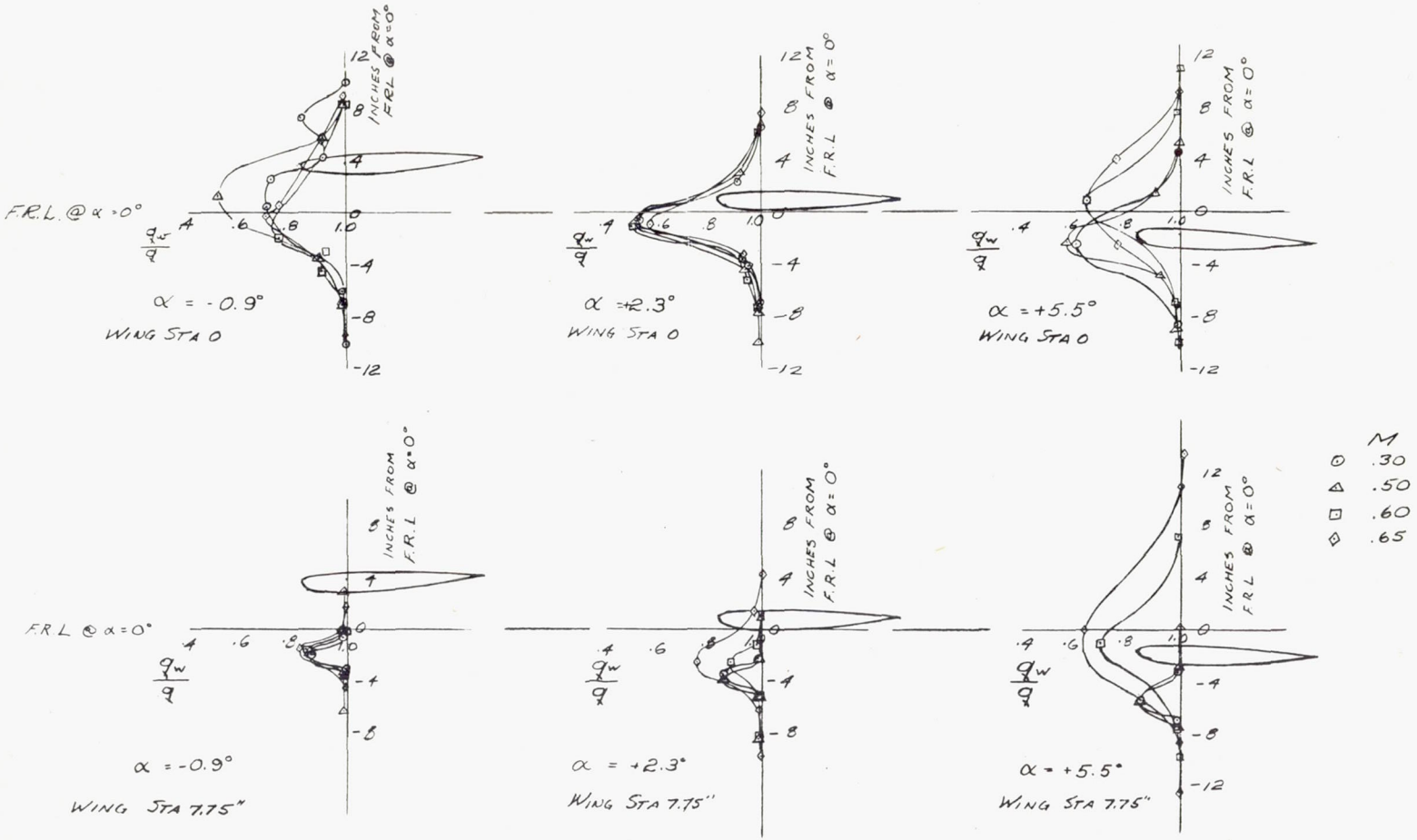

$\frac{q_w}{q}$ = RATIO OF q IN WAKE TO q OUTSIDE OF WAKE

NATIONAL ADVISORY COMMITTEE FOR AERONAUTICS

Figure 23.- Wake position at tail; 230 wing, large booms, fuselage, all accessories.

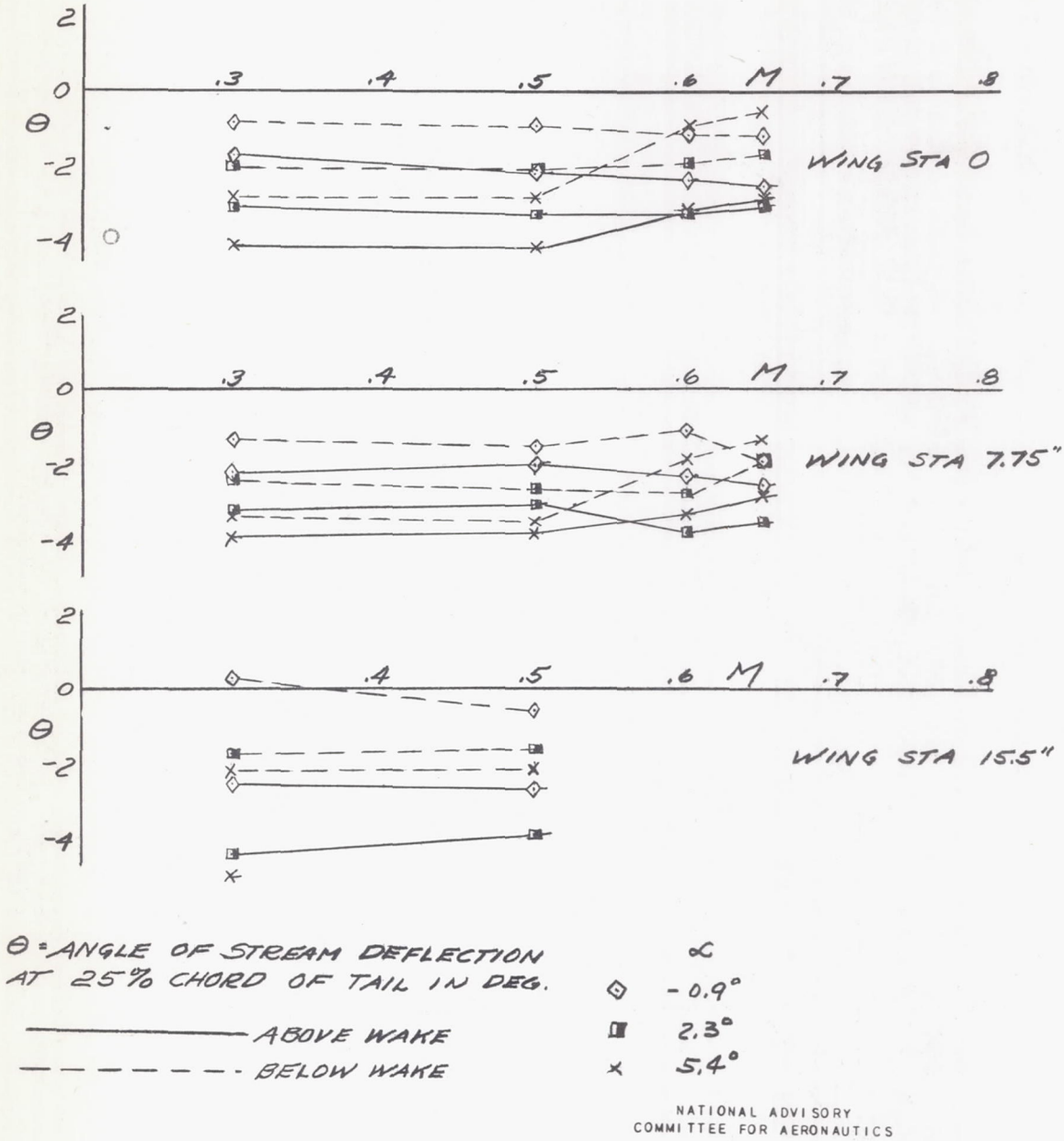

Figure 24.- Flow angles at tail; 230 wing, large booms, fuselage, all accessories.

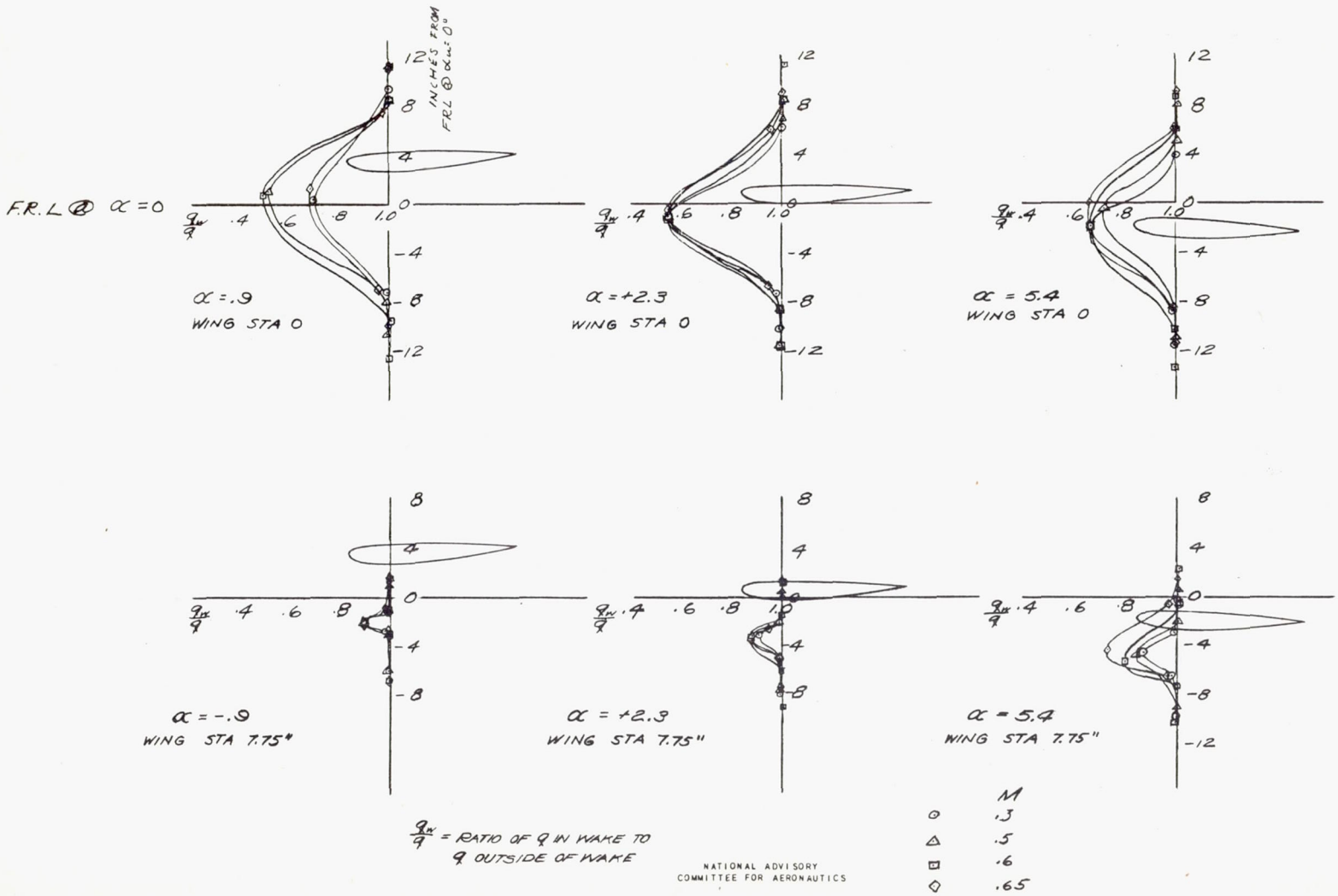

Figure 25.- Wake position at tail; 66 wing, large booms, fuselage, all accessories.

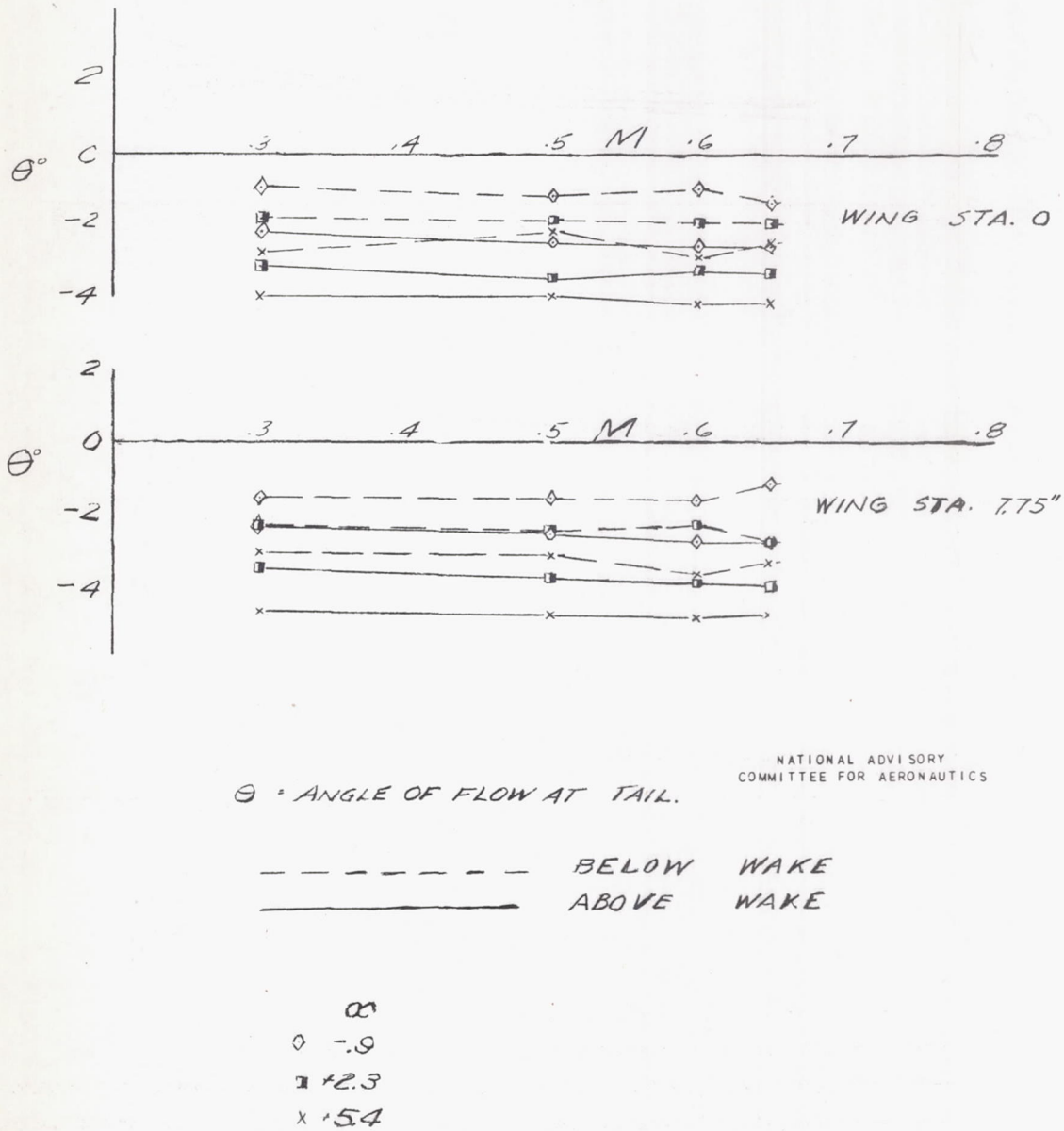

Figure 26.- Flow angles at tail; 66 wing, large booms, fuselage, all accessories.

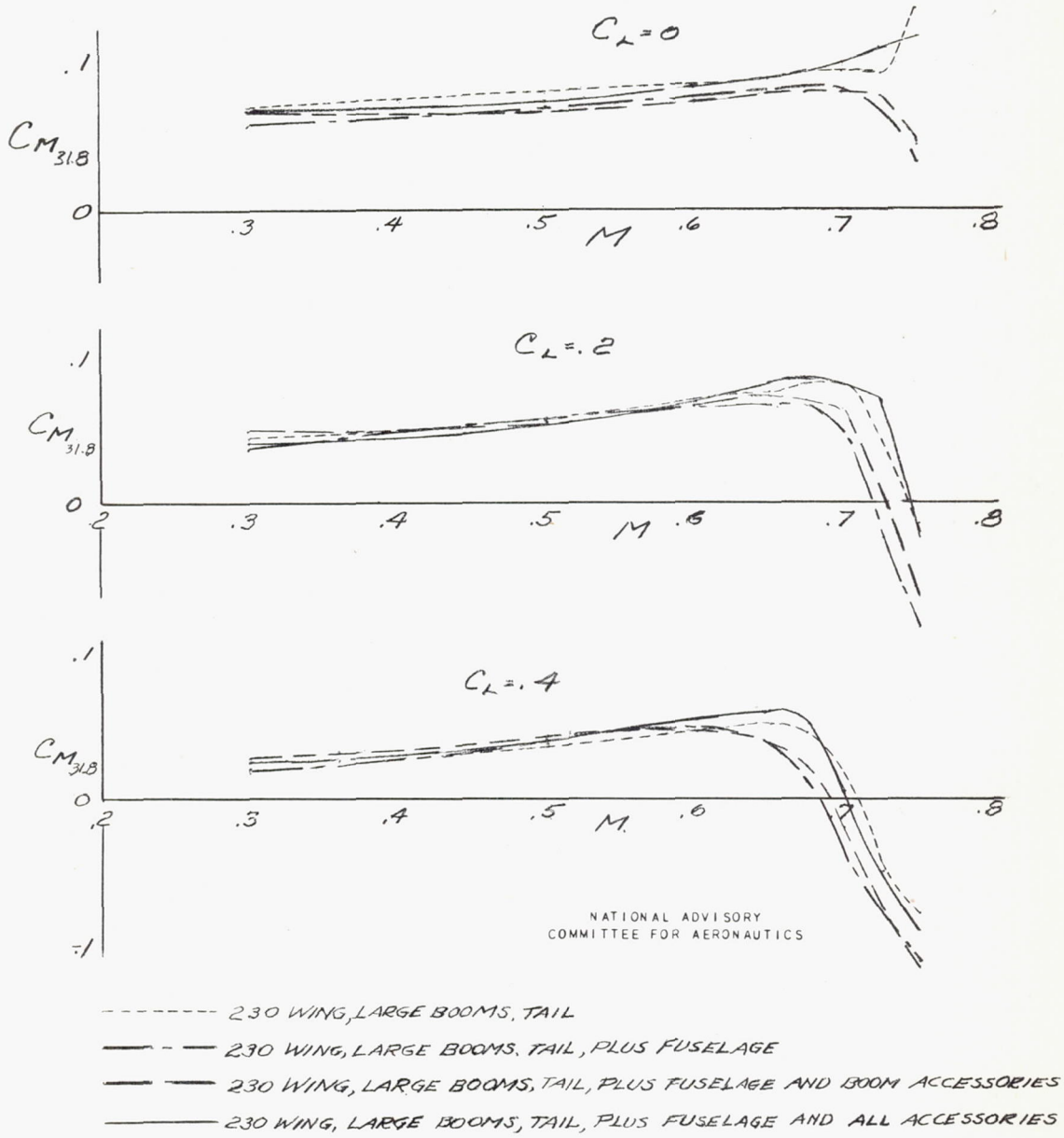

Figure 27.– Effect of build-up on C_M with 230 wing, large booms, tail.

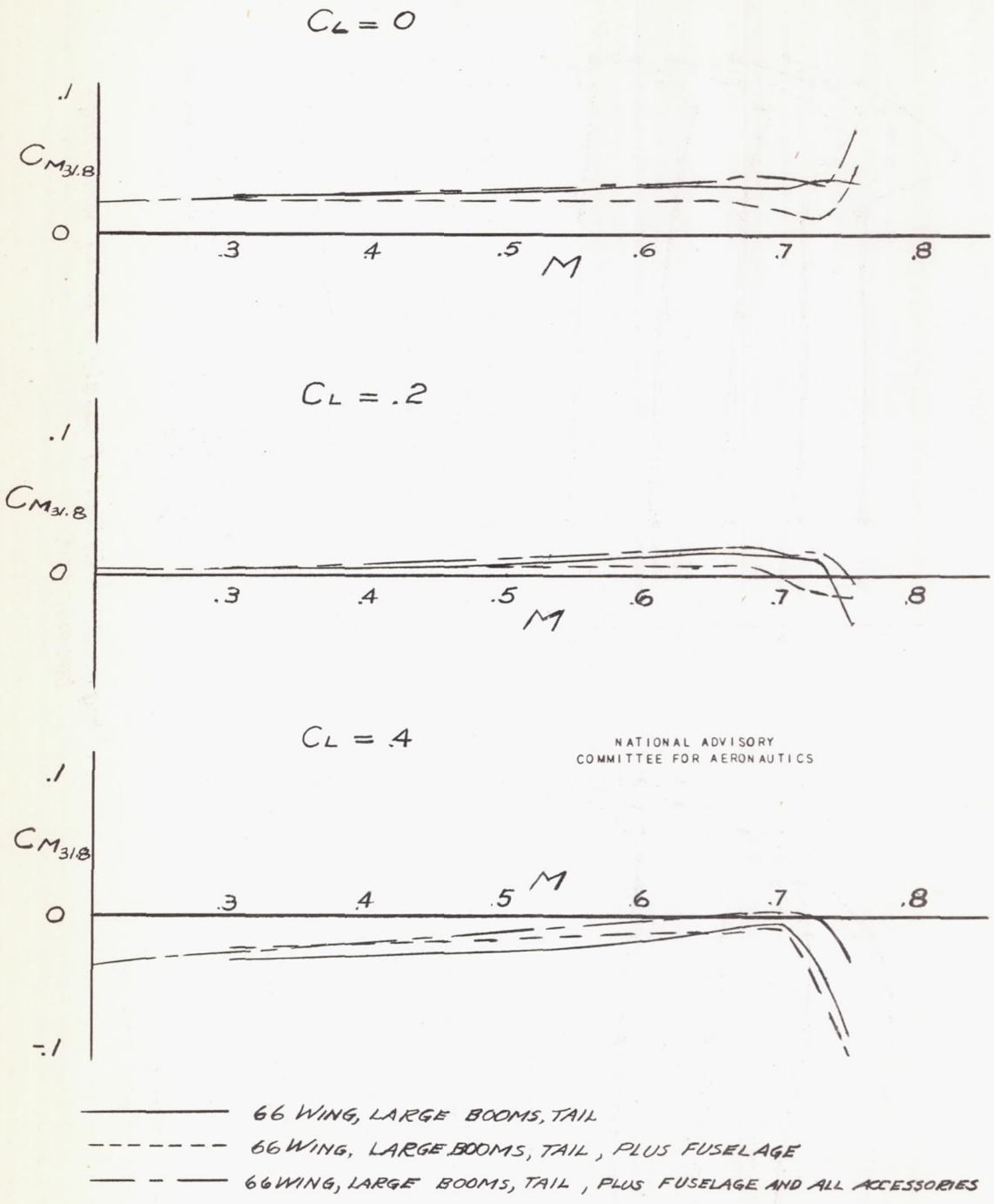

Figure 28.- Effect of build-up on C_M with 66 wing, large booms, tail.

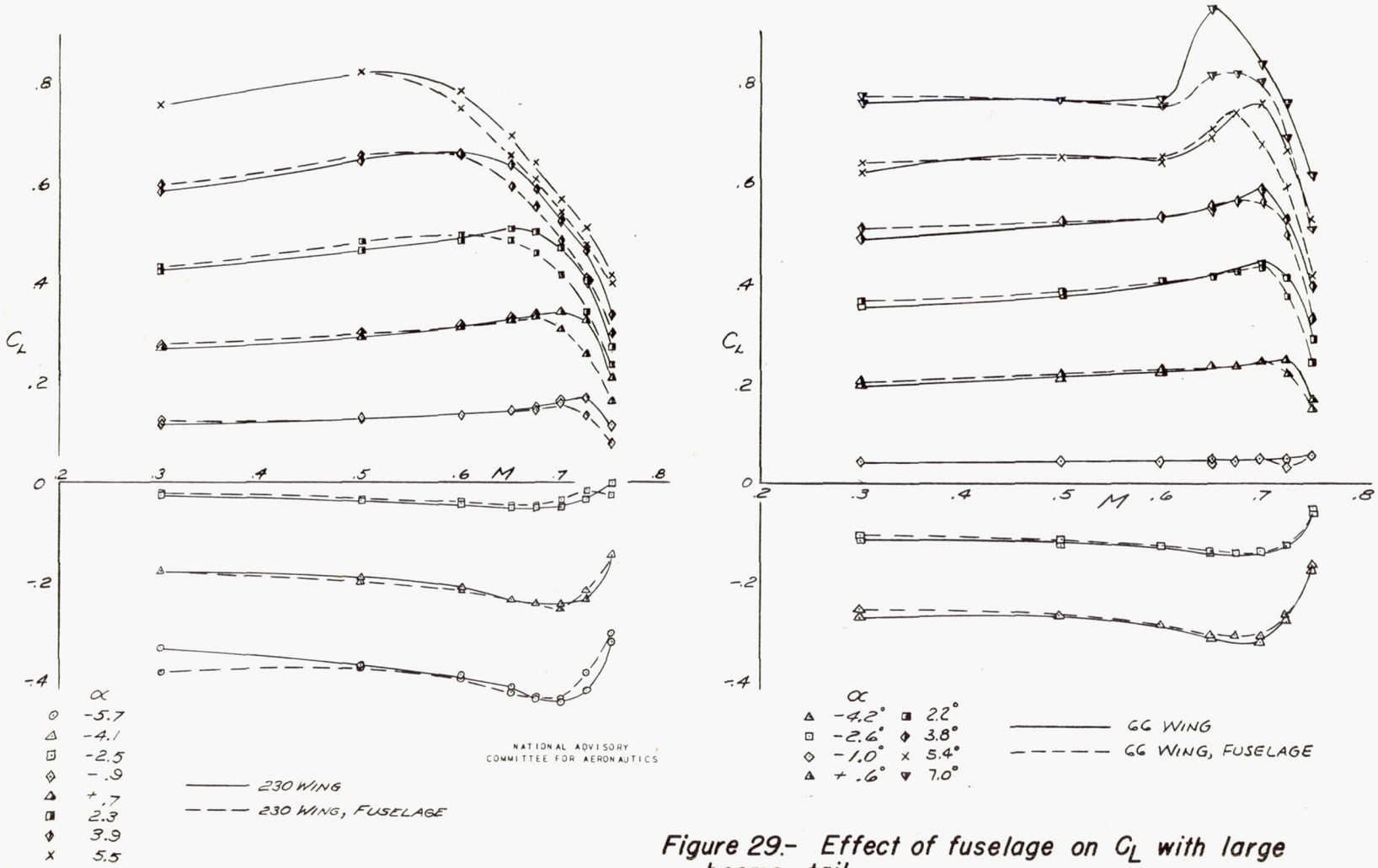

Figure 29.- Effect of fuselage on C_L with large booms, tail.

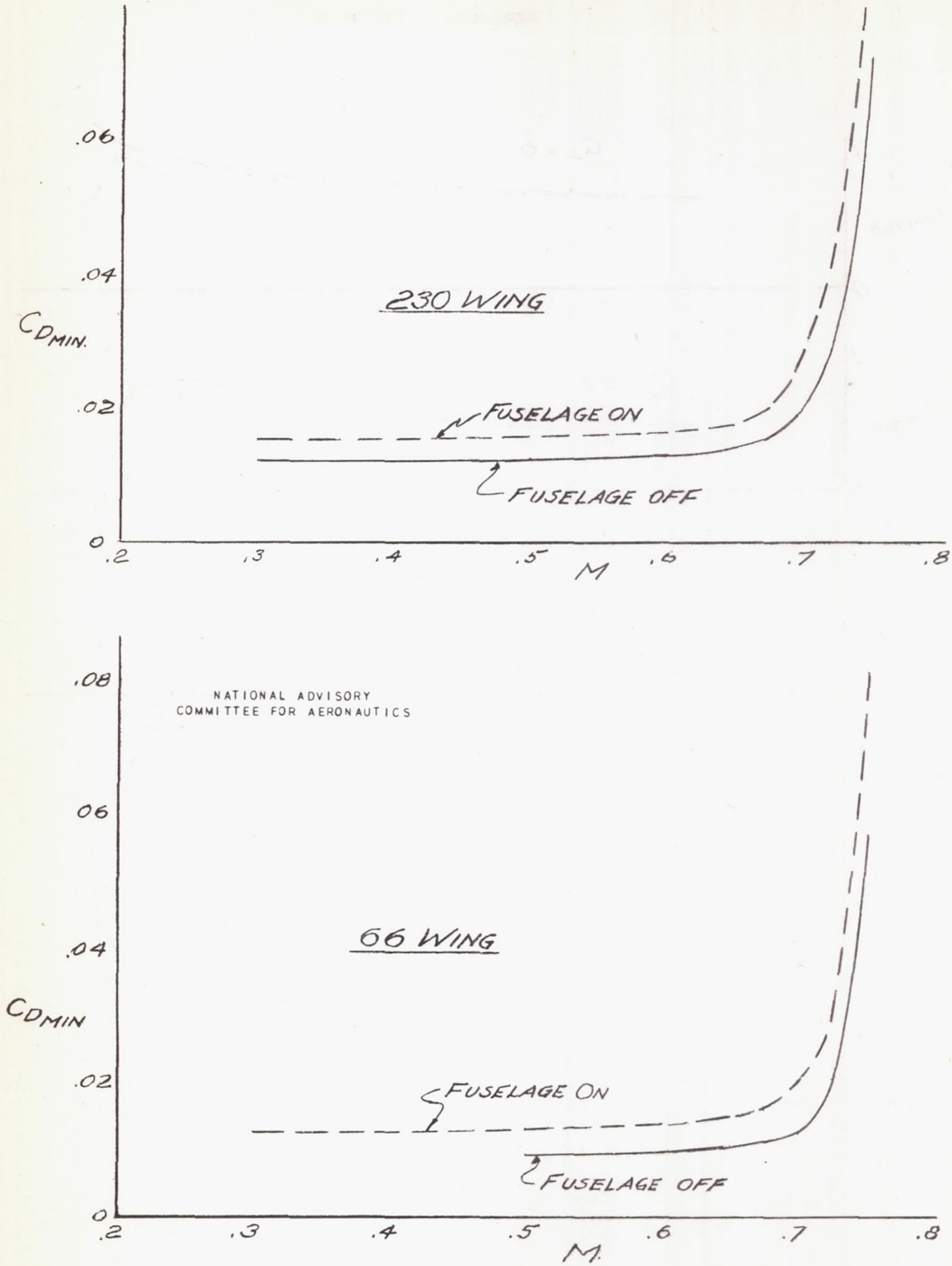

Figure 30.– Effect of fuselage on $C_{D_{min}}$ with large booms, tail.

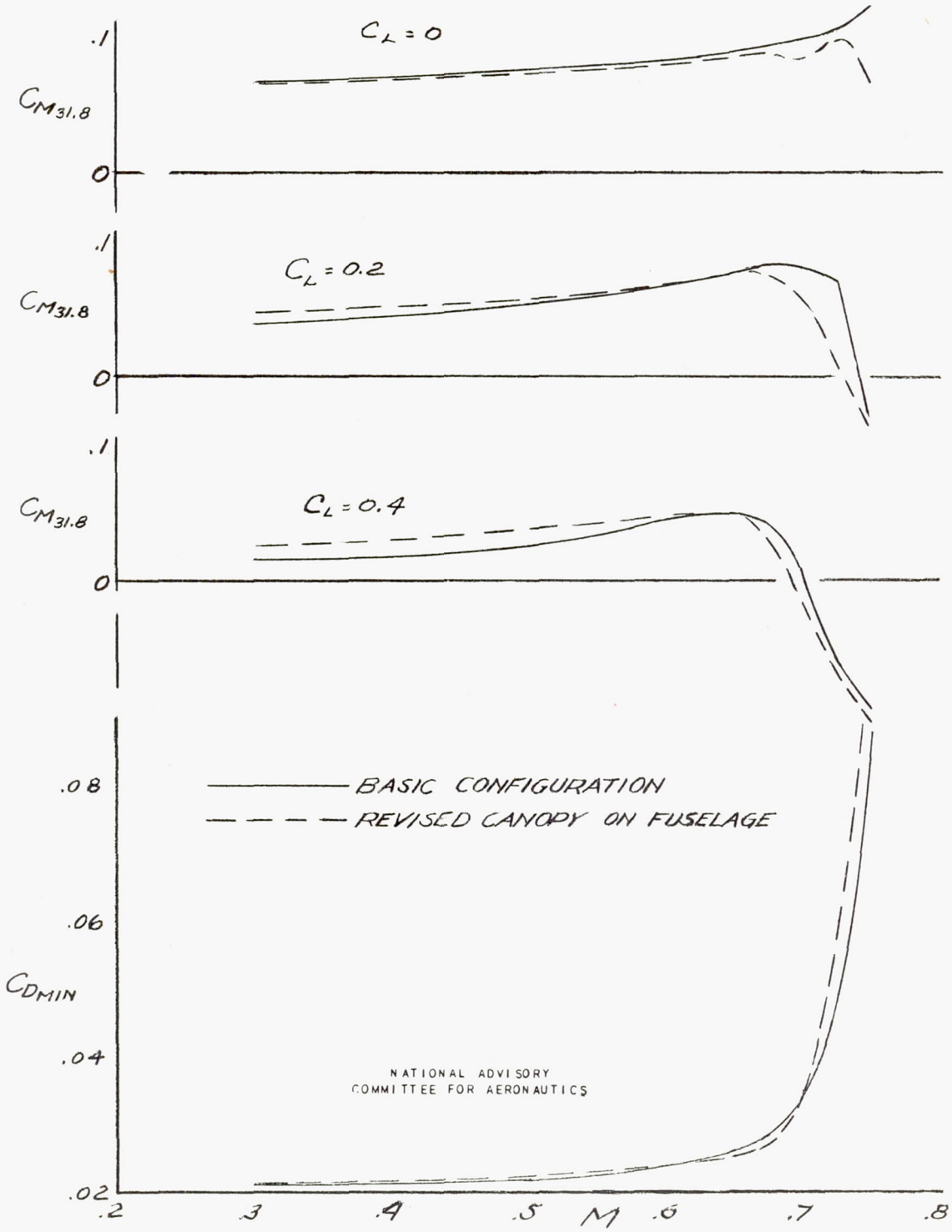

Figure 31.- Effect of canopy revision on C_M and $C_{D_{min}}$; 230 wing, large booms, fuselage, all accessories, tail.

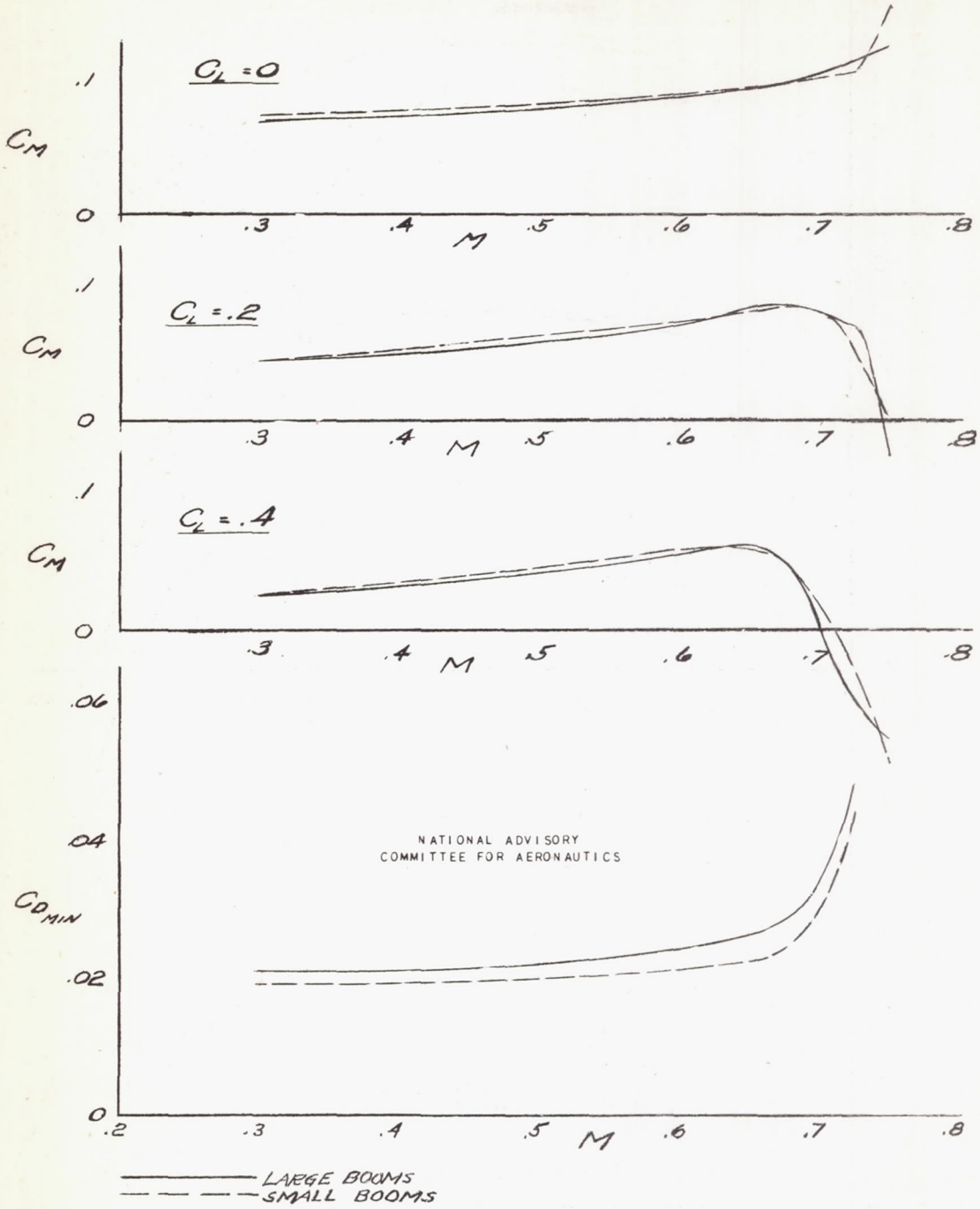

Figure 32.- Effect of boom size on C_M and $C_{D_{min}}$; 230 wing, fuselage, all accessories, tail.

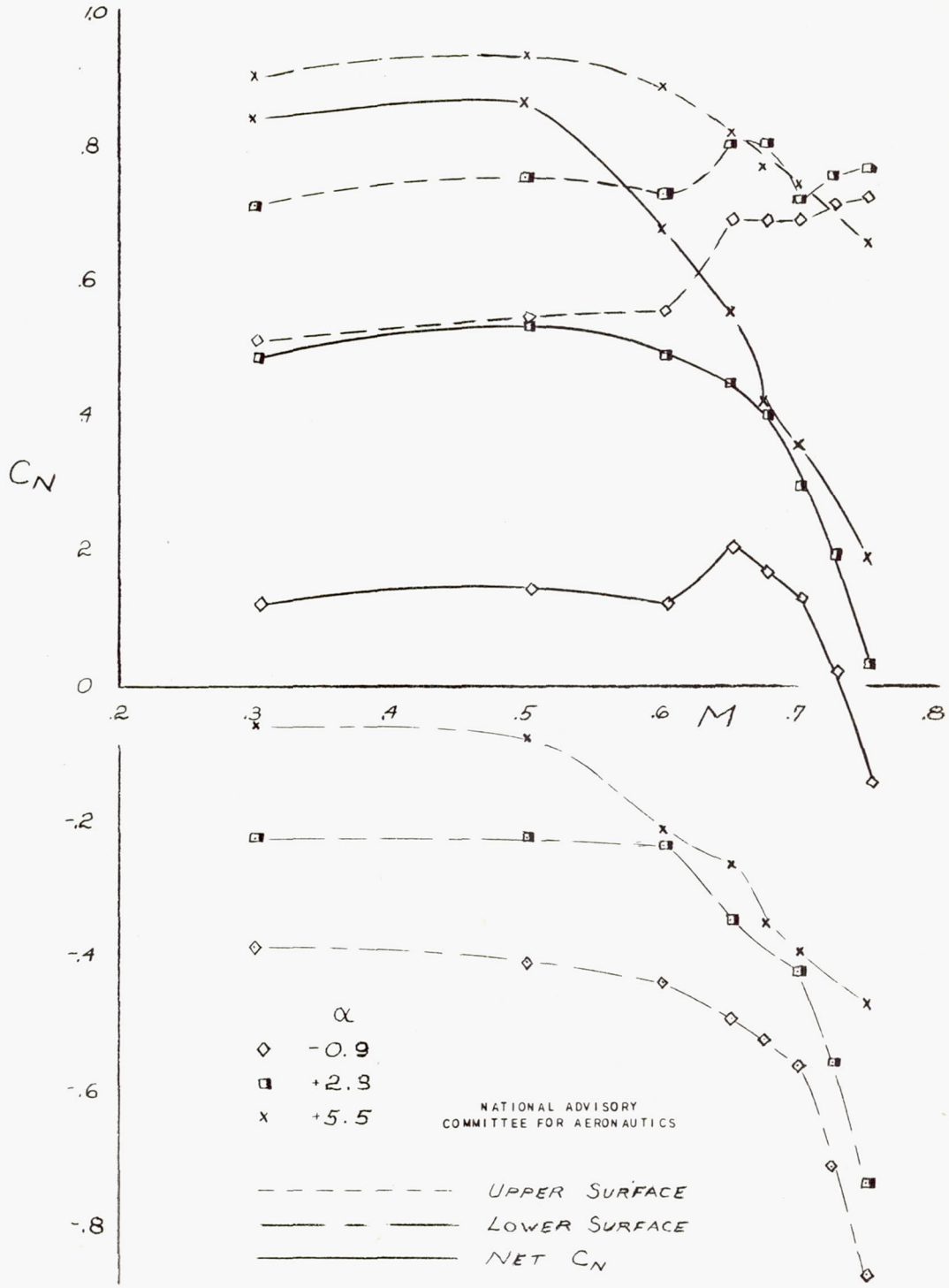

Figure 33.- Normal force coefficients, wing station 9.6; 230 wing, large booms, fuselage, tail.

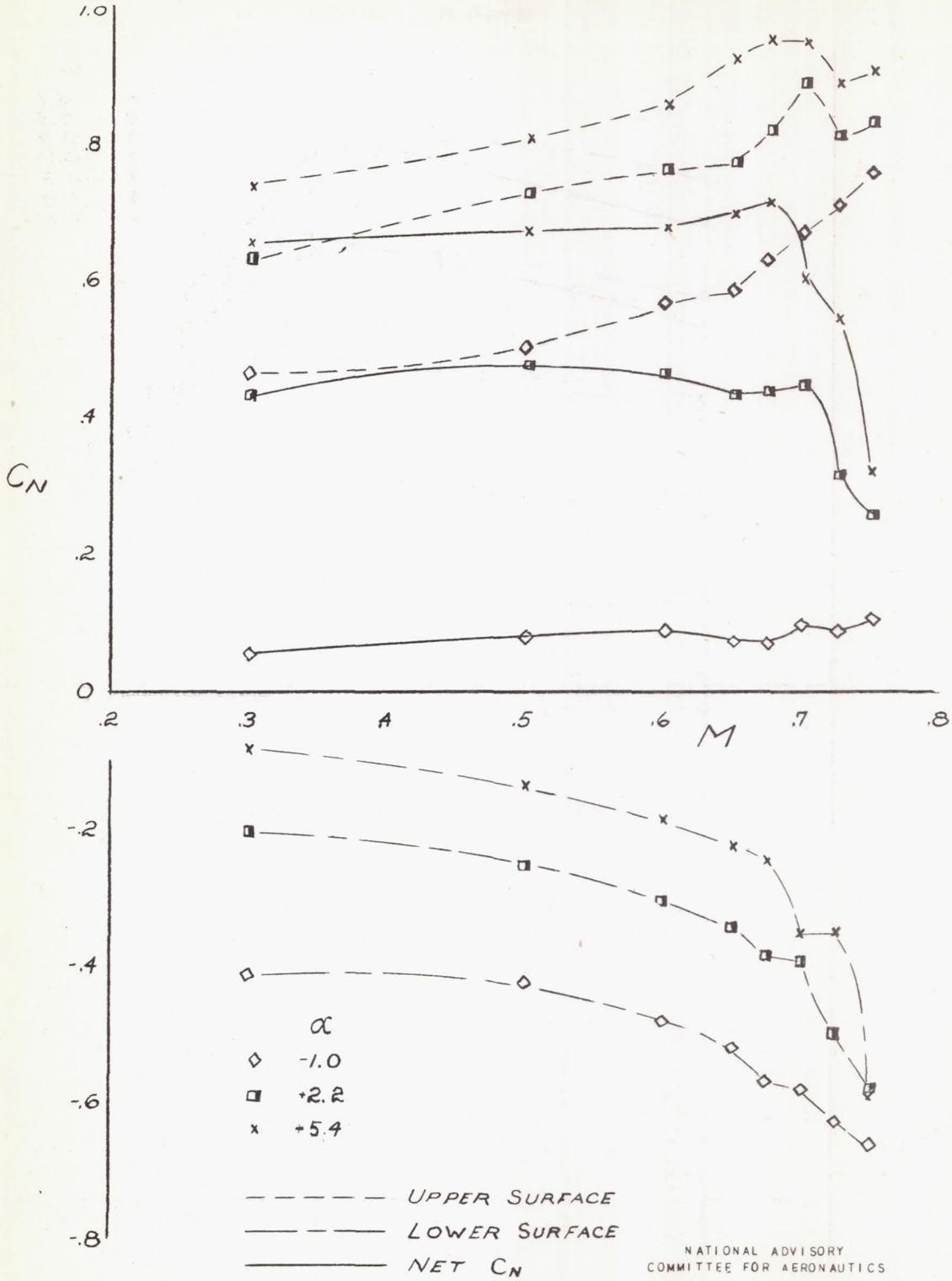

Figure 34.- Normal force coefficients, wing station 9.6; 66 wing, large booms, fuselage, tail.

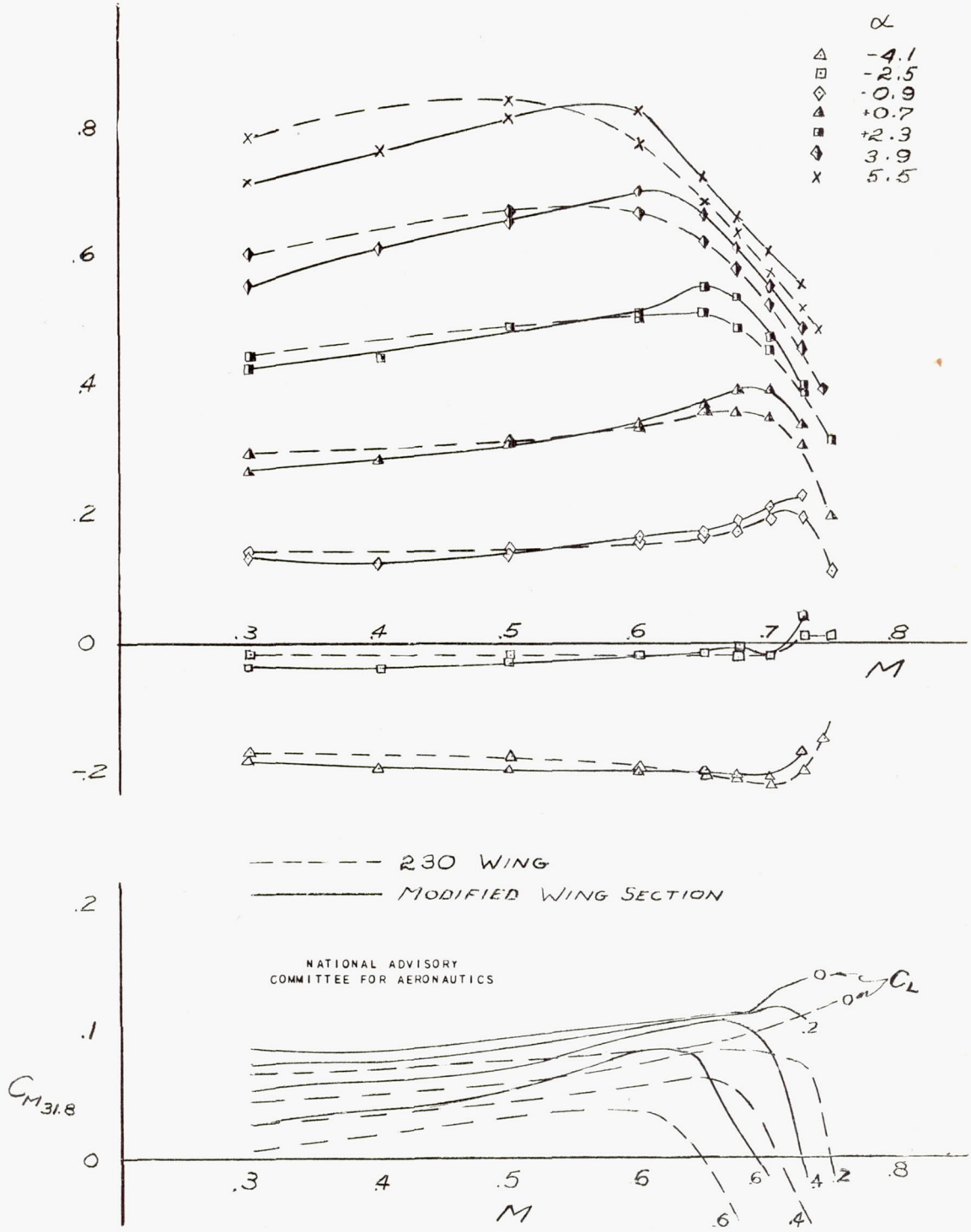

Figure 35.– Effect of 230 wing modification on C_L and C_M with large booms, fuselage, all accessories, tail.

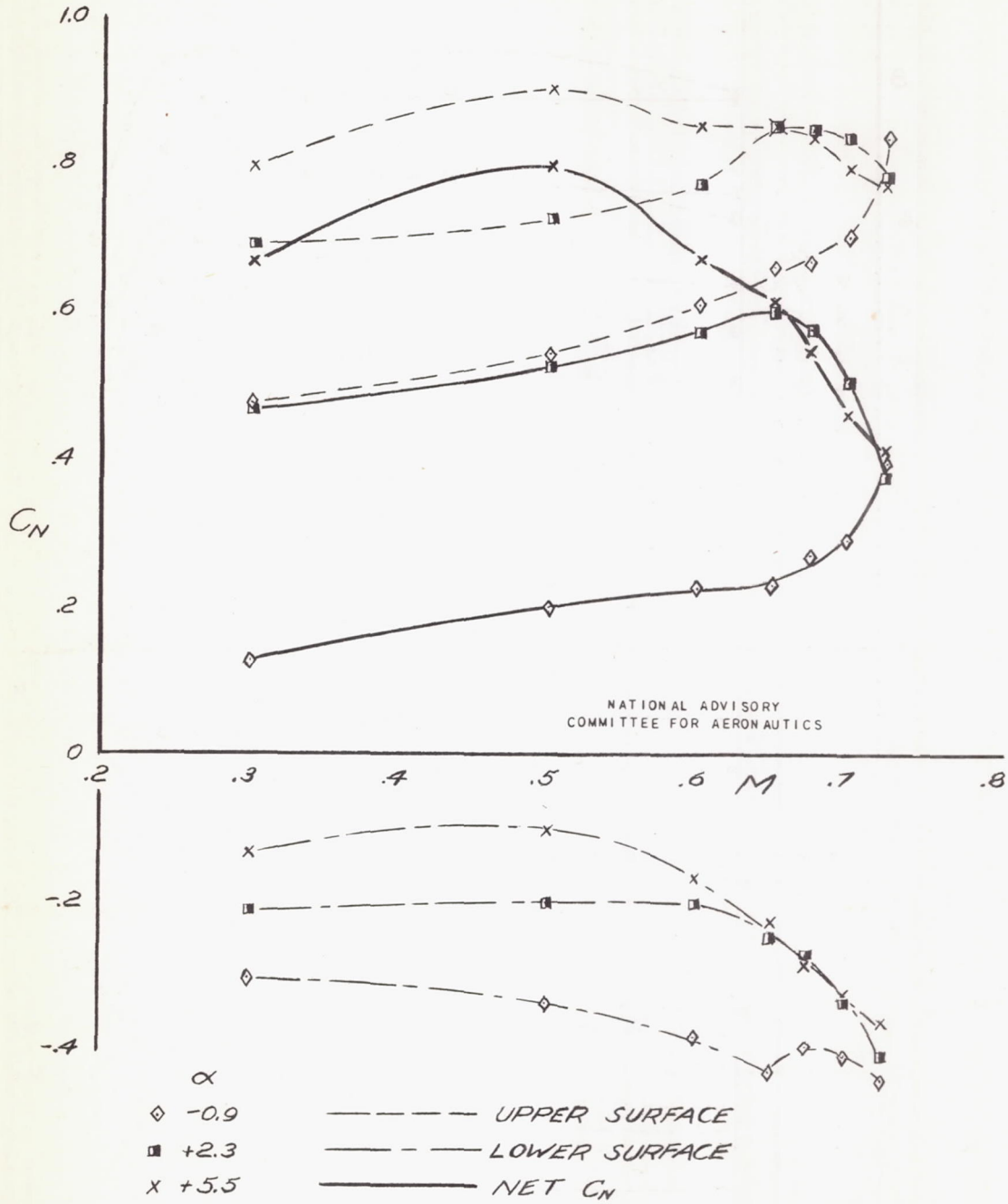

Figure 36.- Normal force coefficients, station 9.6; modified 230 wing, large booms, fuselage, all accessories, tail.

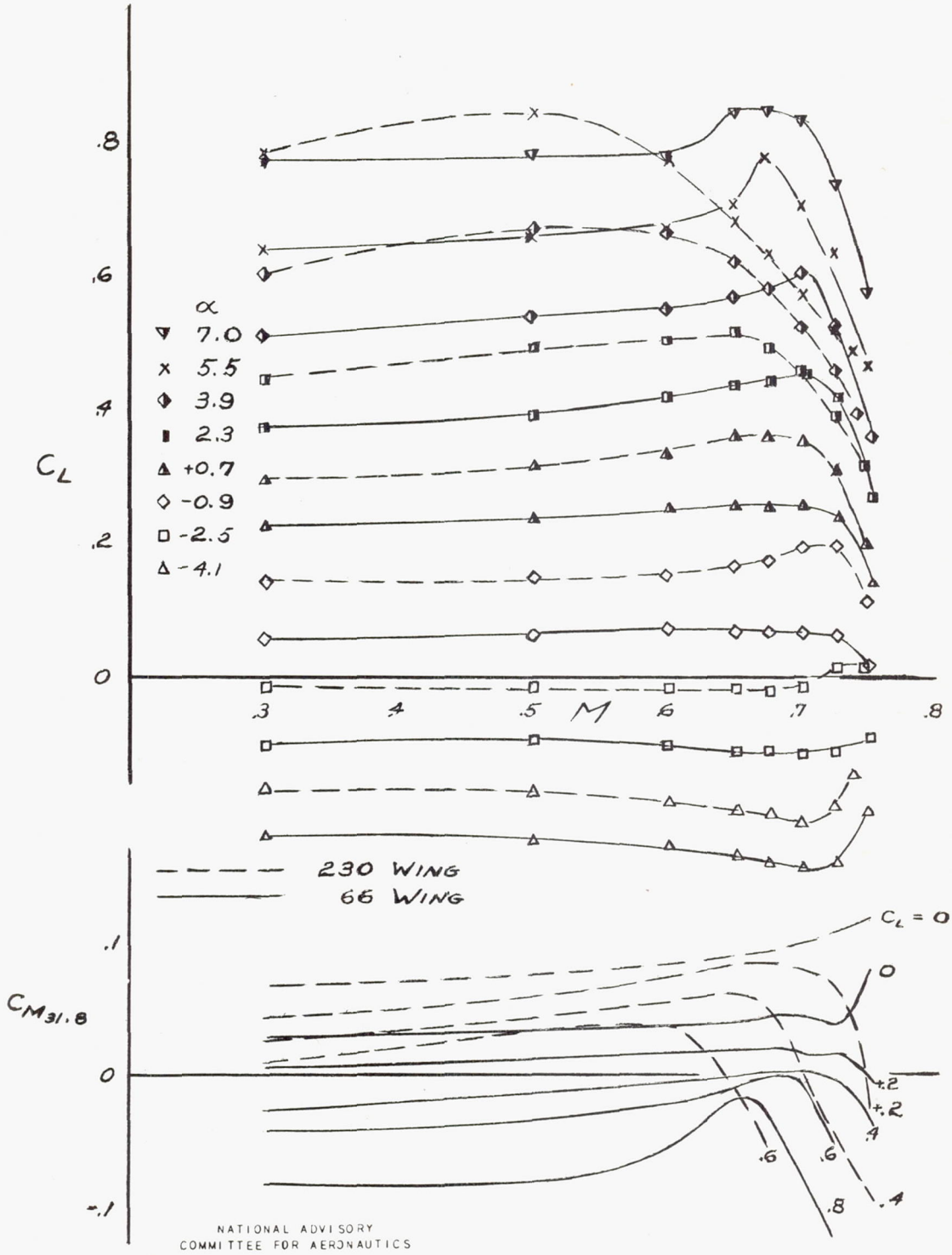

Figure 37.- Comparison of 230 wing and 66 wing with large booms, fuselage, all accessories, tail.

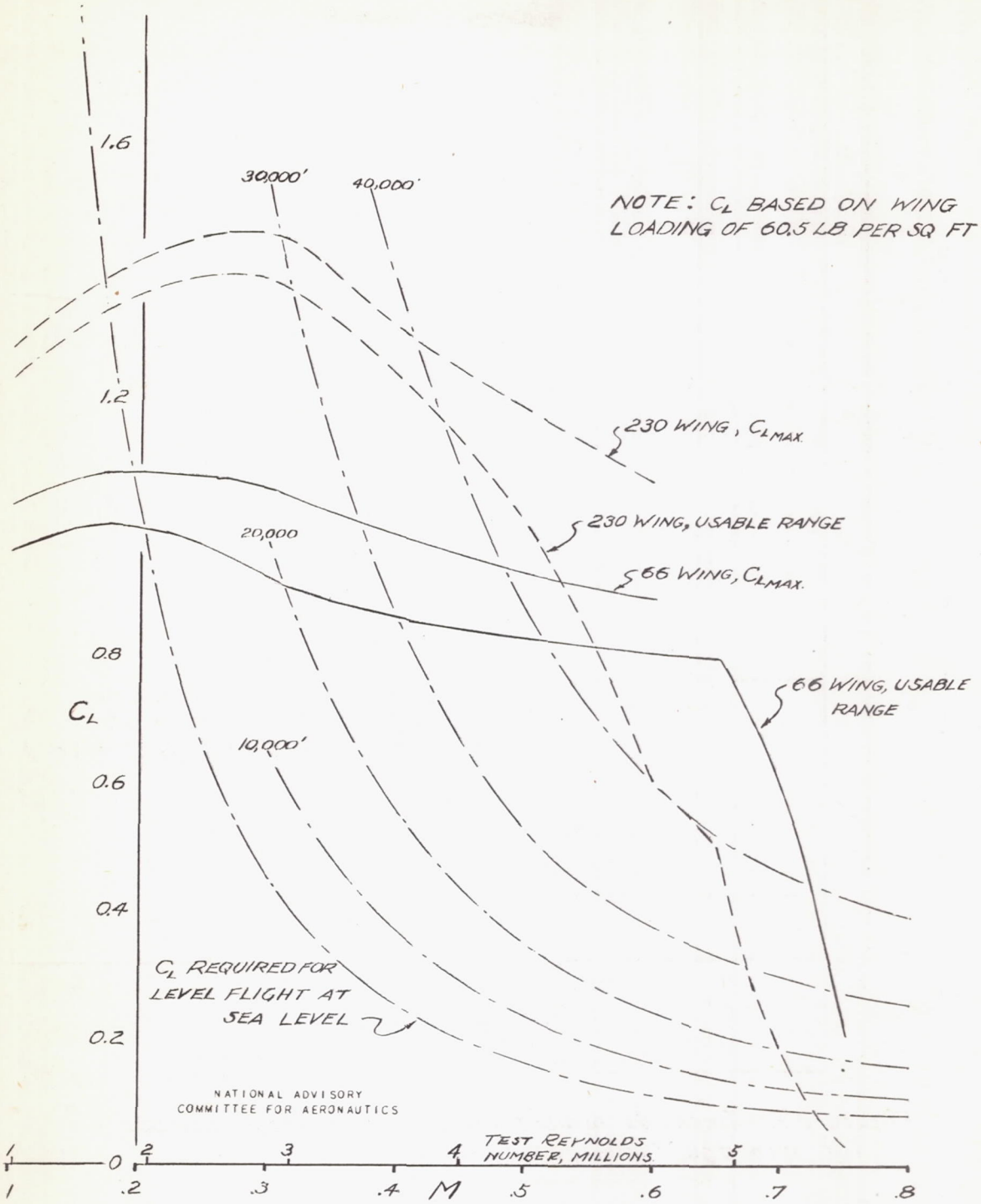

Figure 38.— Maximum C_L, usable C_L range, and C_L for level flight for 230 wing and 66 wing with large booms, fuselage, all accessories, tail.

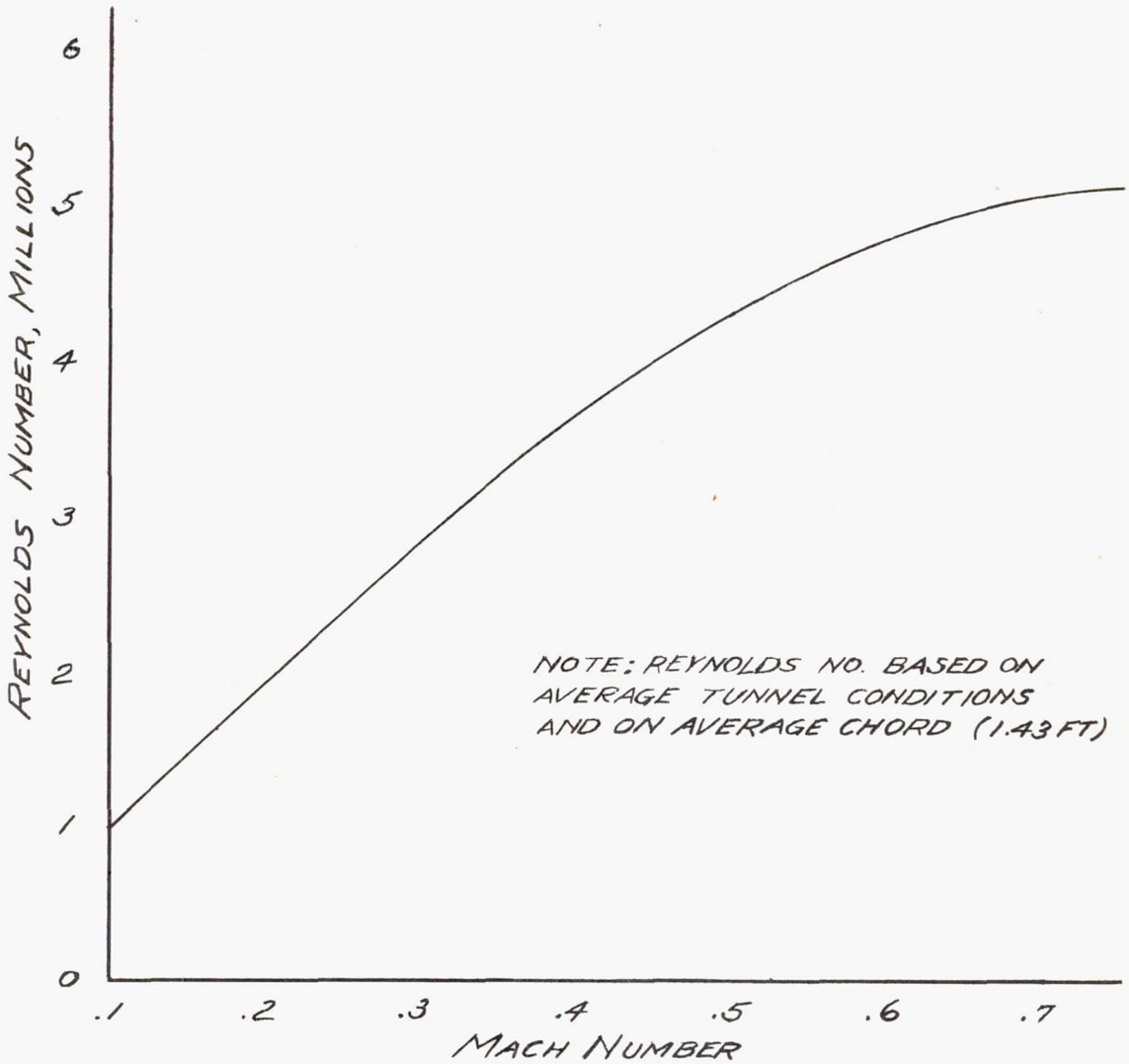

NATIONAL ADVISORY
COMMITTEE FOR AERONAUTICS

Figure 39.- Reynolds number variation with Mach number for average tunnel conditions.

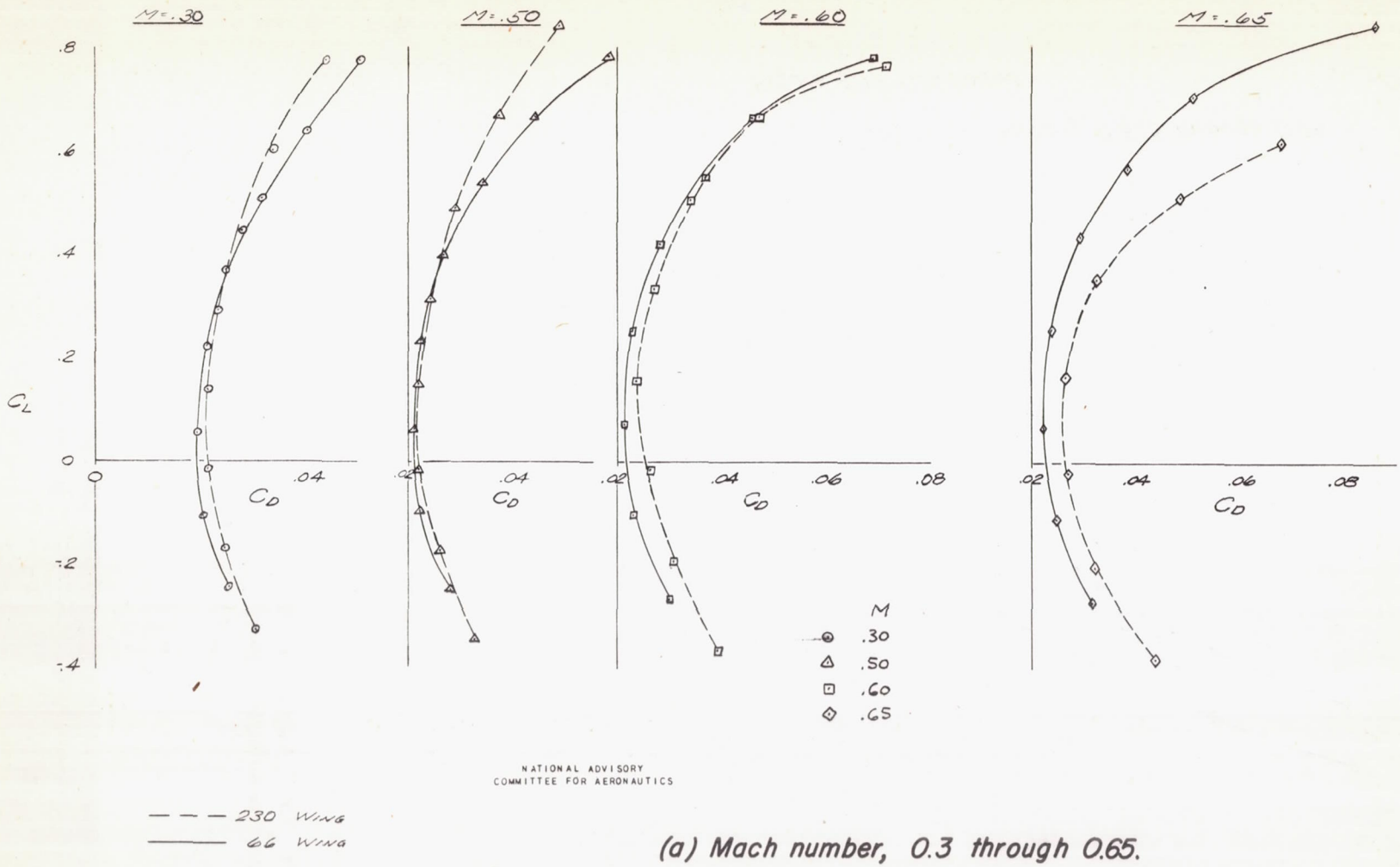

(a) Mach number, 0.3 through 0.65.

Figure 40.- Comparison of 230 wing and 66 wing in drag with large booms, fuselage, all accessories, tail.

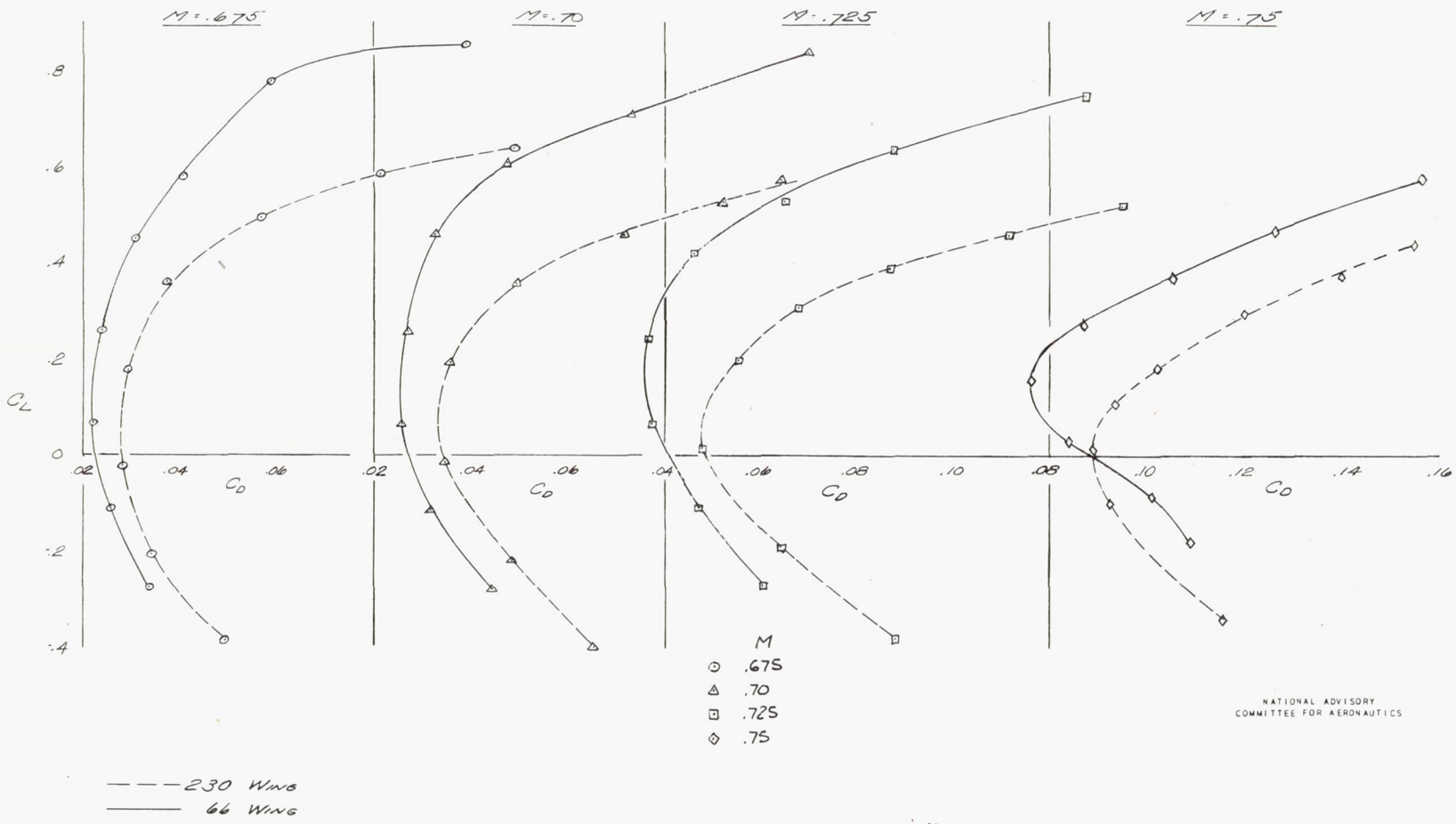

(b) Mach number, 0.675 through 0.75.

Figure 40.- Concluded.

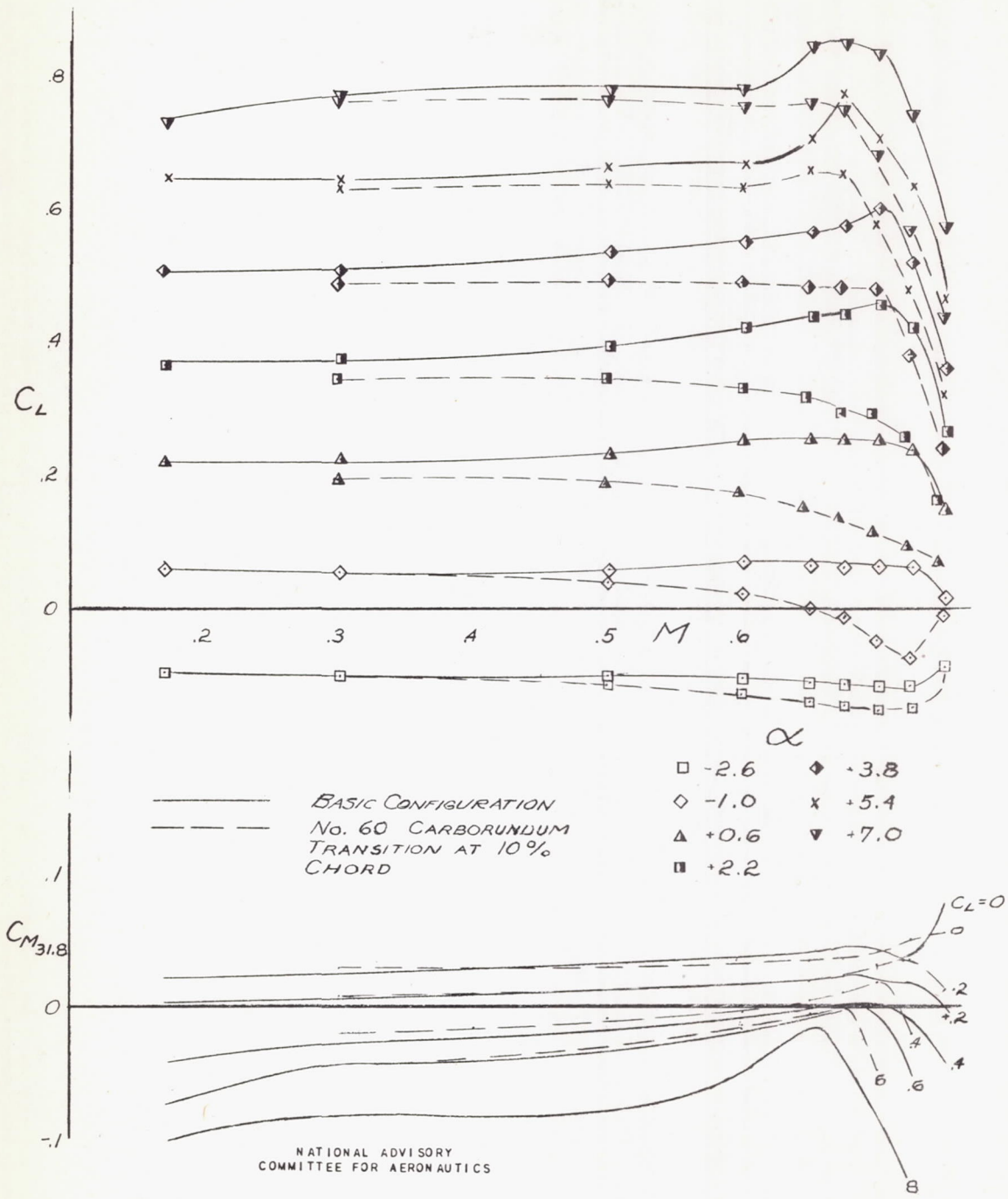

Figure 41.- Effect of fixing transition on C_L and C_M; 66 wing, large booms, fuselage, all accessories, tail.